STABILITY OF STRUCTURES
XIVTH SYMPOSIUM

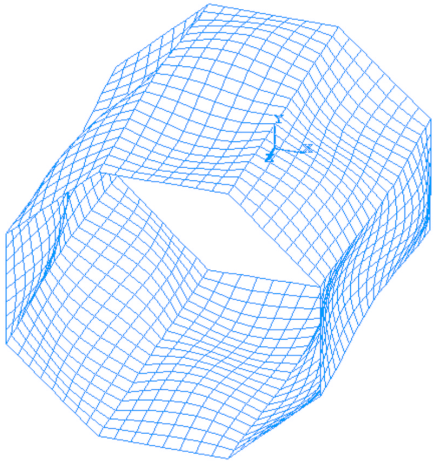

XIV SYMPOZJUM STATECZNOŚCI KONSTRUKCJI

70 LAT POLITECHNIKI ŁÓDZKIEJ

ZAKOPANE 08 - 12. 06. 2015

Proceedings of
the STABILITY of STRUCTURES
XIV-th SYMPOSIUM
Zakopane 2015

Under the auspices of
Dean of Mechanical Faculty of Lodz University of Technology

Professor Bogdan Kruszyński

Editor:

Radosław J. Mania

Organisers

- Department of Strength of Materials, Lodz University of Technology
- Theoretical and Applied Mechanics Polish Society, Lodz Branch

Zakopane, June, 08-12, 2015

SCIENTIFIC COMMITTE

Marian Królak – *honorary chairman*
Zbigniew Kołakowski - *chairman*
Ryszard Grądzki, Stefan Joniak, Maria Kotełko, Katarzyna Kowal-Michalska, Vasily Krasowsky (*Ukraine*), Tomasz Kubiak, Joseph Loughlan (*Great Britain*), Martin Macdonald (*Great Britain*), Krzysztof Magnucki, Arkadij Manevich (*Ukraina*), Radosław Mania, Aleksander Muc, Jacek Przybylski, James Rhodes (*Great Britain*), Shigeru Shimizu (*Japan*), Czesław Szymczak, Lech Tomski, Viorel Ungureanu (*Romania*), Czesław Woźniak, Jerzy Zielnica

ORGANISING COMMITTE

Tomasz Kubiak – *chairman*
Radosław Mania – *scientific secretary*
Mariusz Urbaniak, Jacek Jankowski, Jan Grudziecki, Anna Kuźniarek

Papers (on the rights of manuscripts) were accepted for publishing by the Scientific Committee members

ISBN 83-914019-8-7

© Publisher:
Katedra Wytrzymałości Materiałów i Konstrukcji Politechniki Łódzkiej ©
ul. Stefanowskiego 1/15, 90-924 Łódź
tel. +48 042 631 22 14, tel./fax: +48 042 636 49 85
www.kwm.p.lodz.pl e-mail: mechmat@info.p.lodz.pl

Printed:
Drukarnia Quick-Druk, 90-532 Łódź, Łąkowa 11

XIV SYMPOZJUM STATECZNOŚCI KONSTRUKCJI

STABILITY OF STRUCTURES XIVth SYMPOSIUM

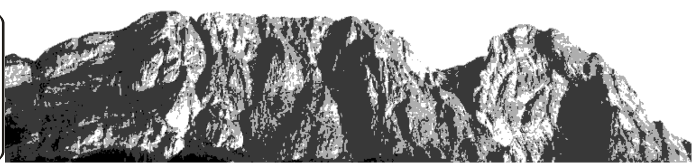

ZAKOPANE, 2015

CONTENTS

Keynote lectures

Session papers

KEYNOTE LECTURES

ON THE FOUNDATION OF NONLOCAL STRUCTURAL MECHANICS FROM LATTICE ELASTICITY

N. CHALLAMEL
Université de Bretagne Sud, LIMATB
Centre de recherche, rue de Saint Maudé, 56321 Lorient, France

1. FROM DISCRETE TO CONTINUOUS ELASTICITY - THE STRING PROBLEM

The source of discreteness in mechanics or physics may come from the inherent nature of matter which is composed of a discrete (or a finite) number of local repetitive cells. Discrete-based medium may be classified as a microstructured medium, and the microstructure can be related to the atomistic composition at a subscale, but also to the molecule, crystal, grain or truss organization at larger scales. Historically, Lagrange during the XVIII-th century first obtained analytical results for the discrete string, which is reconsidered here as a paradigmatic structural model. The free vibrations equation of the microstructured string of length *L* is governed by a linear difference equation:

$$T\,\frac{w_{i+1}-2w_i+w_{i-1}}{a^2}+\mu\omega^2 w_i=0 \tag{1}$$

where *a* is the distance between the nodes (*L*=*na*), μ is the line density, ω is the frequency, T is the applied tensile force, and w_i is the transverse deflection at node *i*. It can be shown that the frequency equation of this discrete problem with the fixed-fixed boundary conditions $w_0=w_n=0$ can be analytically solved and the exact frequencies are given by Lagrange [1]:

$$\omega_{k,n}=\frac{2n}{L}\sin\left(\frac{k\pi}{2n}\right)\sqrt{\frac{T}{\mu}} \tag{2}$$

The difference operator in Eq. (1) can be expanded using a differential approximation scheme, thus leading to the nonlocal differential approximation (see also [3] for the axial lattice or more recently [4])

$$Tw''+\mu\omega^2 w\underline{-\mu\omega^2 l_c^2 w''}=0 \qquad \text{with} \qquad l_c^2=\frac{a^2}{12} \tag{3}$$

where the underlined term is responsible for nonlocal effects. The vibration frequency of the fixed-fixed nonlocal string is then obtained by introducing a sinusoidal mode shape in Eq. (3), thereby leading to:

$$\frac{\omega_{k,n}^2}{\omega_{k,\infty}^2}=\frac{1}{1+\dfrac{k^2\pi^2 l_c^2}{L^2}}=1-\frac{k^2\pi^2}{12n^2}+o\left(\frac{1}{n^4}\right) \tag{4}$$

The discrete string problem has been revisited in the light of nonlocal mechanics. The same reasoning may be followed for discrete beams or discrete plates.

2. NONLOCAL STRUCTURAL MECHANICS

The present analysis may be also applied to bending systems. Hencky's model [2] composed of rigid links connected by concentrated elastic springs can be considered as a discrete beam model, where the bending moment is related to the deflection as:

$$M_i = EI \frac{w_{i+1} - 2w_i + w_{i-1}}{a^2} \tag{5}$$

which may be approximated, after a continualization process, by the nonlocal constitutive law, whose differential format is of Eringen's type [5]:

$$M - (e_0 a)^2 M'' = EI\kappa \qquad \text{with} \qquad \kappa = w'' \quad \text{and} \quad e_0 = \frac{1}{2\sqrt{3}} \tag{6}$$

These results may be generalized to the in-plane and out-of-plane motion (see Challamel [6, 7, 8]), statics versus dynamics, one-dimensional versus two-dimensional plate media. Nonlocal structural mechanics is definitely an efficient engineering theory that may be able to capture the fundamental scale effects related to the microstructure of the discrete element. A lot of applications may be found in the small-scale world but also for large scale structures in civil engineering such as truss structures for instance.

REFERENCES

[1] Lagrange J.L., Mécanique analytique, Paris, 1788 – 3rd Edition, Mallet-Bachelier, Gendre et successeur de Bachelier, Imprimeur-Libraire du bureau des longitudes, de l'école Polytechnique, de l'école centrale des arts et manufactures, Paris, 1853 (page 367).

[2] Hencky H., Über die angenäherte Lösung von Stabilitätsproblemen im Raummittels der elastischen Gelenkkette, Der Eisenbau, 11, 1920, pp. 437-452.

[3] Rosenau P., Dynamics of nonlinear mass-spring chains near the continuum limit, Physics Letters A, 118, 5, 1986, pp. 222-227.

[4] Andrianov I.V., Awrejcewicz J., Weichert D., Improved continuous models for discrete media, Mathematical Problems in Engineering, 986242, 2010, pp. 1-35.

[5] Eringen A.C., On differential equations of nonlocal elasticity and solutions of screw dislocation and surface waves, J. Appl. Phys., 54, 1983, pp. 4703-4710.

[6] Challamel N., Wang C.M., Elishakoff I., Discrete systems behave as nonlocal structural elements: bending, buckling and vibration analysis, Eur. J. Mech. A/Solids, 44, 2014, pp. 125-135.

[7] Challamel N., Lerbet J., Wang C.M., On buckling of granular columns with shear interaction: discrete versus nonlocal approaches, J. Applied Physics, 115, 234902, 2014.

[8] Challamel N., Camotim D., Wang C.M., Zhang Z., On lateral-torsional buckling of discrete elastic systems: a non-local approach, Eur. J. Mech. A/Solids, 49, 2015, pp. 106-113.

[9] Zhang Z., Wang C.M. and Challamel N., Eringen's length scale coefficient for buckling of nonlocal rectangular plates from microstructured beam-grid model, Int. J. Solids Structures, 51, 25-26, 4307-4315, 2014.

DEFORMATION AND BUCKLING OF AXIALLY COMPRESSED CYLINDRICAL SHELLS WITH ESSENTIALLY NON-UNIFORM STRESS-STRAIN STATE

V.L. KRASOVSKY
Department of Structural Mechanics and Strength of Materials
Prydniprovs'ka State Academy of Civil Engineering and Architecture
Chernyshevskogo 24a, 49-600 Dnipropetrovsk, Ukraine

Experiments show that the major feature of buckling process of real shells is the locality of its beginning connected with non-uniformity of precritical stress-strain state (SSS) caused by non-uniform perturbations fields. These factors concern local perturbations dominating over a spectrum of initial imperfections and external actions, non-uniform loading, discontinuities (cuts, openings), non-uniform loads application and non-uniform boundary conditions. In this case the theoretical analysis of stability based on linear precritical and bifurcation models is insufficient. An adequate approach to the real buckling process is a consecutive geometrically nonlinear analysis until the shell collapse. Until recently, a successful carrying out of such analysis was unreal, but now due to modern computers and software based on finite element method (FEM), this analysis appears quite possible. The article examines numerical results within ANSYS software of **three groups of problems** of deformation and buckling of axially compressed elastic circular cylindrical shells with essentially non-uniform precritical SSS.

Problems of the group 1 are devoted to the investigation of geometrically nonlinear behaviour of axially compressed shells under transversal kinematic local quasi-static actions (LQA) [1]. As LQA cause a strong non-uniform SSS of shells, the nature and conditions of load application influence on the features of shell behaviour. In this connection, geometrical and FE models of shells and also simulation models of five schemes of application and removal of an axial loading and LQA have been developed. The axial loading is applied through rigid disks according to two types: force (schemes 1, 3, 5) and kinematic (schemes 2, 4) loading. The models of shells also consider three types of boundary conditions on the edges. For two types the shell edges are hinged to rigid disks (schemes 1-4). Thus, for one type free out-of-plane rotations are possible (schemes 1, 2), and for another one parallel edge displacements are supposed (schemes 3, 4). For the third type of boundary conditions radial and tangent displacements are restricted on the edges, but out-of-plane edge displacements are allowed (scheme 5). Numerical buckling simulations have been carried out by means of geometrically nonlinear analyses realized for step-by-step loading of a shell. This research also studies the influence of the sequence of the axial load and LQA application (typical or initial LQA).

For 5 mentioned schemes in a wide range of axial loads, dependences of transversal reactions on typical lateral LQA are received. These dependences completely reflect main features of shells behaviour for desired axial load and LQA. For the schemes 1-4 in the certain area of axial loads these dependences show an existence of the stable buckling mode of a shell with one local dent that corresponds to the experimental data and analytical solutions. For the scheme 5 these dependences have a different character in comparison with other schemes. The visualisation results and comparisons of numerical buckling modes with experimentally tested patterns of compressed shells under LQA prove the opportunity of detection of bifurcation points in geometrically nonlinear analyses within ANSYS software. In this case, the criterion of bifurcation points is a divergence of numerical solutions.

Problems of the group 2 concern the buckling behaviour of axially compressed shells with one transversal (in the middle section) or one longitudinal cut of various lengths [2]. FE models reflect 5 mentioned loading schemes. Besides, numerical simulations repeat 60 own buckling tests of shells with cuts compressed according to the scheme 1. Numerical problems consider three buckling analyses: linear (solution *I*), geometrically nonlinear (solution *II*) and geometrically nonlinear analysis of shells with imperfections (solution *III*). The solution *III* provides the best correspondence to the experimental data for any cuts. The main features of linear and geometrically nonlinear analyses of buckling problems are determined depending on loading schemes 1-5 and on cut lengths. A high efficiency of ANSYS software has been proved for numerical simulations of shells buckling taking into account a physical nonlinearity of material.

Problems of the group 3 deal with numerical analyses [3] of deformation and stability of elastic circular cylindrical shells undergoing periodically non-uniform SSS of different nature: periodical axial loading and periodical initial imperfections. The study is focused on the effect of “static resonance”. This effect consists in the increase of static lateral deformation of the shell and decrease of limit load in a case of non-uniform SSS similar to the form of first Eigen vibration mode of a shell.

The present research also contains an important number of comparisons of numerical solutions with experimental, analytical and other numerical researches. For all the groups of problems an excellent correspondence between the numerical results and known solutions confirms a good applicability of ANSYS software for the deformation and buckling problems of axially compressed cylindrical shells with essentially non-uniform SSS.

This work is supported by Alexander von Humboldt Foundation (Institutional academic cooperation program, grant no. 3.4 – Fokoop – UKR/1070297).

REFERENCES

[1] Krasovsky V., Marchenko V., Schmidt R., Deformation and buckling of axially compressed cylindrical shells with local loads in numerical simulation and experiments, Thin-Walled Structures, 49, 2011, pp. 576-580.

[2] Lykhachova O.V., Schmidt R., Deformation and buckling of axially compressed elastic cylindrical shells with transversal cut in experiments and numerical simulations, Shell Structures: Theory and Applications, (eds.) W. Pietraszkiewicz, J. Gorski, London, 3, 2013, pp. 219-222.

[3] Krasovsky V.L., Kolesnikov M.V., “Static resonance” in cylindrical shells with periodical non-uniform strain-stress state conditioned by load or initial imperfections, in “Static, Dynamics and Stability of Structures. Review and Current Trends in Stability of Structures”, (eds.) Kowal-Michalska K., Mania R. J., Lodz, Vol. 3, 2013, pp. 289-312.

EQUILIBRIUM PATHS OF SELECTED ELASTIC STRUCTURES

K. MAGNUCKI
Institute of Applied Mechanics, Poznan University of Technology
Jana Pawła II 24, 60-965 Poznań, Poland

1. INTRODUCTION

The information on a post-buckling behaviour of structures is important for design engineers. Post-buckling behaviour of columns, frames, plates, thin-walled beams and shells was described and discussed for example by Hutchinson and Koiter (1970), Thompson and Hunt (1973), Budiansky (1974), Bushnell (1989), Bažant and Cedolin (1991) and Kubiak (2013). These authors indicated the stable/unstable equilibrium paths.

The paper is devoted to post-buckling behaviour of selected elastic structures, in particular the shells of revolution with positive and negative Gaussian curvature, and also a seven-layer orthotropic cylindrical shell.

2. COLUMNS, RECTANGULAR PLATES AND CYLINDRICAL SHELLS

The equilibrium paths for the columns and rectangular plates are stable, however for the cylindrical or conical shells (zero of the Gaussian curvature) are unstable (Fig. 1).

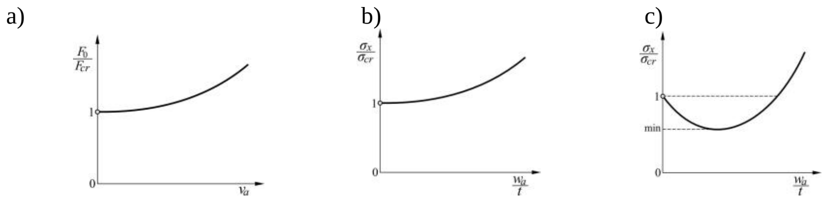

Fig. 1. The equilibrium paths for columns - a), rectangular plates - b), cylindrical shells - c)

The stabilisation problem of equilibrium paths considered as an optimization problem of structures was described by Bochenek and Krużelecki [2].

3. SHELLS OF REVOLUTION WITH VARIABLE GAUSSIAN CURVATURES

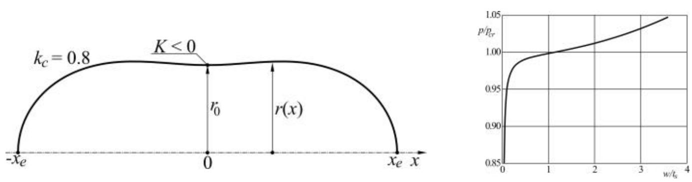

Fig. 2. The scheme of the Cassini ovaloidal shell and the equilibrium path

The stabilisation problem of equilibrium paths of shells of revolution considered as meridian shape problem was studied and described by Jasion [6]. The shells of revolution with positive and negative Gaussian curvature are distinguished by stable equilibrium paths. The example of this shell is the Cassini ovaloidal shell (Fig. 2), where k_c is a dimensional parameter, K is Gaussian curvature, $r(x)$ is radius of the meridian.

4. SEVEN-LAYER CYLINDRICAL SHELL

The seven-layer elastic cylindrical shell with main corrugated core and two three-layer faces is an untypical sandwich structure (Fig. 3). The buckling and post-buckling behaviour of a family of these shells under external pressure were numerically FEM investigated by Malinowski *et al* [8]. The distinguishing mark of these shells are the stable equilibrium paths (Fig. 3).

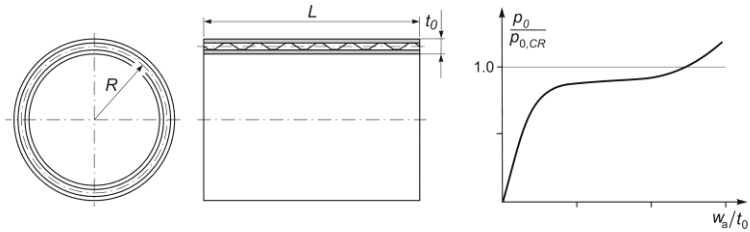

Fig. 3. Scheme of the seven-layer cylindrical shell and the equilibrium paths

The research was conducted within the framework of Statutory Activities in 2015.

REFERENCES

[1] Bažant Z.P., Cedolin L., Stability of structures, Oxford Univ. Press, New York, Oxford, 1991.

[2] Bochenek B., Krużelecki J., Optimization of structures stability, Modern problems, Wyd. Politechniki Krakowskiej, Kraków 2007, (in Polish).

[3] Budiansky B., Theory of buckling and post-buckling behaviour of elastic structures, Advances in Applied Mechanics, 14, 1974, pp. 1-65.

[4] Bushnell D., Computerized buckling analysis of shells, Kluwer Academic Publishers, Dordrecht, Boston, London, 1989.

[5] Hutchinson J.W., Koiter W., Postbuckling theory, Applied Mechanics Reviews, 23, 1970, pp. 1353-1366.

[6] Jasion P., Buckling and post-buckling analysis of shells of revolution with positive and negative Gaussian curvature, Publ. House of Poznan Univ. of Technology, Poznan, 2015.

[7] Kubiak T., Static and dynamic buckling of thin-walled plate structures, Springer, Cham, Heidelberg, New York, Dordrecht, London, 2013.

[8] Malinowski M., Belica T., Magnucki K., Buckling of sandwich cylindrical shell with corrugated main core and three-layer faces, App. Comp. Science, 10, 4, 2014, pp. 18-25.

Thompson J.M.T., Hunt G.W., A general theory of elastic stability, John Wiley & Sons, London, New York, Sydney, Toronto, 1973.

STABILITY OF COLD-FORMED STEEL BEAMS OF CORRUGATED WEBS. EXPERIMENTAL AND NUMERICAL INVESTIGATIONS

V. UNGUREANU, D. DUBINA
Politehnica University of Timisoara, Timisoara, Romania
Romanian Academy – Timisoara Branch, Timisoara, Romania

The beams of thin corrugated web afford a significant weight reduction compared with hot-rolled or welded ones. In the initial solutions, the flanges are made of flat plates, welded to the sinusoidal web sheet, requiring a specific welding technology. A new solution is proposed by the authors, in which the beam is composed by a web of trapezoidal cold-formed steel sheet and flanges of back-to-back lipped channel sections. For connecting flanges to the web self-drilling screws are used. The paper summarizes the experimental and numerical investigations carried out at the CEMSIG Research Centre of the Politehnica University of Timisoara and, at the end, presents an investigation of sensitivity of webs to distortion of corrugations when the size of corrugations increases.

Five beams with corrugated webs (CWB) with a span of 5157 mm and a height of 600 mm have been tested, considering different arrangements for self-drilling screws and shear panels. References [1] and [2] show detailed information related to the behaviour of each tested specimen. Figure 1 shows, as an exemplification, the deformed shape of the CWB-5 beam at collapse and the distortion of the web corrugation in the region with the reduced number of screws. Additional tests in order to determine the material properties and connections behaviour have been performed.

(a) (b)

Fig. 1. (a) Deformed shape of CWB-5 beam at failure; (b) the distortion of the web corrugation

Based on the above results and considering the FEM models validated in [1], the next step was to evaluate the behaviour and capacity of a beam of 12 m span with trapezoidal shape and a another one of 16 m with parallel flanges using numerical simulations [3]. The numerical model has been created using the commercial FE program ABAQUS/CAE v.6.7.1. Details related to the type of finite elements, material behaviour, contact parameters, modelling of screws and bolts are presented in [3].

Based on the conclusions of the second beam, of 16 m span with parallel flanges, on the following, the influence of the depth of corrugation on the global behaviour was studied. In this sense, three different depths for the corrugated web have been chosen, i.e. 30 mm, 43 mm (presented above) and 85 mm, in all the cases the thickness being 0.7 mm. For this analyses the case with transversal translational and rotational springs at the top flange in the position of purlins, corresponding to axial and bending rigidities of a Z200/2 purlin including fly bracings corresponding to the first purlin adjacent to the ridge has been considered. Also, it should be mention that in case of screws, the optimized solution used for beam CWB-5 was adopted, i.e. by adapting both the flange-to-web connections and seam fasteners to the distribution of shear stresses.

Plotting all three curves on the same graph, it is easy to see that curve for corrugation A85 has a reduced stiffness compared to the other two due to the fact the depth of the corrugations is more sensible to the end distortion of the corrugations. More, after reaching the maximum load the curve drop suddenly and a stable path can be seen due to the buckling coming from in-plane loading of the web. The curves for corrugation A30 and A45 have the same stiffness, but the maximum force is lower in case of A45 and a "plateau" can be seen. Another aspect is related to the optimisation of screws used both as seam fasteners and for connecting the web to the flanges. A better distribution of self-drilling screws together with reduced thicknesses for the web will put better in evidence the influence of the sheeting.

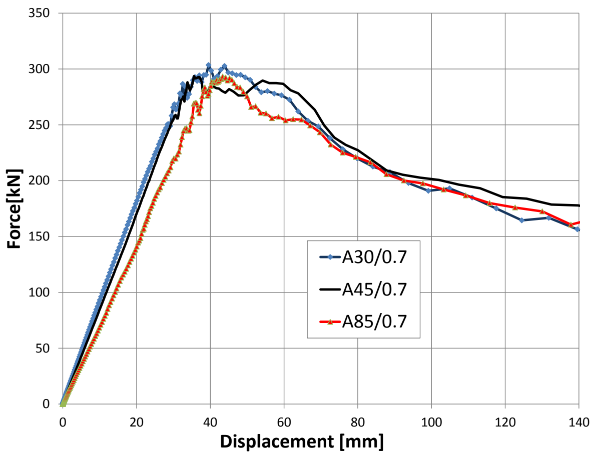

Fig. 2. Force-displacement curve for the three different depths of corrugated web

On the aim of optimizing the technical solution for a mass production of such beams, the further investigations will focus on these aspects.

REFERENCES

[1] Dubina D., Ungureanu V., Gîlia, L., Cold-formed steel beams with corrugated web and discrete web-to-flange fasteners, Steel Constructions.Design & Research,6(2), 74–81,2013.

[2] Dubina D., Ungureanu V., Gîlia L., Experimental investigations of cold-formed steel beams of corrugated web and built-up section for flanges, Thin-Walled Structures, 90(2015), 159–170.

[3] Dubina D., Ungureanu V., Gîlia L., Cold-formed steel beams of corrugated web and built-up section chords, Proceedings of the 7th European Conference on Steel and Composite Structures - EUROSTEEL 2014, Naples, Italy, (10-12/09), 429-430, 2014.

INFLUENCE OF *BENDING–TWISTING* COUPLING ON COMPRESSION AND SHEAR BUCKLING STRENGTH FOR INFINITELY LONG CARBON-FIBRE AND FIBRE-METAL LAMINATED PLATES

C. B. YORK
Aerospace Sciences, School of Engineering, University of Glasgow
James Watt (South) Building, Glasgow G12 8QQ, UK

Loughlan [3] reminded us that the structural design engineer who is unaware of the degrading influence of *Bending–Twisting* coupling on buckling response may choose a lay-up configuration for which a simple orthotropic analysis approach leads to a significant overestimate of the critical shear stress, i.e., on the unsafe side. This degrading influence applies equally to the critical compressive stress, yet recent studies [1] illustrate that the exact closed form solution for othotropic laminates continues to be incorrectly applied to *Bending–Twisting* coupled designs. This is in spite of the fact that approximate closed form solutions for long 'flexurally anisotropic' plates with simply supported edges were developed by Weaver (see [7]), in order to help the designer quickly assess the impact of 'flexural/twist anisotropy' on compression buckling loads.

For laminated plates that have a fixed number of constant-thickness plies, Loughlan [3] demonstrated, by a finite strip approach, that, for a given degree of 'material anisotropy', the stacking sequence of the plies significantly alters the degree of Bending–Twisting coupling in the laminate and hence the shear buckling performance. Composite plates that have the same dimensions and are of the same weight behave very differently as a result of lay-up configuration. It should also be noted that these effects are direction dependent, i.e., the shear buckling performance may be augmented, rather than degraded, if the loading direction is reversed.

The current article serves to provide more clarity on this subject by identifying laminates with matching stiffness properties, which differ only by their coupling terms (D_{16}, D_{26}), thus offering a clearer understanding on their isolated influence on buckling performance. The (non-dimensional) bounds on both compression ($k_{x,\infty}$) and shear ($k_{xy,\infty}$) buckling strength have previously been assessed using closed form solutions, applied to a definitive listings of *Bending–Twisting* coupled laminates [7]:

$$k_{x,\infty} = 2\left\{1 + \beta - (\gamma - 3\delta)^2 \big/ (\beta + 3)\right\} \tag{1}$$

$$k_{xy,\infty} = 3.42 + 2.05\beta - 0.13\beta^2 - 1.79\gamma - 6.89\delta + 0.36\beta(2\gamma + \delta) - 0.25(2\gamma + \delta)^2 \tag{2}$$

These assessments involve the non-dimensional parameters, proposed by Nemeth [5], consisting of an othotropic parameter, β, and two anisotropic parameters, γ and δ.

$$\beta = (D_{12} + 2D_{66}) \big/ (D_{11}D_{66})^{1/2} \tag{3}$$

$$\gamma = D_{16} \Big/ \left(D_{11}{}^{3} D_{22} \right)^{1/4} \tag{4}$$

$$\delta = D_{26} \Big/ \left(D_{11} D_{22}{}^{3} \right)^{1/4} \tag{5}$$

Here the use of a finite strip or similar method would clearly have been impractical for what amounts to an assessment of tens of thousands of stacking sequences. However, subsequent comparisons of these approximate closed form solutions, against an exact infinite strip method, has revealed that whilst high level inaccuracy is obtained for certain anisotropy characteristics, there are significant errors on the unsafe side, for others.

Compression buckling assessments were found to be within 0.1% of the exact result when the two anisotropic parameters were within 5% of each other; outside this range, the buckling assessments could be in excess of 10%, on the unsafe side, of the exact result. Shear buckling assessments revealed a rather more random distribution with much larger inaccuracies. These inaccuracies will be addressed in this article and the applicability of the revised closed form buckling solutions to fibre-metal laminates (FML) will be demonstrated.

Application to FML is explored in the context of Aluminium and Carbon-Fibre epoxy woven cloth (TeXtreme™) layers, since recent research [6] has revealed that thin ply laminate technology with areal weights of 50g/m^2, compared to standard materials with 250 g/m^2, allows the possibility of designing isotropic layers, e.g. $[\alpha/\beta_2/\alpha/\beta/\alpha_2/\beta]_T$, with $\alpha = \beta + \pi/4$, possessing identical moduli to Aluminium, and within the thickness constraints found in standard FML, such as Glare, e.g.: $[$Al./TeXteme/Al./TeXteme/Al.$]_T$.

ACKNOWLEDGMENTS: Results of the research carried out within the project UMO-2012/07/B/ST8/04093 funded by the state funds designated by NCN.

REFERENCES

[1] Irisarri F.-X., Lasseigne A., Leroy F.-H., Stacking sequence tables for laminate blending optimization. Proc. 19th International Conference on Composite Materials, Montreal, Canada, 2013.

[2] Irisarri F.-X., Lasseigne A., Leroy F.-H., Le Riche R., Optimal design of laminated composite structures with ply drops using stacking sequence tables, Composite Structures, 107, 2014, pp. 559-569.

[3] Loughlan J., The influence of bend–twist coupling on the shear buckling response of thin laminated composite plates, Thin-Walled Structures, 34, 1999, pp. 97-114.

[4] Loughlan J., The shear buckling behaviour of thin composite plates with particular reference to the effects of bend-twist coupling, International Journal of Mechanical Sciences, 43, 2001, pp. 771-792.

[5] Nemeth M. P., Nondimensional parameters and equations for buckling of symmetrically laminated thin elastic shallow shells, NASA TM-104060, 1992.

[6] Shamsudin M.H., York C.B., Mechanically coupled laminates with balanced plain weave, Composite Structures, 107, 2014, pp. 416-428.

[7] York C.B., Weaver P.M., Balanced and symmetric laminates - New perspectives on an old design rule, Proc. 51st AIAA/ASME/ASCE/AHS/ASC Structures, Structural Dynamics, and Materials Conf., Paper No. AIAA-2010-2775, Orlando, Florida, 2010.

SESION LECTURES

COMPARISON OF FAILURE CRITERIA APPLICATION FOR FML BUCKLING STRENGTH ANALYSIS

D. BANAT, R. J. MANIA
Department of Strength of Materials, Lodz University of Technology
Stefanowskiego 1/15, 90-924 Łódź, Poland

1. FIBRE METAL LAMINATE (FML)

The subject of this study is a thin-walled profile made of Fibre Metal Laminate - material which is a hybrid composite consisting of alternating thin layers of aluminium and fibre-reinforced epoxy. That combination provides many benefits such as higher bearing strength and huge impact resistance comparing pure metallic material. Connection with fibre reinforced material also guarantees better fatigue characteristics as well as high strength and stiffness of the structure. FMLs are also characterized by relatively high corrosion and fire resistance which increase significantly its durability [1]. Furthermore, Fibre Metal Laminate composites can be designed to be strong in a specific direction which gives engineers a lot of possibilities for specific industrial application. Another great advantage of FMLs over conventional material is a low density of the material which results in lower mass of entire structure.

For the purpose of this study, the 3-2 FML profiles of Z-section were designed by appropriate composite layers arrangement. To obtain accurate profile geometry and properties samples were manufactured in the pressure chamber of the autoclave system. Performing curing cycle of that system at a specific heating rate and pressures allowed to obtain high-quality composite structures [5].

2. NUMERICAL MODEL AND STRUCTURAL STABILITY ANALYSIS

Numerical analysis was performed with ANSYS software application, where structural element SHELL181 was applied to create a discrete model of experimentally tested Z-shape profiles. In FEM model 3-2 FML stacking was defined by the Lay-up technique which allowed to specify each layer separately. Simply support boundary conditions were defined by blocking kinematic degrees of freedom of loaded edges [4]. Specific nodes were coupled to guarantee the equal displacement and uniform compression in axial direction.

Numerical analyses of the structure stability were performed in two stages. First, linear eigenvalue buckling technique was used to predict buckling load and corresponding buckling mode shape. Next, a post-buckling behaviour was studied by means of nonlinear buckling analysis which included large deflection response and initial imperfections of chosen magnitude. Furthermore, the structure stability was examined under various laminate configuration and reinforcement directions. For determined buckling load and load carrying capacity cases, the comparative analysis of failure criteria applications was performed. As an example, the table below shows that each considered criterion gives different results for the single FML layer under the same load.

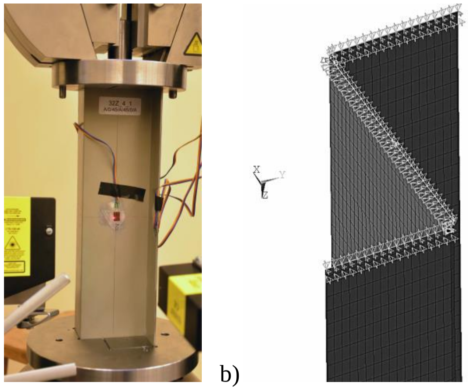

Fig. 1. Experimental test rig (a) and B-C of discrete model (b)

In Table 1 the headings stand for: TWSI - Tsai-Wu strength index; TWSR - inverse of Tsai-Wu strength ratio index; HFIB - Hashin fiber failure criterion; HMAT - Hashin matrix failure criterion; PFIB - Puck fiber failure criterion; PMAT - Puck inter-fiber (matrix) failure criterion - respectively [3].

Table 1. Comparison of failure criteria results for selected FML layer

Type of load	Failure criteria					
	TWSI	TWSR	HFIB	HMAT	PFIB	PMAT
Buckling load	0.400	0.665	0.009	1.242	0.093	0.663
Load carrying capacity	1.005	1.002	0.020	2.193	0.141	0.999

Further detailed analysis allows to assess the stress tensor components participation in the FML failure. Implementing real parameters and strengths of the material obtained in laboratory tests allowed to estimate the potential failure of the structure in a buckling and post-buckling range. Determined FC results also were mapped onto the profile geometry to indicate regions greatly exposed to failure.

Acknowledgments: Research carried out within the project UMO-2012/07/B/ST8/04093.

REFERENCES

[2] Chang P., Yeh P., Yang J., Fatigue crack initiation in hybrid boron/glass/aluminum fiber metal laminates, Materials Science and Engineering, 2008, pp. 273-280.

[3] Hintona M.J., Kaddourb A.S., Soden P.D., A comparison of the predictive capabilities of current failure theories for composite laminates, judged against experimental evidence, Com. Science and Technology, 62, 2002, pp. 1725-1797.

[4] Mania RJ. Comparative static buckling study of FML thin-walled profiles. ECCM16 - 16th European Conference on composite materials. Seville, Spain, 2014.

[5] Vlot A., Gunnink J.W., Fibre Metal Laminates - An Introduction, Kluwer academic publishers, Delft, 2001.

EXPERIMENTAL INVESTIGATIONS OF THIN WALLED, SQUARED CROSS – SECTION COMPOSITE TUBES APPLIED TO STATIC COMPRESSION

P. CZAPSKI, T. KUBIAK
Department of Strength of Materials, Lodz University of Technology
Stefanowskiego 1/15, 90-924 Łódź, Poland

1. ABSTRACT

This paper deals with the experimental investigations of thin-walled, squared cross-section composite tubes subjected to a static compression. The main purpose of this paper is to present and discuss different methods of data analysis while investigating stability of thin-walled structures. Performed experiments were conducted by employing Zwick/Roel universal test stand; non-contact, geometrical - optical principled system Aramis produced by GOM company and strain-gauge technique. Different methods of determining buckling loads were employed, discussed and compared. Moreover all problems, occurring during experiments and data analysis were emphasized in order to show what kind of difficulties could appear during processing the results of measurements. As an example, comparing non-dimensional strain-gauges data with dimensional non-contact system Aramis results of measurements can quoted.

2. SCOPE OF THE RESEARCH

Tests were performed on composite, thin-walled columns with square cross-section with dimensions presented in the Fig. 1. Walls were made of 8th layered GFRP prepreg tape.

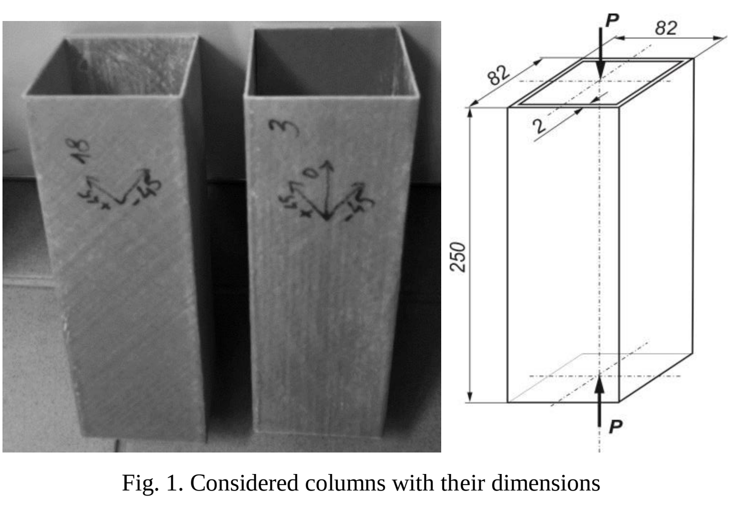

Fig. 1. Considered columns with their dimensions

Following six different layer arrangements of the plies were considered:

- $[45^o/-45^o/45^o/-45^o]_S$
- $[45^o/-45^o/0^o/0^o]_S$
- $[45^o/-45^o/45^o/0^o]_S$
- $[45^o/-45^o/45^o/0^o/0^o/-45^o/45^o/-45^o]_T$
- $[0^o/45^o/-45^o/45^o/-45^o/45^o/-45^o/0^o]_T$
- $[-45^o/45^o/45^o/45^o/-45^o/-45^o/-45^o/45^o]_T$.

Buckling loads were determined on the basis of the two main methods [1], [2]:

- inflection point method,
- P-w^2 method.

Moreover applicability of this two methods and others was discussed. In Fig. 2. is an example of limited applicability of some methods, as well. The paper tries to answer how to deal with such a problem.

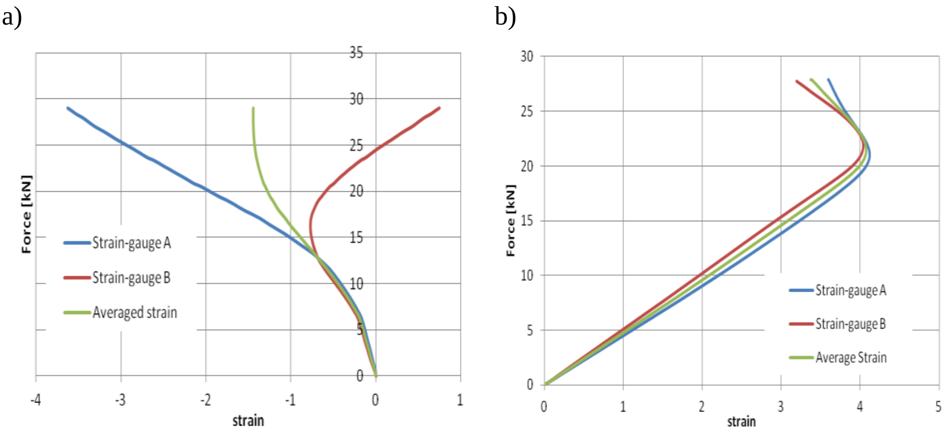

Fig. 2. Exemplary strain - load relationship for possible (a) and impossible (b) application of Averaged Strain Method

ACKNOWLEDGMENT

The investigations has been performed under the research project financed by the National Centre for Science - decision number DEC-2011/03/B/ST8/06447.

REFERENCES

[1] Kolakowski Z., Kowal-Michalska K. (Eds.), Selected problems of instabilities in composite structures, A series of monographs, Technical University of Lodz Press, Lodz, 1999.

[2] Singer J., Arbocz J., Weller T., Buckling experiments. Experimental methods in buckling of thin-walled structure. Basic concepts, columns, beams, and plates, vol. 1. New York: John Wiley & Sons Inc., 1998 (vol. 2, 2002).

DYNAMIC RESPONSE OF PLATE UNDER TEMPERATURE FIELD PULSE

L. CZECHOWSKI
Department of Strength of Materials, Lodz University of Technology
Stefanowskiego 1/15, 90-924 Łódź, Poland

1. INTRODUCTION

FGMs are composed of a mixture - mostly of metal and ceramics, in different proportions across the wall thickness. The material properties can slightly and continuously change from one surface to another one, excluding the stress concentration e.g. FGMs can be used in the ultrahigh temperature field such as nuclear plants, aerospace, thermal ballistic shields or space vehicles etc.

Na and Kim [1] conducted the thermal buckling and postbuckling analyses for FGMs up to an uniform and non-uniform temperature rise on the basis of the finite element method. Authors of paper [2] analysed the buckling phenomenon for static and dynamic loading (pulse of finite duration) of functionally graded plates subjected to uniform temperature increment.

2. PROBLEM DESCRIPTION

The presented studies concern the behavior of functionally graded square plate of the side length of 1 m and thickness of 0.01 m, subjected to the thermal pulse loading. The problem was solved by means of the finite element method. The temperature rise through the plate thickness was assumed to be uniform, linear or sinusoidal. The analysis was developed in the ANSYS 14.5 software. The duration of thermal loading equal to a period or half a period of natural fundamental flexural vibrations of given structures has been taken into consideration. An evaluation of dynamic response of structures was carried out on the basis of Budiansky-Hutchinson criterion [2].

3. COMPUTATION RESULTS

The plates analysed in current paper have continuously varying material properties only in the thickness direction. On the top surface of the plate, pure metal was assumed and it grades up to the bottom surface containing ceramics only.

The overall material properties (for each component, see Table 1) in relation to the layer position (denoted as z) through the plate thickness (denoted as h) can be expressed as:

$$P(z) = P_m \cdot V_m(z) + P_c \cdot V_c(z) = P_c + (P_m - P_c) \cdot \left(1 - \frac{z}{h}\right)^n \tag{1}$$

Figs. 6a and 6b show the plate response maximal deflections under the thermal pulse loading for linear temperature rise and sinusoidal temperature rise, respectively. The diagrams show the plate deflection for the pulse duration equal to one period.

Table 1. Material properties of components

properties	ceramics	metal
Young's modulus [GPa]	393	200
Thermal expansion coefficient [$1/K$]	$13.3 \cdot 10^{-6}$	$8.8 \cdot 10^{-6}$
Poisson's ratio [-]	0.25	0.3
Density [kg/m^3]	2000	7800

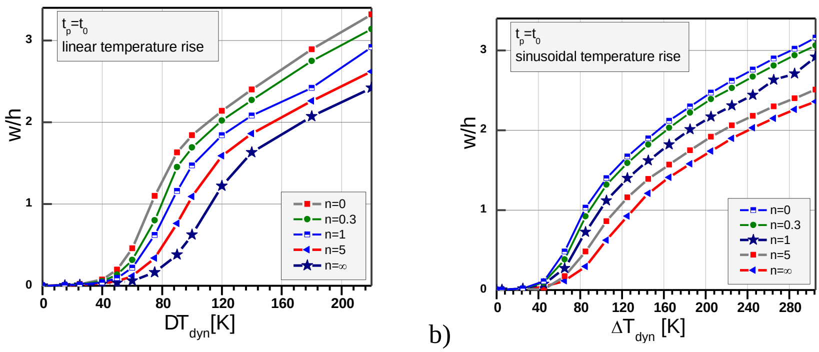

a) b)

Fig. 1. Maximal deflection of the plate vs. dynamic thermal loading for a) linear temperature rise and b) sinusoidal temperature rise

4. SUMMARY

The work dealt with the numerical simulation of functionally graded plate under thermal pulse loading. It was stated that the great influence on the plate response had the distribution index, the duration and the kind of the temperature rise.

ACKNOWLEDGMENTS

The work was carried out within the financial support of the National Science Centre of Poland 2011/B/ST8/07441.

REFERENCES

[1] Na K. S., Kim J. H., Thermal postbuckling investigations of functionally graded plates using 3-D finite element method, Finite Elements in Analysis and Design, 42, 2005, pp. 749-756.

[2] Czechowski L., Kowal-Michalska K., Static and Dynamic Buckling of Rectangular Functionally Graded Plates Subjected to Thermal Loading, Strength of Materials, 6, 2013, pp. 45-55.

MODELOWANIE PROCESU ZNISZCZENIA ŚCISKANYCH SŁUPÓW KOMPOZYTOWYCH Z WYKORZYSTANIEM NAPRĘŻENIOWYCH KRYTERIÓW ZNISZCZENIA

H. DĘBSKI
Department of Machine Design and Mechatronics, Lublin University of Technology
Nadbystrzycka 36, 20-618 Lublin, Poland

T. KUBIAK
Department of Strength of Materials, Lodz University of Technology
Stefanowskiego 1/15, 90-924 Łódź, Poland

1. KRYTERIA ZNISZCZENIA KOMPOZYTÓW

W analizie zniszczenia kompozytów stosuje się wiele kryteriów umożliwiających analizę zniszczenia, co jest uzasadnione dużą różnorodnością właściwości mechanicznych kompozytów [1, 2]. W laminatach materiał pojedynczej warstwy traktowany jest makroskopowo jako materiał jednorodny, natomiast samo kryterium formułowane jest dla k-tej warstwy w lokalnym układzie współrzędnych związanym z głównymi kierunkami ortotropii warstwy. Szeroko stosowane do oceny zniszczenia są kryteria naprężeniowe, bazujące na parametrach granicznych kompozytu, określających naprężenia niszczące przy ściskaniu, rozciąganiu w głównych kierunkach ortotropii warstwy oraz ścinaniu [3].

W pracy wykorzystano naprężeniowe kryteria zniszczenia do opisu zniszczenia ściskanych osiowo cienkościennych słupów kompozytowych o przekroju ceowym, wykonanych z kompozytu węglowo-epoksydowego techniką autoklawową. Konstrukcja słupów wykonana była w symetrycznym układzie ośmiu warstw kompozytu w konfiguracji $[0/-45/45/90]_s$. Zakres badań obejmował numeryczne obliczenia nieliniowej stateczności konstrukcji z wykorzystaniem metody elementów skończonych w programach ANSYS® oraz ABAQUS®.

2. ANALIZA NUMERYCZNA – DYSKUSJA WYNIKÓW

Realizację obciążenia modeli numerycznych kontynuowano do poziomu osiągnięcia parametru krytycznego określonego dla każdego zastosowanego kryterium. Na podstawie stanu naprężeń wyznaczono wartość obciążenia inicjującego zniszczenie pierwszej warstwy laminatu $P_{f(ini)\text{-}MES}$ oraz wartość obciążenia niszczącego $P_{f\,\text{–}MES}$. Założono, że zniszczenie następuje poprzez spełnienie kryterium zniszczenia we wszystkich warstwach kompozytu, zakładając, że do momentu wyczerpania nośności ostatniej warstwy, wszystkie warstwy pracują.

Przykładowe mapy parametru krytycznego dla wartości obciążenia odpowiadającego zniszczeniu pierwszej warstwy $P_{f(ini)\text{-}MES}$ przedstawiono na Rys. 1.

Wartości obciążeń inicjujących zniszczenie i obciążeń niszczących dla przyjętych kryteriów oraz wyniki badań eksperymentalnych zestawiono w Tabeli 1.

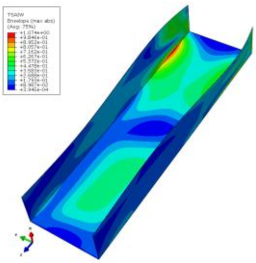

a)

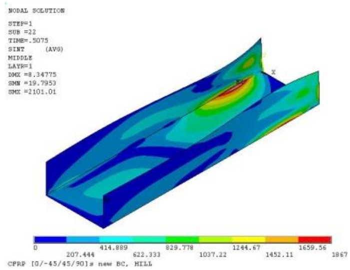

b)

Rys. 1. Mapy parametru krytycznego: a) Tsai-Wu (ABAQUS®), b) Hill (ANSYS®)

Tablica 1. Zestawienie sił [N] inicjujących zniszczenie i sił niszczących

<table>
<tr><th>kryterium</th><th>MES
$P_{f(ini)\text{-}MES}$</th><th>Eksperyment
$P_{f(ini)\text{-}EKSP}$</th><th>MES
$P_{f\ \text{-}MES}$</th><th>Eksperyment
$P_{f\ \text{-}EKSP}$</th></tr>
<tr><td>Max. naprężeń</td><td>5469</td><td rowspan="8">5064
5466</td><td>8329</td><td rowspan="8">9010
7073</td></tr>
<tr><td>Tsai-Hilla</td><td>5490</td><td>9002</td></tr>
<tr><td>Tsai-Wu</td><td>5500</td><td>8750</td></tr>
<tr><td>Azzi-Tsai-Hilla</td><td>5484</td><td>9019</td></tr>
<tr><td>Wilczyńskiego</td><td>4987</td><td>6905</td></tr>
<tr><td>Hoffmana</td><td>4953</td><td>6866</td></tr>
<tr><td>Pucka, Cui</td><td>4948</td><td>6864</td></tr>
<tr><td>Hilla</td><td>4927</td><td>6661</td></tr>
</table>

Poddając analizie otrzymane wyniki stwierdzono maksymalne różnice obciążenia inicjującego zniszczenie pierwszej warstwy kompozytu dla wszystkich zastosowanych kryteriów zniszczenia na poziomie 10.4% w przypadku obliczeń numerycznych oraz 9.8% pomiędzy wynikami obliczeń i eksperymentu. Maksymalna rozbieżność wyników w przypadku obciążenia niszczącego kształtuje się na poziomie 26% w obydwu przypadkach, tj. pomiędzy poszczególnymi kryteriami zniszczenia w obliczeniach MES oraz w stosunku do wyników badan doświadczalnych. Potwierdza to zbieżność zastosowanych naprężeniowych kryteriów zniszczenia w stopniu akceptowalnym dla zastosowań w analizie stateczności oraz stanów granicznych badanych konstrukcji cienkościennych.

PODZIĘKOWANIA: Badania realizowane w ramach Projektu Nr N N507 241440 finansowanego przez Narodowe Centrum Nauki.

LITERATURA

[1] Muc A., Mechanika kompozytów włóknistych, Księgarnia Akademicka, Kraków,2003.
[2] Kowal-Michalska K. (red.), Stateczność dynamiczna kompozytowych konstrukcji płytowych, WNT, Łódź-Warszawa, 2007.
[3] Reddy Y.S.N., Pandey A.K., A first-ply failure analysis of composite laminates, Comput. Struct., 25, 3, 1987, pp. 371-93.

STANY GRANICZNE KOMPOZYTOWYCH SŁUPÓW O PRZEKROJU OMEGOWYM

H. DĘBSKI
Katedra Podstaw Konstrukcji Maszyn i Mechatroniki, Politechnika Lubelska
ul. Nadbystrzycka 36, 20-618 Lublin

S. SAMBORSKI, A.TETER
Katedra Mechaniki Stosowanej, Politechnika Lubelska
ul. Nadbystrzycka 36, 20-618 Lublin

1. ZNISZCZENIE SŁUPÓW KOMPOZYTOWYCH

Dotychczasowe badania wykazują, że konstrukcje cienkościenne po utracie stateczności lokalnej są w stanie przenosić obciążenie [1]. Istotna staje się znajomość zachowania konstrukcji w pełnym zakresie obciążenia. Proces degradacji struktury wskutek narastania obciążenia wciąż jest niedostatecznie przebadany. Szczególnie ważne jest określenie warunków granicznych oraz określenie obciążeń niszczących. Znane z literatury kryteria zniszczenia laminatów [2] stanowią jedynie wstępne oszacowanie obciążeń, które inicjują proces zniszczenia struktury kompozytu. Brakuje pogłębionej eksperymentalnej weryfikacji stosowanych kryteriów zniszczenia rzeczywistej struktury.

W prezentowanej pracy wykorzystano naprężeniowe kryteria zniszczenia do opisu stanów granicznych ściskanych osiowo cienkościennych słupów kompozytowych o przekroju typu omega (*hat*). Badane słupy zostały wykonane z ośmiowarstwowego kompozytu węglowo-epoksydowego o symetrycznym układzie warstw względem płaszczyzny środkowej laminatu, w konfiguracji $[0/\text{-}45/45/90]_s$. Przeprowadzono symulacje numeryczne metodą elementów skończonych. W obliczeniach zastosowano komercyjny pakiet ABAQUS®. Wyniki symulacji numerycznych zweryfikowano eksperymentalnie.

2. WYNIKI BADAŃ I WNIOSKI

Analizę stanów pokrytycznych i granicznych ściskanych słupów cienkościennych prowadzono w ujęciu nieliniowym zakładając duże przemieszczenia (zagadnienie geometrycznie nieliniowe) [3]. Dodatkowo przyjęto liniowy model materiału. Do oceny nośności konstrukcji zastosowano kryterium Tsai-Wu. We wstępnych badaniach eksperymentalnych wyznaczono wartości graniczne stosowanego materiału kompozytowego. Jako moment inicjacji zniszczenia kompozytu przyjmowano wartość obciążenia $P_{f(ini)\text{-}MES}$ odpowiadającego spełnieniu parametru zniszczenia w pierwszej warstwie kompozytu. Natomiast wartość obciążenia granicznego $P_{f\text{-}MES}$ określano jako obciążenie odpowiadające spełnieniu kryterium zniszczenia Tsai-Wu we wszystkich warstwach układu. Wyznaczone numerycznie wartości obciążenia granicznego porównano z wartościami tych obciążeń określonych doświadczalnie. Deformację konstrukcji odpowiadającą momentowi utraty nośności słupa przedstawiono na Rys. 1.

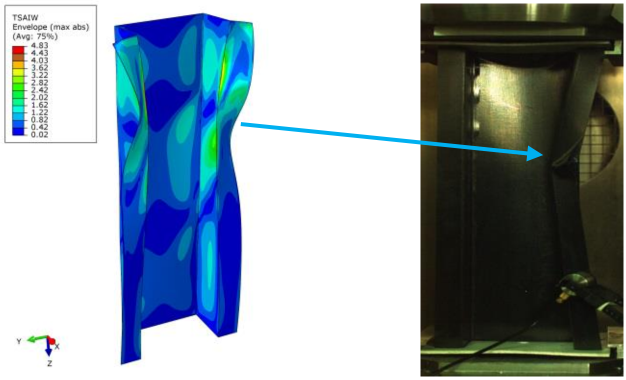

Rys. 1. Utrata nośności słupa: a) wynik symulacji numerycznej, b) badania doświadczalne

Tabela 1. Zestawienie sił inicjujących zniszczenie i sił niszczących

MES $P_{f(ini)\text{-}MES}$ [N]	MES $P_{f\,-MES}$ [N]	Eksperyment $P_{f\,-EKSP}$ [N]
16 500	19 910	Pr1: 19 506 Pr2: 20 307 Pr3: 21 813

Prezentowane wyniki wykazały dużą zgodność wyznaczonych numerycznie oraz doświadczalnie wartości obciążenia niszczącego. Maksymalne rozbieżności dla próbki nr Pr3 nie przekroczyły 9%. W badaniach eksperymentalnych nie potwierdzono wyznaczonych numerycznie obciążeń inicjujących zniszczenie pierwszej warstwy, a inicjacja zniszczenia następowała tuż przed całkowitą utratą nośności słupa. Zachowanie rzeczywistej konstrukcji cienkościennej zdeterminowane jest przez wiele czynników pomijanych w symulacjach numerycznych wynikających np. z losowych ugięć wstępnych, niedokładności obciążenia oraz warunków brzegowych. Dalsze badania numeryczne oraz eksperymentalne są konieczne do pełnego opisu procesu degradacji struktury oraz samego procesu zniszczenia.

Praca została dofinansowana ze środków Narodowego Centrum Nauki przyznanych na podstawie decyzji numer DEC-2013/11/B/ST8/04358.

REFERENCES

[1] Bloom F., Coffin D.: Handbook of thin plate buckling and postbuckling, Chapman & Hall/CRC Boca Raton, London, New York, Washington, D.C., 2001.

[2] Reddy YSN, Pandey AK., A first-ply failure analysis of composite laminates, Com. Struct. 25(3), 1987, pp. 371-93.

[3] Cichoń C., Nieliniowa analiza stateczności konstrukcji prętowych w ujęciu MES, Wydaw. Politechniki Krakowskiej, Monografia, 38, Kraków, 1985.

ANALIZA NUMERYCZNA STANÓW POKRYTYCZNYCH ŚCISKANEJ PŁYTY Z WYCIĘCIEM

K. FALKOWICZ, M. FERDYNUS, H. DĘBSKI
Department of Machine Design and Mechatronics, Lublin University of Technology
Nadbystrzycka 36, 20-618 Lublin, Poland

1. PRZEDMIOT I ZAKRES BADAŃ

Przedmiot badań stanowiły dwie grupy prostokątnych płyt o wymiarach gabarytowych A×B = 250×150 mm i grubości g = 1 mm, wykonane ze stali sprężynowej 50HS oraz kompozytu węglowo-epoksydowego. Analizowane płyty posiadały symetryczne, usytuowane centralnie wycięcie, o kształcie prostokąta i klepsydry (Rys. 1 i 2), którego wymiary obrysowe a i b stanowiły parametry geometryczne o kluczowym znaczeniu, jeśli chodzi o charakterystykę podkrytyczną płyty. Parametry geometryczne wycięcia zmieniały się w zakresie: a = 80÷200 mm oraz b = 20÷50 mm.

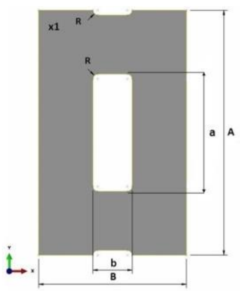

Rys. 1. Wymiary geometryczne płyty z prostokątnym wycięciem

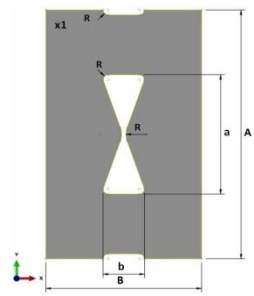

Rys. 2. Wymiary geometryczne płyty z wycięciem w kształcie klepsydry

Płyta została podparta przegubowo i obciążona siłą ściskającą równomiernie rozłożoną na górnej krawędzi płyty. Aby zwiększyć nośność płyt zdecydowano się na wymuszenie utraty stateczności według wyższej, giętno-skrętnej postaci wyboczenia. Pożądane zachowanie się konstrukcji bylo realizowane w uchwycie, w którym zamocowano płytę. Zakres badań obejmował analizę numeryczną MES (program ABAQUS) zagadnienia nieliniowej stateczności, w której obliczenia prowadzone były na modelach z zainicjowaną imperfekcją geometryczną odpowiadającą giętno- skrętnej postaci wyboczenia konstrukcji.

W badanym ustroju wyraźnie konstrukcyjnie wydzielone są pasy pionowe, gdzie element cienkościenny jest ściskany i zginany oraz pasy poziome, gdzie występuje głównie skręcanie. W zależności od tego, jaki obszar zajmują poszczególne strefy, element płytowy uzyskuje odmienną charakterystykę. Ta właściwość może być bardzo istotna w aspekcie ewentualnych zastosowań, gdyż łatwo można uzyskać elementy o identycznych wymiarach do zabudowy, a o krańcowo różnej charakterystyce.

Zagadnienia stateczności, zachowań pokrytycznych oraz nośności granicznej ustrojów płytowych z otworami zostały opisane m.in. w pracach [1÷4].

2. WYNIKI ANALIZY NUMERYCZNEJ

Otrzymane wyniki obliczeń pozwalają na dokonanie jakościowej i ilościowej oceny pracy konstrukcji w zakresie pokrytycznym. Formy deformacji pokrytycznej płyty dla wszystkich badanych przypadków stanowiły pogłębienie deformacji zaimplementowanej postaci wyboczenia. Uzyskane ścieżki równowagi prezentowane są do pojawienia się uplastycznienia w narożu wycięcia. Zmniejszenie działania karbu w narożu wycięcia powinno zwiększyć zakres pracy konstrukcji. Przykładowe charakterystyki ukazujące pokrytyczne ścieżki równowagi przedstawiono na Rys. 3. Dotyczą one wybranej grupy płyt o szerokości wycięcia b = 20 mm wykonanych z materiału izotropowego.

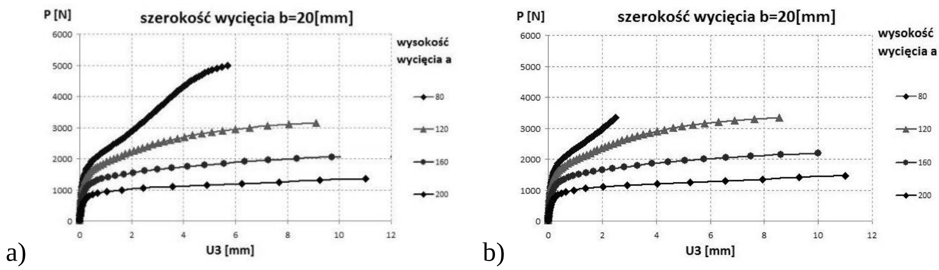

Rys. 3. Pokrytyczne ścieżki równowagi w zależności od wysokości wycięcia
a) wycięcie prostokątne; b) wycięcie w kształcie klepsydry

Przebieg zależności pomiędzy obciążeniem a ugięciem bocznym płyty, wskazuje na silną zależność zakresu tych charakterystyk od parametrów geometrycznych wycięcia. Jak się okazuje kształt wycięcia nie jest tak istotny, jak jego wymiary obwiedniowe. Zaprezentowane krzywe wskazują, że przy tych samych wymiarach gabarytowych płyty można uzyskać zdecydowanie odmienne charakterystyki pracy konstrukcji, kształtowane wymiarami wycięcia. Otrzymane wyniki potwierdzają decydujący wpływ wysokości wycięcia a na charakterystykę pokrytyczną badanych płyt. Powyższe wnioski mają istotne znaczenie praktyczne w aspekcie obliczania tego typu ustrojów do zastosowań jako elementy sprężyste.

LITERATURA

[1] Narayanan R., Chow F.Y., Ultimate capacity of uniaxially compressed perforated plates, Thin-Walled Structures, 2, 2, 1984, pp. 241-264.

[2] Prabhakara D.L., Datta P.K., Vibration, buckling and parametric instability behaviour of plates with centrally located cutouts subjected to in-plane edge loading (Tension or Compression), Thin-Walled Structures, 27, 4, 1997, pp. 287-310.

[3] Ritchie D., Rhodes J., Buckling and post-buckling behaviour of plates with holes, The Aeronautical Quarterly, 26, 4, 1975, pp. 281-296.

[4] Shanmugam N.E., Openings in Thin-walled Steel Structures, Thin-Walled Structures, 28, 3/4, 1997, pp. 355-372.

DYNAMIC AXIAL CRUSHING OF FLAWED THIN-WALLED SQUARE SECTION TUBES

M. FERDYNUS
Department of Machine Construction & Mechatronics, Lublin University of Technology
Nadbystrzycka 36, 20-618 Lublin, Poland

M. KOTEŁKO
Department of Strength of Materials, Łódź University of Technology
Stefanowskiego 1/15, 90-924 Łódź, Poland

1. INTRODUCTION

In the case of thin-walled members subjected to axial compression, which act as energy absorbers, a substantial issue is such a design, which promotes a progressive buckling mechanism, stimulating the highest energy absorption capacity. One of the possible design solutions is the application of a trigger (notch or dent), which releases the most desirable crushing mechanism. There are numerous published results of research concerning energy absorption of thin-walled tubes [1, 2], however, very few deal with tubular structures with dents or other flaws. In [3] the authors studied the behavior of tubular columns with dents, but these flaws were treated as imperfections coming from damage. The static analysis of axially compressed square section tube with dents in the corners is presented in [4].

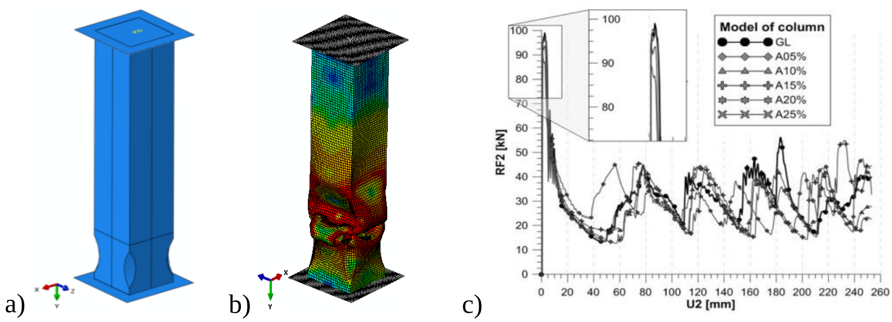

Fig. 1. Subject of analysis: a) - theoretical model (A15%), b) - numerical model - failure pattern, c) - comparative load-shortening diagram

2. SUBJECT OF RESEARCH

The subject of investigation was a thin-walled square section aluminum tube with four indentations in the corners. The tubes of dimensions 70x2 and height l = 335 mm, were made of aluminum alloy EN AW6060-T6 (R_e = 175 MPa, R_m = 250 MPa, ν = 0.33). This material exhibits linear hardening during plastic flow (E = 70GPa, E_t = 937,5MPa). The process of modeling of the column with dents was realized with the Catia v5 software package in the Generative Shape Design module. The dent's geometry was characterized by the main radius R = 50 mm. The depth of the dent was 2.5; 5; 7.5: 10, 12.5 mm, what is 5; 10; 15; 20; 25 % of its diagonal of cross- section. Dents were made at the bottom of the column (Fig. 1a). The models were designated by the symbols from A05% to A25%, where the number stands for the relative depth of the dent. The column with smooth walls was designated as GL.

3. NUMERICAL ANALYSIS - PARAMETRIC STUDY

A parametric study into an optimal dents situation and geometry with respect to the energy absorption capacity of tubes was performed on the basis of FE simulations. FE explicit analysis was carried out using ABAQUS 6.13 code. An impact of energy E = 10 kJ was assumed. A bi-linear material model was applied. As the preliminary results of the parametric study have showed that the best energy absorption indicators for examined columns, namely EA - energy absorption, MCF - mean crushing force, CLE - mean to ultimate crushing force ratio were obtained for columns A20%, the further analysis was performed for these columns, with different distance of a dent from the bottom end, 5,10,15 and 20 [mm]. The columns were indicated as B20_05 to B20_20, respectively. Energy absorption indicators for those columns are shown in Table 1.

Table 1. Energy absorption indicators for columns type B

	Model of column			
Parameter	GL	B20_05	B20_15	B20_20
EA [J]	6748.91	6327.37	6271.96	8274.59
MCF [kJ/mm]	31.27	29.30	29.04	38.34
CLE [%]	31.58	33.09	32.21	42.34

As shown in the Table 1 the energy indicators increase rapidly for column B20. The research presented in the paper is a part of a wider project. Further investigation will be continued into an experimental validation of theoretical results and more detailed parametric study into an optimal situation and dimensions of dents. Also an optimization using a technique of metamodels is planned.

REFERENCES

[1] Hamouda AMS, Saied RO, Shuaeib FM, Energy absorption of square tubular structures, J. of Achievements in Materials and Manufacturing Engineering, 24, 2007, pp. 36-42.

[2] Langseth M, Hopperstad OS, Hanssen AG, Crash behaviour of thin-walled aluminium members, Thin Walled Structures, 32, 1998, pp. 127-150.

[3] Lancaster ER, Palmer SC, Model testing of mechanically damaged pipes containing dents and gouges.,ASME Pressure Vessels & Piping Conference, New York, 235, 1992, pp. 143-148.

[4] Ferdynus M., An energy absorber in the form of a thin-walled column with square cross-section and dimples, Eksploatacja i Niezawodnosc/Maintenance and Reliability, 15, 3, 2013, pp. 253-258.

STATECZNOŚĆ ZDELAMINOWANYCH CIENKOŚCIENNYCH KOMPOZYTOWYCH KOLUMN PODDANYCH ŚCISKANIU

A. GLISZCZYŃSKI, T. KUBIAK, J. ŚLIWIŃSKI
Katedra Wytrzymałości Materiałów i Konstrukcji, Politechnika Łódzka
Stefanowskiego 1/15, 90-924 Łódź, Polska

1. WPROWADZENIE

Elementem badań konstrukcji kompozytowych jest analiza zjawisk towarzyszących powstawaniu delaminacji. Źródeł ich powstawania należy poszukiwać już na etapie wytwórczym, kiedy delaminacja może pojawić się na skutek błędnie dobranych parametrów procesu autoklawowego. Inicjację delaminacji zapoczątkować również może uderzenie z niską prędkością [1], wpływające na lokalną degradację sztywności materiału. Uszkodzenia w postaci mikropęknięć bądź delaminacji najczęściej modelowane są jako podobszary (w kształcie okręgu bądź elipsy) posiadające odmienne własności materiałowe lub w postaci rozwarstwień nieciągłości pomiędzy warstwami [1-2]. W pracy rozpatrzono krótki, ośmiowarstwowy ceownik kompozytowy poddany ściskaniu, w którym obszar delaminacji został zamodelowany w postaci rozwarstwienia na granicy sąsiadujących warstw. Rozważano następujące quasi-izotropowe schematy ułożenia włókien: $[0/90/0/90]_S$ oraz $[45/-45/45/-45]_S$. W pracy nie uwzględniano lokalnej degradacji sztywności i całemu obszarowi analizy przyporządkowano tożsamy model materiałowy. Liniowe oraz nieliniowe analizy stateczności analizowanych struktur zostały przeprowadzone metodą elementów skończonych w środowisku programu ANSYS®.

Tabela 1. Własności mechaniczne

E_1 [GPa]	E_2 [GPa]	G_{12} [GPa]	v_{12} [GPa]	T_1 [GPa]	T_1 [GPa]	S_{12} [GPa]	C_1 [GPa]	C_2 [GPa]
38.5	8.1	2.0	0.27	792	39	108	679	71

2. MODEL MATERIAŁOWY

Własności mechaniczne analizowanego typu kompozytu zostały wyznaczone w badaniach eksperymentalnych. Testy wytrzymałościowe obejmowały rozciąganie i ściskanie próbek z wzdłużnym oraz poprzecznym ułożeniem włókien oraz próbę ścinania. Próba ścinania została przeprowadzona na podstawie normy ASTM D 3518, jako próba rozciągania quasi-izotropowej próbki kompozytowej o ułożeniu warstw pod kątem $\pm 45^0$. W przeprowadzonych próbach wytrzymałościowych wyznaczono niezbędne własności materiałowe, które przedstawnionio w Tabeli 1.

3. MODEL NUMERYCZNY

Analizowana kolumna została poddana ściskaniu, odpowiadającemu równomiernemu skróceniu słupa. W węzłach, stanowiących podparcie słupa zamodelowano przegubowe podparcie, odbierając przemieszczenie w kierunku wzdłużnym i poprzecznym. Węzłom obciążanym przyporządkowano stałą wartość przemieszczeń wzdłuż osi słupa uy=const. oraz odebrano możliwość przemieszczeń w kierunkach prostopadłych do kierunku działającego obciążenia. Ze względu na stałą wartość przemieszczeń przekroju obciążanego, siła ściskająca została zaimplementowana do modelu numerycznego w postaci siły skupionej F.

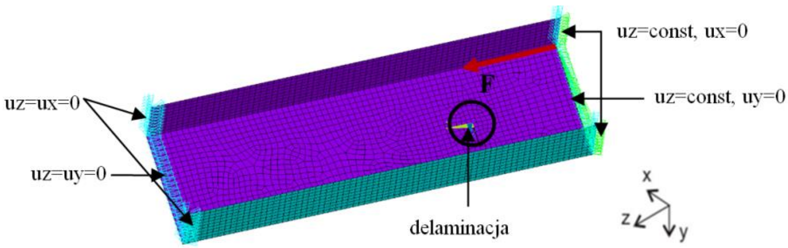

Rys. 1. Model dyskretny z przyjętymi warunkami brzegowymi

Obszar analizy został zdyskretyzowany czterowęzłowym, wielowarstwowym elementem powłokowym o sześciu stopniach swobody w każdym węźle (SHELL181).

4. ANALIZA WYNIKÓW

Z przeprowadzonych analiz wynika, że główny wpływ na wartość siły krytycznej wyznaczanej w liniowej analizie stateczności ma wielkość delaminacji oraz miejsce jej występowania w schemacie międzywarstwowym. Najniższe wartości krytyczne osiągają ustroje, w których delaminacja znajduje się w najbliższym sąsiedztwie warstw zewnętrznych a najwyższe wartości sił krytycznych towarzyszą przypadkom kiedy delaminacja jest zlokalizowana w najbliższej odległości względem płaszczyzny środkowej. W świetle przeprowadzonych obliczeń na pierwszą wartość własną nie ma natomiast wyraźnego wpływu geometryczna lokalizacja strefy zdelaminowanej względem długości i szerokości analizowanej kolumny, a także faktu czy delaminacja występuje na środniku czy też jednej z półek rozpatrywanego słupa. Liniowe analizy stateczności stanowią jedynie wstęp do analizy stateczności i pokrytycznego zachowania analizowanych kolumn, które zostały przeprowadzone celem wyznaczenia postaci własnych oraz wartości krytycznych. Analizy stateczności stanowić będą dalszą część badań, których rezultaty zostaną przedstawione podczas sympozjum.

LITERATURA

[1] Aymerich F., Priolo P., Characterization of fracture modes in stitched and unstitched cross-ply laminates subjected to low-velocity impact and compression after impact loading. International Journal of Impact Engineering, 2008.

[2] Jeon B.S., Lee J.J., Kim J.K., Low velocity impact and delamination buckling behavior of composite laminates with embedded optical fibers. Smart Material Structures, 1999.

Praca została napisana w ramach realizacji projektu badawczego finansowanego przez Narodowe Centrum Nauki Nr DEC-2011/03/B/ST8/06447.

STRENGHT AND BUCKLING OF THE SHELL OF REVOLUTION WITH THE BOOTH LEMNISCATE MERIDIAN

M. GRYGOROWICZ, P. JASION, P. PACZOS, K. MAGNUCKI
Institute of Applied Mechanics, Poznan University of Technology
ul. Jana Pawła II 24, 60-965 Poznań, Poland

1. INTRODUCTION

The shells of revolution are basic elements of thin-walled structures, such as pressure vessels, tanks, space crafts or submersibles. There are a lot of publications describing that kind of structures. Strength and stability of shells of revolution are dscribed in details, *e.g*. [1, 2, 3, 4, 5]. The presented paper is devoted to the Booth's ovaloidal shell. The meridian of this shell is in the elliptic Booth lemniscate shape.

The Booth oval as a plane curve in Cartesian coordinates is defined as follows

$$y = \pm \frac{1}{\sqrt{2}}\left[-\left(2x^2 - b^2\right) + \sqrt{4\left(a^2 - b^2\right)x^2 + b^2}\right]^{\frac{1}{2}}, \tag{1}$$

where a and b are the parameters of the above function.

The shape of the middle surface of the barrelled shell is shown in Fig. 1.

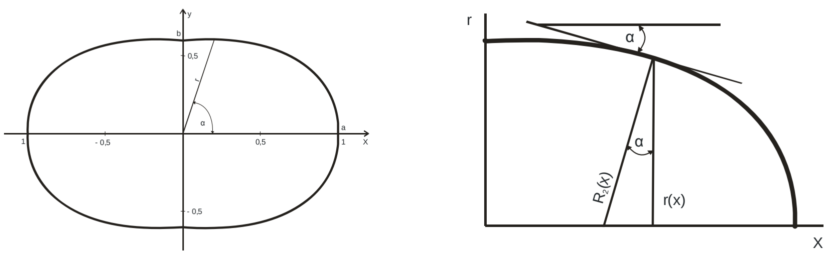

Fig. 1. The elliptic Booth lemniscate for a = 1.0 and b = 0.6

The capacity of the shell is

$$V_0 = 2\pi \int_0^a \left[r\left(x\right)\right]^2 dx \ , \tag{2}$$

The mass of the shell

$$m_s = A_s t_s \rho_s \ , \tag{3}$$

where: $A_s = 4\pi \int_0^a r \sqrt{1 + \left(\frac{dr}{dx}\right)^2} dx$ - lateral area, t_s - thickness of the shell, ρ_s - mass density.

The principal radii of the surface

$$R_1(x)=\frac{R_2^3(x)}{r^2(x)\left[1-\frac{x^2}{r^2(x)}\left(\frac{a^2-b^2}{\sqrt{f_0(x)}}-1\right)\right]\left(\frac{a^2-b^2}{\sqrt{f_0(x)}}-1\right)-\frac{4\left(a^2-b^2\right)^2x^2}{\left[4\left(a^2-b^2\right)x^2+b^4\right]^{\frac{3}{2}}}}\,, \qquad (4)$$

$$R_2(x)=\left\{r^2(x)+x^2\,\frac{\left[a^2-b^2-\sqrt{4\left(a^2-b^2\right)x^2+b^4}\,\right]^2}{4\left(a^2-b^2\right)x^2+b^4}\right\}^{\frac{1}{2}}. \qquad (5)$$

2. THEORETICAL STUDY OF STRENGTH AND BUCKLING OF THE SHELL

The membrane forces of the Booth's ovaloidal shell under uniform pressure p_0

$$N_1(x)=\frac{1}{2}R_2(x)p_0\,, \qquad N_2(x)=\left[1-\frac{R_2(x)}{2R_1(x)}\right]R_2(x)p_0\,. \qquad (7)$$

The pre-buckling and buckling states of this shell are numerically analysed with FEM application and calculated with the use of the ANSYS system.

ACKNOWLEDGMENTS

The research was conducted within the framework of Statutory Activities in 2015.

REFERENCES

[1] Błachut J., Magnucki K., Strength, stability and optimisation of pressure vessels - review of selected problems, Applied Mechanics Reviews, 61(6), November 2008, Article Number 060801.

[2] Bushnell D., Computerized buckling analysis of shells, Kluwer Academic Publishers, Dordrecht, Boston, London, 1989.

[3] Jasion P. Buckling and post-buckling analysis of shells of revolution with positive and negative Gaussian curvature. Publ. House of Poznan University of Technology, Poznan, 2015.

[4] Jasion P., Magnucki K., Elastic buckling of clothoidal-spherical shells under external pressure - theoretical study, Thin-Walled Structures, 86, 2015, pp. 18-23.

[5] Thompson J.M.T., Hunt G.W., A general theory of elastic stability, John Wiley & Sons, London, New York, Sydney, Toronto, 1973.

POSTBUCKLING OF IMPERFECT PLATE LOADED IN COMPRESSION

J. HAVRAN, M. PSOTNÝ
Department of Structural Mechanics, Slovak University of Technology
Radlinského 11, 810 05 Bratislava, Slovakia

1. INTRODUCTION

The stability analysis of thin plate loaded in compression is presented. The non-linear FEM equations are derived from the variational principle of minimum of potential energy. To obtain the non-linear equilibrium paths, the Newton-Raphson iteration algorithm is used. The peculiarities of the effects of the initial imperfections are investigated using user program. Special attention is paid to the influence of imperfections on the post-critical buckling mode.

2. THEORY

From the condition of the minimum of the increment of the total potential energy $\delta \Delta U = 0$ can be obtained the system of conditional equations in the form:

$$\mathbf{K}_{inc} \, \Delta \boldsymbol{\alpha} + \mathbf{F}_{int} - \mathbf{F}_{ext} - \Delta \mathbf{F}_{ext} = \mathbf{0} \, , \tag{1}$$

where $\mathbf{K}_{inc}$ is the incremental stiffness matrix of the plate, $\mathbf{F}_{int}$ is the internal force (plate), $\mathbf{F}_{ext}$ - the external load (plate), $\Delta\mathbf{F}_{ext}$ - the increment of the external load (plate). Isotropic elastic material is considered. Initial geometric imperfection is chosen in the form:

$$w_0 = \alpha_{01} \sin \frac{\pi x}{a} \sin \frac{\pi y}{b} + \alpha_{02} \sin \frac{2 \pi x}{a} \sin \frac{\pi y}{b} \, . \tag{2}$$

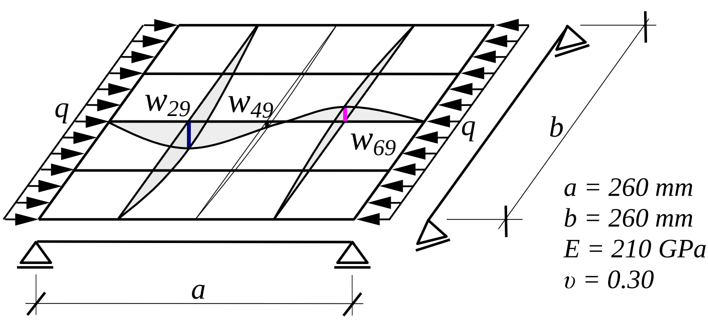

Fig. 1. Notation of the quantities of the plate loaded in compression

3. FEM NONLINEAR ANALYSIS

The FEM computer program using a 48 DOF element has been used for analysis. FEM model consists of 4x4 finite elements. Full Newton-Raphson procedure has been applied. Illustrative examples of steel plate loaded in compression from Fig. 1 are presented as load-displacement paths in Fig. 2 and Fig.3.

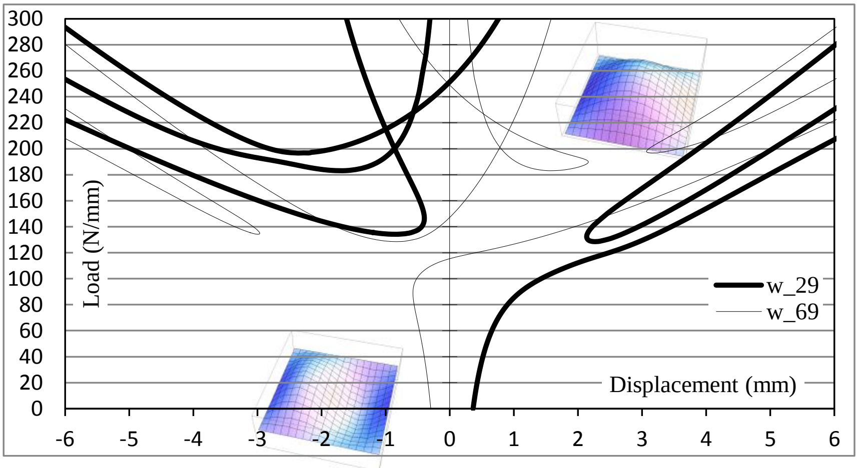

Fig. 2. Plate with initial imperfection (α_{01}=0.05 and α_{02}=0.33)

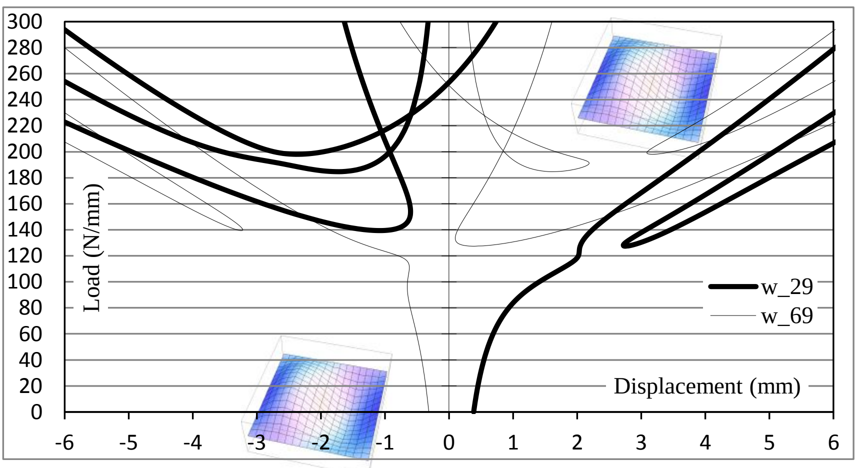

Fig. 3. Plate with initial imperfection (α_{01}=0.05 and α_{02}=0.35)

From Figs. 2 and 3 it is obvious that two almost identical modes of initial imperfection at the beginning of the loading process offer two different solutions in postbuckling range. More details in the full text.

SOME ASPECTS OF AIR-CENTRE STRUCTURE OF AUTOMOTIVE HEAT EXCHANGERS IN VIEW OF ITS POST-BUCKLING BEHAVIOUR

S. KEDZIORA
Faculty of Science, Technology and Communication University of Luxembourg
Campus Kirchberg, 6 rue Coudenhove-Kalergi
L-1359 Luxembourg, Luxembourg

1. INTRODUCTION

Air-centres are the key components of automotive heat exchangers [1] taking into account heat transfer requirements and air pressure drop. In other words, their main goal is to provide a sufficient surface needed to transfer heat with minimum pressure drop of an airside. The air-centres are thin-walled structures made of wrought aluminium alloy with a ratio between a minimum dimension and a thickness at least of 85. In addition, they create a necessary structural support for heat exchanger tubes and thanks to them a heat exchanger cores have a required structural resistance. The Figure 1 shows main components of the typical automotive heat exchanger (heater core).

The current heat exchanger structural designs were developed based on ground of many years' developments having regard to field failures and complex manufacturing processes. Unfortunately, there are still design issues, which need to be clarified and one of them is the structural design requirements of the air centres.

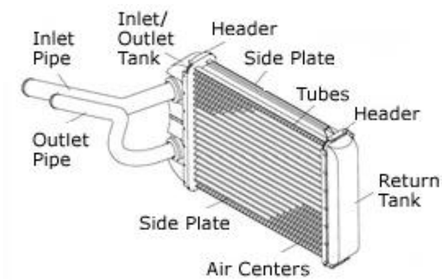

Fig. 1. Main components of automotive heat exchanger (heater core) - nomenclature
Source: http://www.delphi.com/manufacturers/auto/heatcool/intheatcool/cores

The goal of this paper is to show importance of the post-buckling resistance of the air-centres on the overall structural integrity of the heat-exchanger core. The work is focused on the post-buckling behaviour of the air-centres taking into consideration different material properties in an elasto-plastic range and the different thickness. Both parameters have influence on stress level in the heat-exchangers tubes. The varying stresses in the tubes are main roots of field failure of the heat exchangers. The buckled shapes of the air centres cause the reduction of the tube stiffness supports. Thus, they causes high tube stresses, which in turn reduce significantly field lifetime of the heat exchangers. The problem is very much practical due to continuous trend on nowadays-automotive market to decrease the thickness of components of heat exchangers in order to cut cost of final products.

Unfortunately, there is not a clear limit of the thickness reduction considering the strength (pressure resistance) of the core. In addition, the strength material requirements are not visibly defined in terms of the overall pressure core resistance. This work is going to bring some estimation of the thickness and the material strength requirements of the air centres taking into consideration the complex buckling problem.

The current nominal thickness of the air-centres is about 0.075 mm with a trend to reduce. The material is typically wrought aluminium alloy 3003-H14 with the trend to change to higher strength materials.

2. ANALYSIS METHOD AND RESULTS

The problem is theoretically solved using the finite element method [2, 3]. A typical design of air centre was selected from heater cores or radiators.

The analysis depends on the nonlinear buckling calculations of the air-centres with initial random complex imperfections since they are never perfect in shape. The calculations are made using the commercial software ANSYS 15/16 of the finite element method [4]. The maximum von Mises stress in the tube was taken as an output parameter, which makes feasible a comparison and an assessment of the dissimilar air-centre designs.

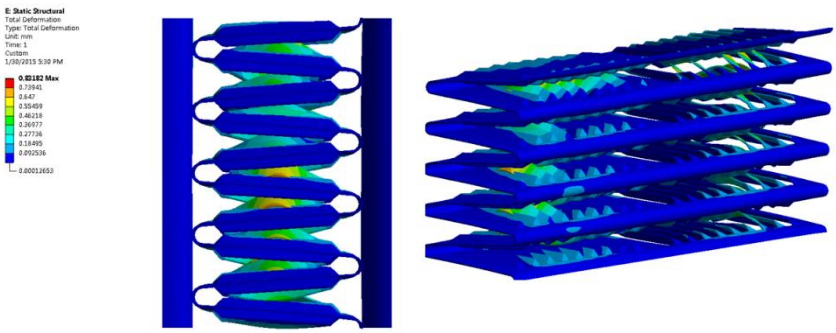

Fig. 2 Post buckling shape of analysed air-centres

REFERENCES

[1] Hesselgreaves J. E., Compact heat exchangers: selection, design and operation, Pergamon, London, 2001.

[2] Kędziora S., Nośność graniczna ortotropowych cienkościennych belek-słupów o przekrojach otwartych i zamkniętych, w zakresie sprężysto-plastycznym, Politechnika Łódzka, Łódź, 2000, (in Polish).

[3] Kubiak T., Static and dynamic buckling of thin-walled plate structures, Springer Science & Business Media, 2013.

[4] User's Guide ANSYS 15, ANSYS Inc., Houston, USA.

INTERACTIVE BUCKLING OF FGM COLUMNS UNDER COMPRESSION

Z. KOŁAKOWSKI
Lodz University of Technology TUL, Department of Strength of Materials (K12)
PL - 90-924 Lodz, Stefanowskiego 1/15, Poland

A. TETER
Lublin University of Technology LUT, Department of Applied Mechanics,
PL - 20-618 Lublin, Nadbystrzycka 36, Poland

The present paper deals with interactive buckling of thin-walled columns, which are made of functionally graded materials (FGMs). FGMs are inhomogeneous composites made up of two constituents: metallic and ceramic phases. The content of the volume of these two phases changes gradually along the thickness of the structures. Al-TiC metal-ceramic material is applied and these FG structures are subjected to axial compression. The structures are simply supported at both ends. The classical laminate plate theory (CLPT) is employed to obtain the governing equations of the thin-walled FG plate equilibrium. A plate model of the FG column has been adopted in the study to describe global buckling which leads to lowering the theoretical value of load carrying capacity. In order to obtain the differential equilibrium equations of individual plates the Hamilton's Principle for the asymptotic analytical-numerical method was applied and the nonlinear theory of composite plates has been modified in such a way that it additionally accounts for the full Green's strain tensor for thin plates and the second Piola-Kirchhoff's stress tensor in Lagrange's description. The study is based on the numerical method of the transition matrix using Godunov's orthogonalization. The solution method assumed in this study allows for interaction analysis of all buckling modes. In the presented considerations, thermal effects are neglected. The most important advantage of this method is that it enables one to describe a complete range of behaviour of thin-walled FG structures under compression. The authors have found no earlier studies on interactive buckling of FGM structures. One can find papers in which the buckling and post-buckling behaviour of thin-walled elements made of FGMs under compression (e.g., plates [1]) is presented. The nonlinear analysis of this type of elements devoted to basic types of loads is covered in [2]. In paper [3], the nonlinear Koiter's theory has been used to explain an effect of the imperfection sign (sense) on the post-buckling equilibrium paths of FG structures. In the case of FG structure, nonzero first-order sectional inner forces that cause an occurrence of nonzero post-buckling coefficients responsible for sensitivity of the system to imperfections appear. It results in the fact that post-buckling equilibrium paths of plate structures made of FGMs are nonsymmetrically stable. This explains the differences in the plate response dependence on the imperfection sign (sense). Using the classical laminate plate theory (CLPT), the stress and moment resultants (**N**, **M**) are defined as:

$$\begin{Bmatrix} \mathbf{N} \\ \mathbf{M} \end{Bmatrix} = \begin{bmatrix} \mathbf{A} & \mathbf{B} \\ \mathbf{B} & \mathbf{D} \end{bmatrix} \begin{Bmatrix} \boldsymbol{\varepsilon} \\ \boldsymbol{\kappa} \end{Bmatrix} \qquad (1)$$

where: **A**, **B**, **D** - are extensional, coupling and bending stiffness matrices, respectively, for the FG structure. Due to the presence of the nontrivial submatrix **B**, the coupling between extensional and bending deformations exists. The interactive buckling of thin-walled beam-columns with closed and open cross-sections (i.e. trapezoidal, square, top hat and lip channel) are considered (Fig. 1). An interaction of various buckling modes, that is to say, from a two-mode up to four-mode approach has been assumed in the analysis. Attention has been drawn to the effect of the imperfection sign (sense) and the nonsymmetrical stable post-buckling equilibrium path on load carrying capacity. The differences in the behavior of the analyzed columns can be easily explained by different effects of adjacent walls of the column and by the nonsymmetrical stable post-buckling path for FG structures [3-4] on the assumption that the values of imperfection are the same.

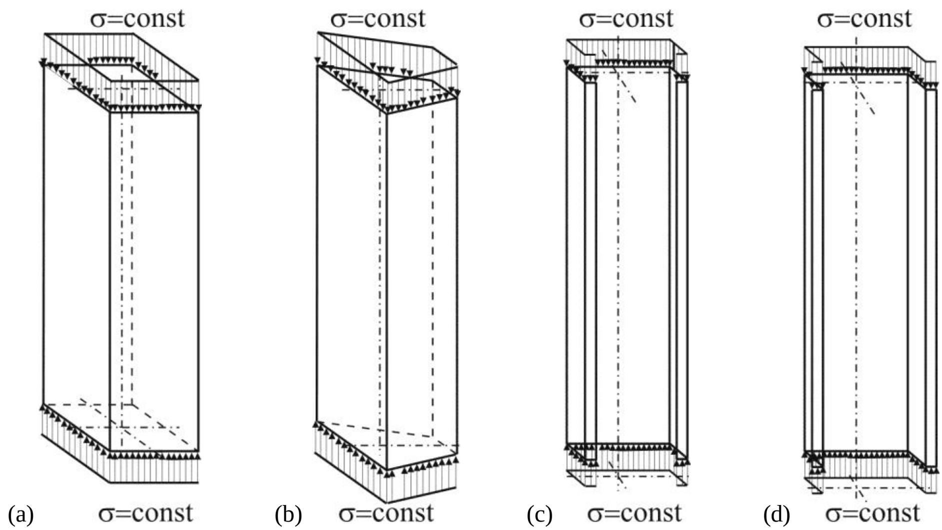

Fig. 1. Thin-walled beam-columns with different cross-sections

This publication is a result of the research carried out within the project subsidized over the years 2012-2015 by the state funds designated for the National Science Centre (NCN UMO-2011/01/B/ST8/07441).

REFERENCES

[1] Jha DK, Tarun Kant, Singh RK, A critical review of recent research on functionally graded plates. Composite Structures 96, 2013, pp. 833–849.
[2] Hui-Shen S. Functionally graded materials - Nonlinear analysis of plates and shells. CRC Press, Taylor & Francis, London, 2009.
[3] Kolakowski Z., Mania R.J., Grudziecki J., Local nonsymmetric post-buckling equilibrium path in thin FGM plate. Eksploatacja i Niezawodnosc/Maintenance and Reliability, 17(1), 2015, pp. 135–142.
[4] Kołakowski Z., Teter A., Static interactive buckling of functionally graded columns with closed cross-sections subjected to axial compression, Composite Structures, 123, 2015, pp. 257–262.

WPŁYW SPRZĘŻENIA STANU BŁONOWEGO WYSTĘPUJĄCEGO W LAMINATACH WŁÓKNISTYCH NA ZACHOWANIE POKRYTYCZNE ŚCISKANEGO SŁUPA

Z. KOŁAKOWSKI
Katedra Wytrzymałości Materiałów i Konstrukcji, Politechnika Łódzka
ul. Stefanowskiego 1/15, 90-924 Łódź

A. TETER, D. PASIERBIEWICZ
Katedra Mechaniki Stosowanej, Politechnika Lubelska
ul. Nadbystrzycka 36, 20–618 Lublin

Laminaty włókniste to kompozyty zbudowane z długich włókien wzmacniających oraz osnowy. W ogólnym przypadku włókniste warstwy laminatu mogą być ułożone w dowolny sposób. Stosując klasyczną teorię laminowanych płyt zależności pomiędzy siłami wewnętrznymi **N**, **M,** a odkształceniami błonowymi $\boldsymbol{\varepsilon}$ oraz krzywizny $\boldsymbol{\kappa}$ można zapisać w ogólnej postaci macierzowej [1]:

$$\begin{Bmatrix} \mathbf{N} \\ \mathbf{M} \end{Bmatrix} = \begin{bmatrix} \mathbf{A} & \mathbf{B} \\ \mathbf{B} & \mathbf{D} \end{bmatrix} \begin{Bmatrix} \boldsymbol{\varepsilon} \\ \boldsymbol{\kappa} \end{Bmatrix} \tag{1}$$

Macierz **A** opisuje stan błonowy, macierz **D** - stan zgięciowy, zaś macierz **B** - sprzężenia zachodzące pomiędzy stanem błonowym oraz zgięciowym. Znane są takie ułożenia warstw laminatu np. $[60/\text{-}60_2/0_3/60_2/0/\text{-}60/60_2/\text{-}60_3/0_2/60]_T$ [2], że możliwe jest pełne rozprzężenie stanu błonowego oraz zgięciowego (tzw. niesprzężony laminat). Dla laminatów o dowolnym układzie warstw zachodzą różne przypadki sprzężeń [1-3]. Ze względów praktycznych szczególnie interesujący jest przypadek sprzężenia stanu błonowego, o którym decydują niezerowe wyrazy A_{16} oraz A_{26} macierzy **A**:

$$\mathbf{A} = \begin{bmatrix} A_{11} & A_{12} & A_{16} \\ & A_{22} & A_{26} \\ Sym. & & A_{66} \end{bmatrix}; \quad \mathbf{B} = 0\,; \quad \mathbf{D} = \begin{bmatrix} D_{11} & D_{12} & 0 \\ & D_{22} & 0 \\ Sym. & & D_{66} \end{bmatrix} \tag{2}$$

Jeżeli $A_{16}=A_{26}=0$ to stany: błonowy oraz zgięciowy są niesprzężone. W przeciwnym przypadku występuje sprzężenie błonowe. Laminaty ze sprzężeniem błonowym można wytwarzać nowoczesnymi technologiami (technologią autoklawową) w podwyższonych temperaturach, ponieważ wytworzone elementy nie ulegają paczeniu w procesie chłodzenia. Nie ma więc konieczności korekty wynikającej z dylatacji termicznej. Przykładem laminatu wykazującego sprzężenie stanu błonowego może być laminat o układzie warstw: $[45/0/\text{-}45/45/\text{-}45_5/(0/\text{-}45)_3/45_2/\text{-}45/]_T$ [2].

Szczegółowe obliczenia przeprowadzono dla słupa o przekroju kwadratowym o wymiarach 250 mm oraz długości 2000 mm, swobodnie podpartego na obu końcach. Przyjęto, że słup wykonano z wielowarstwowego kompozytu IM7/8552 o właściwościach mechanicznych: E_1=161 GPa, E_2=11.38 GPa, G_{12}=5.17 GPa, ν_{12}=0.38 [2] oraz grubości warstwy 0.14 mm. Jako przypadek referencyjny (Wariant 1) przyjęto laminat niesprzężony o układzie 18 warstw: $[60/-60_2/0_3/60_2/0/-60/60_2/-60_3/0_2/60]_T$. Laminat wykazujący sprzężenie błonowe to $[45/0/-45/45/-45_5/(0/-45)_3/45_2/-45/]_T$ (Wariant 2). Ugięcia wstępne wynoszą: w_o=0.25 mm. Dodatkowo przedstawiono wyniki dla słupa izotropowego (Wariant 3), przyjmując stałe materiałowe: E_1=161GPa, ν_{12}=0.38.

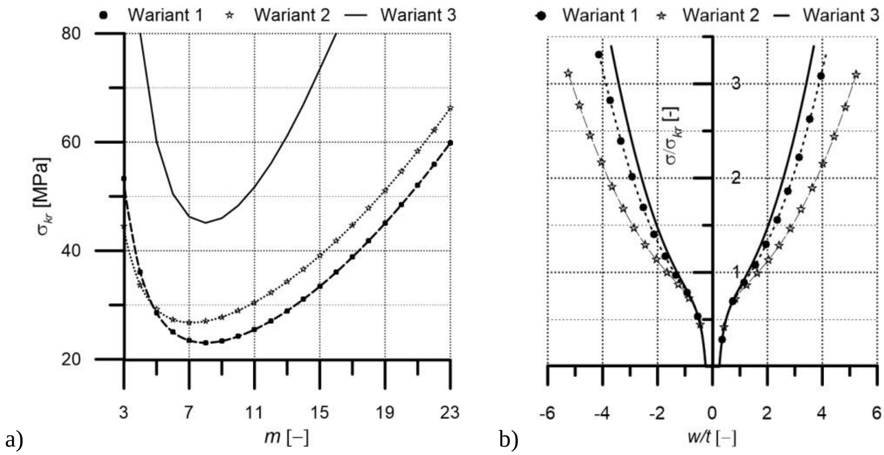

Rys. 1. Stan krytyczny (a) oraz pokrytyczna ścieżka (b) dla analizowanego słupa

Z analizy stanu krytycznego wynika, że najniższe naprężenia krytyczne σ_{kr} odpowiadające wyboczeniu lokalnemu dla słupa wykonanego z kompozytu wykazującego efekt sprzężenia (Wariant 2 - Rys. 1a) wynoszą: 26.8 MPa dla m=7, zaś dla słupa referencyjnego (Wariant 1 - Rys. 1a) odpowiednie naprężenia wynoszą 23,1 MPa dla m=8. W przypadku słupa izotropowego otrzymano odpowiednio: 45.1 MPa dla m=8. Obserwujemy zarówno różnicę ilościową jak i jakościową wynikającą ze zmiany długości półfali wyboczenia. Pokrytyczne zachowanie dla analizowanych wariantów przedstawiono na Rys. 1b, gdzie σ - naprężenie ściskające, w - ugięcie oraz t - grubość laminatu. Wszystkie wyznaczone ścieżki pokrytyczne są stateczne oraz symetryczne.

Praca została dofinansowana ze środków Narodowego Centrum Nauki przyznanych na podstawie decyzji numer DEC-2013/11/B/ST8/04358.

LITERATURA

[1] Jones R.M., Mechanics of composite materials, Taylor & Francis, Inc., Philadelphia, 1999.
[2] York C.B., On extension–shearing coupled laminates, Composite Structures, 120, 2015, pp. 472–482.
[3] York C.B., Coupled quasi-homogeneous orthotropic laminates, Mechanics of Composite Materials, 47, (4), 2011, pp. 405-426.

POST-CRITICAL DEFORMATION STATES OF COMPOSITE THIN-WALLED AIRCRAFT LOAD-BEARING STRUCTURES

T. KOPECKI, P. MAZUREK, T. LIS
Rzeszów University of Technology, Department of Aircrafts and Aeroengines
Al. Powstańców Warszawy 12, 35-959 Rzeszów, Poland

J. BAKUNOWICZ
Aviation Training Centre, Rzeszów University of Technology

1. INTRODUCTION

The study presents results of experimental examination of a model representing a fragment of an aircraft wing structure with skin made of glass fibre/epoxy composite. For such system, the deformation pattern has been found and the representative equilibrium path determined. The finite element method was used to develop corresponding numerical model correctness of which has been then verified by comparing the obtained results with the course of relevant experiment. Conformity of the results allowed to determine usefulness of the applied methods to assessment of mechanical properties of modified solutions involving integral skin stiffening elements.

2. EXPERIMENTAL RESEARCH.

The subject of the analysis was a fragment of a monospar wing structure with constant chord along the whole span and stiffened front torsion box (Fig. 1).

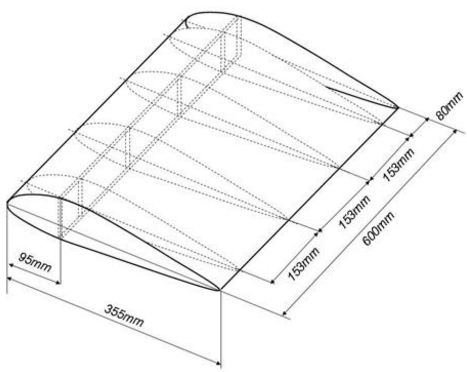

Fig. 1. An overall outline of the examined structure

Three different variants of the structure were considered and compared. First, exactly corresponding to outline presented on figure 1, second, reference structure without two ribs in the central area and third, containing integral stiffeners instead of mentioned ribs.

The skeleton portion of the model used in the experiment was made of plywood and wooden slats with known mechanical parameters. The skin was an epoxy composite reinforced with glass fibre (GFRP). In the course of experiment, the model was subjected to simultaneous bending and torsional deflection (Fig. 2) on a specially constructed experimental set-up. The deformations of the structure were obtained by means of optical scanner ATOS.

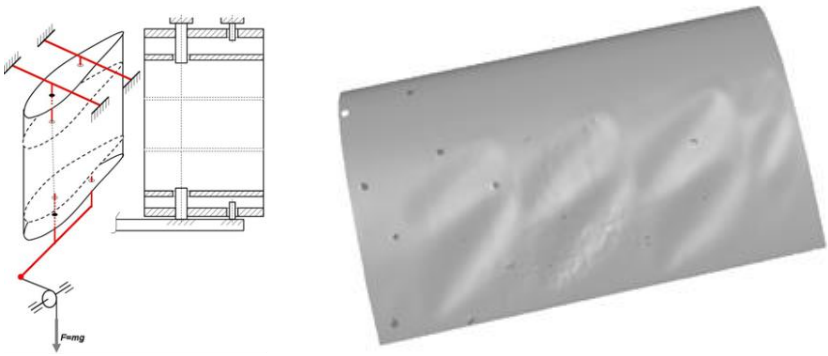

Fig. 2. An outline of model fastening and load application (left) and model deformations determined by means of ATOS scanner (right)

3. NUMERICAL CALCULATIONS

As the result of nonlinear numerical analyses using MSC MARC software, the replacement and effective stress distributions were obtained (Fig. 3)

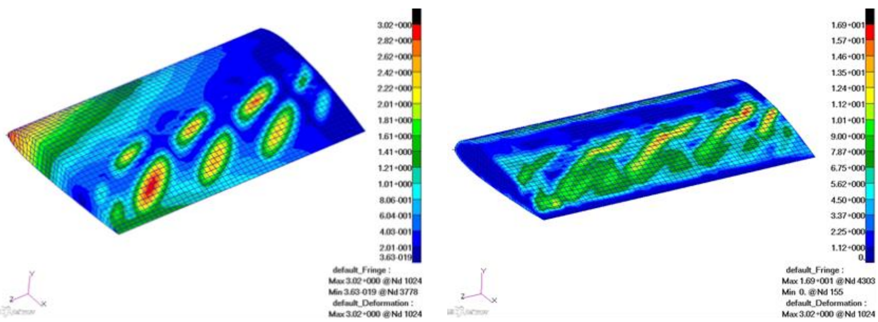

Fig. 3 Resultant displacement distribution (left) and reduced stress distributions according to σ_{max} hypothesis (in MPa) (right)

REFERENCES

[1] Bathe K.J, Finite element procedures, Prentice Hall, 1996.

[2] Buckling and Postbuckling Behaviour of Composite Laminated Shell Structures, Proceedings of 2nd International Conference, Braunschweig 2008.

POST-CRITICAL DEFORMATION STATES OF THIN-WALLED SEMI-MONOCOQUE AIRCRAFT LOAD-BEARING STRUCTURE WITH LARGE OPENING

T. KOPECKI, P. MAZUREK

Rzeszów University of Technology, Department of Aircrafts and Aeroengines
Al. Powstańców Warszawy 12, 35-959 Rzeszów, Poland

D. CHODOROWSKA
State Higher Vocational School in Krosno
ul. Wyspiańskiego 20, 38-400 Krosno, Poland

1. INTRODUCTION

The study presents results of experimental examination of a model representing a fragment of an aircraft structure, weakened by a large opening. The main goal of the research constituted the determination of the influence of the skeleton variant on critical load and post-critical deformations pattern of the skin. The deformation patterns have been obtained using optical scanner and the representative equilibrium paths were determined. The finite element method was used to develop corresponding numerical model correctness of which has been then verified by comparing the obtained results with the course of relevant experiment. Conformity of the results allowed to use obtained numerical models to try out the influence of some skeleton modifications on post-critical properties of the structure.

2. EXPERIMENTAL RESEARCH.

The subject of the analysis was a fragment of typical structure with large opening, which corresponds to a part of an aircraft fuselage or a helicopter tail rotor beam. In the course of experiment, the model was subjected to torsion by means of special stand (Fig. 1).

Fig. 1. Experimental stand with fixed model

Two different variants of the structure, with different thickness of the opening frames were considered and compared. The change of the frame thickness result in the different pattern of post-critical deformations of the skin. The deformations of the structure were obtained by means of optical scanner ATOS.

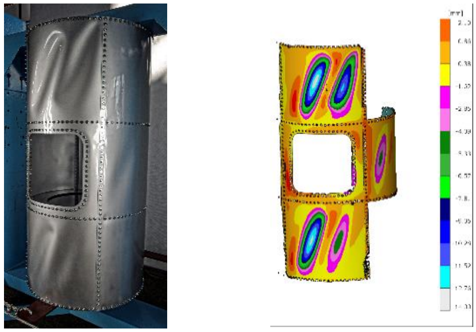

Fig. 2. Post-critical deformations of the model (left) and model deformations determined by means of ATOS scanner (right)

3. NUMERICAL CALCULATIONS

As the result of nonlinear numerical analyses using MSC MARC software, the replacement and effective stress distributions were obtained (Fig. 3). Verified numerical models were a base to work out some modified solutions of the structure with different forms of skeletons.

Fig. 3. The pattern of post-critical displacements (left) and resultant displacement distribution (in mm) (right)

REFERENCES

[1] Bathe K.J, Finite element procedures, Prentice Hall, 1996.

[2] Arborcz J., Post-buckling behavior of structures, Numerical techniques for more complicated structures, Lecture Notes in Physics, 1985.

[3] Crisfield M. A., Non-linear finite element analysis of solid and structures, J. Wiley & Sons, 1997.

IMPACT BEHAVIOUR OF SPOT-WELDED THIN-WALLED FRUSTA

M. KOTEŁKO, A. MOŁDAWA

Department of Strength of Materials, Łódź University of Technology
Stefanowskiego 1/15, 90-924 Łódź, Poland

1. INTRODUCTION

Dynamic response of structures in the plastic range is a significant problem in the case of energy absorbers. Such a structural member converts totally or partially the kinetic energy into another form of energy. One of the possible design solutions is the conversion of the kinetic energy of impact into the energy of plastic deformation of a thin-walled metallic structural member. There are numerous types of energy absorbers of that kind cited in the literature. Among others, there are compressed thin-walled frusta (truncated circular cones or prisms) [1], currently used as impact attenuation members in car structures. A designer of any impact attenuation device must meet two main requirements. The initial collapse load must not be too high in order to avoid unacceptably high impact velocities of the vehicle. On the other extreme, the main requirement is a possibly highest energy dissipation capacity, which may not be achieved if the collapse load of the impact device is too low. The shape of the thin-walled member and the manufacturing technology (e.g. spot welding) influence substantially quantities mentioned above. There are very few fragmented information about an influence of spot welding on the crushing behavior of thin-walled members subjected to axial impact [2]. In the paper the results of the parametric study into the energy absorption capacity, ultimate load and mean crushing load of thin-walled prismatic frusta subjected to axial impact compressive force are presented. Particularly, the influence of a diameter and number of spot welds was investigated as well as preliminary parametric analysis into an optimal angle of inclination of the frustum wall was performed.

a) 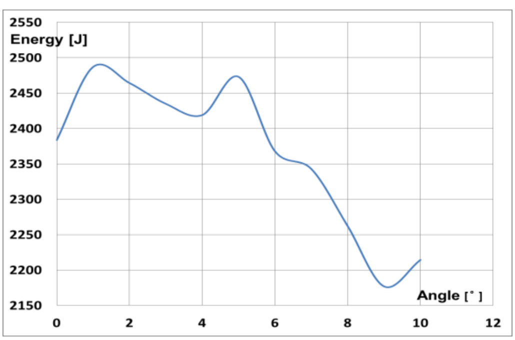

b) 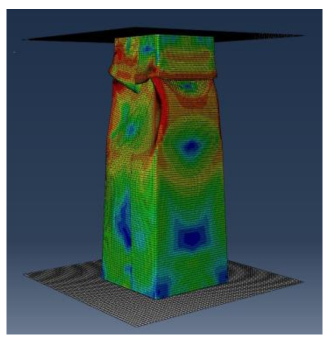

Fig. 1. Numerical results a) - energy absorption versus wall inclination angle (8 spot welds of diameter d = 8 [mm]) - b) - numerical model

2. NUMERICAL ANALYSIS

The subject of investigation was a thin-walled prismatic frustum on square foundation shown in Fig.1, under axial dynamic compressive force. The numerical explicit dynamic analysis of crushing behaviour of the frustum was carried out using FE commercial code ABAQUS. An FE model of the frustum (Fig. 1b) was created using 4-node shell elements S4R. A column model situated between two rigid elements R3D4. Between upper and lower rigid elements and the column Tie links were applied. The rate-dependent material elasto-plastic model, taking into account the strain rate and strain hardening has been applied. Material parameters were determined in tensile and compressive tests. It was steel Dual Phase DP 800, with main parameters: E= 210 GPa, Re= 590 MPa. There, calibration of the material model was carried out using ABAQUS program [3]. The spot welds were modelled using the rigid beam elements, situated between two overlapping column surfaces.

3. RESULTS OF ANALYSIS AND FINAL REMARKS

Results of preliminary analysis showed that the diameter and number of spot welds had a minor influence on the crushing behaviour of examined frusta.

The further analysis was focused on the parametric study into an optimal angle of frustum wall inclination with respect to the energy absorbed. The results show the optimum of magnitude about 5º (Fig. 1) for the examined wall thickness. The ultimate load decreases linearly with the increase of the angle of inclination. The research presented in the paper is a part of a wider project. Further investigation will be continued into an experimental validation of theoretical results.

REFERENCES

[1] Alghamdi, Collapsible impact energy absorbers: an overview, Thin-Walled Structures, 39, 2001, pp. 189-213.

[2] Rusiński E. et al., Tests of thin-walled beams joined by spot welding. J. of Materials Processing Technology, 157-158, 2004, pp 405-409.

[3] Abaqus 6.13 Documentation, Abaqus Online Documentation, Simulia, Dassault Systems, 2013.

Finite Element calculations carried out in Abaqus by CYFRONET AGH. MNiSW/IBM_BC_HS21/PŁódzka/013/2013

ELASTIC-PLASTIC STABILITY OF FML COLUMNS OF OPEN CROSS-SECTIONS

K. KOWAL-MICHALSKA, Z. KOŁAKOWSKI

Department of Strength of Materials, Lodz University of Technology
Stefanowskiego 1/15, 90-924 Łódź, Poland

1. INTRODUCTION

Fiber Metal Laminates (FMLs) are hybrid materials, built from thin layers of metal alloy and fiber reinforced epoxy resin. These materials are manufactured by bonding composite plies to metal ones. FMLs, with respect to metal layers, can be divided into FMLs based on aluminum alloys (ARALL reinforced with aramid fibers, GLARE - glass fibers, CARALL - carbon fibers) and others. Nowadays material such as GLARE (glass fiber/aluminum) due to their very good fatigue and strength characteristics combined with the low density find increasing use in aircraft industry [1].

When the plate structures made of GLARE subject to in-plane uniform compression in the elasto-plastic range of stresses, the buckling occurs in such a way that aluminum layers become plastic but the glass layers remain elastic. Therefore the behavior of such structures differs significantly from the behavior of pure aluminum ones.

2. SUBJECT OF CONSIDERATION

A prismatic thin-walled structure built of FML plates connected along longitudinal edges has been considered (Fig. 1). The structure is simply supported at its ends. In order to account for all modes of global, local and coupled buckling, a plate model of thin-walled structure has been applied. It is also assumed that both component materials the structure is made of obey Hooke's law.

3. METHOD OF SOLUTION

The problem of inelastic buckling is examined using the analytical-numerical method elaborated for the analysis of the elastic stability of multi-layered thin-walled columns [2]. The layers can be isotropic or orthotropic. Determination of buckling stresses and buckling modes of thin-walled plate structures in the elastic plastic range requires the material characteristic to be known for a material under consideration. In case of aluminum it can be described in an analytical way by Ramberg-Osgood formula or Needleman-Tvergaard relation [2]. The relationships between stress and strain for a component elasto-plastic layer are derived on the basis of the J_2-deformation theory of plasticity and/or J_2-flow theory (incremental theory). On the other side the same relations are written for an orthotropic elastic layer. Comparing the appropriate coefficients in both relations the instantaneous "conventional" parameters of orthotropy can be found out.

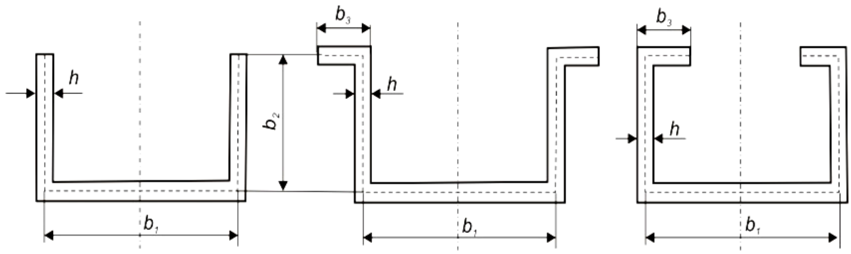

Fig. 1. Cross-sections of analysed columns

The columns are built of rectangular flat plates. The material is GLARE 3 [1] with an even number of glass reinforced layers, the outer layers are always aluminum. The overall laminate is symmetric. The dimensions of structures are chosen in such a way that the stability loss occurs in the elastic-plastic range for aluminum layers.

4. SOME RESULTS OF CALCULATIONS

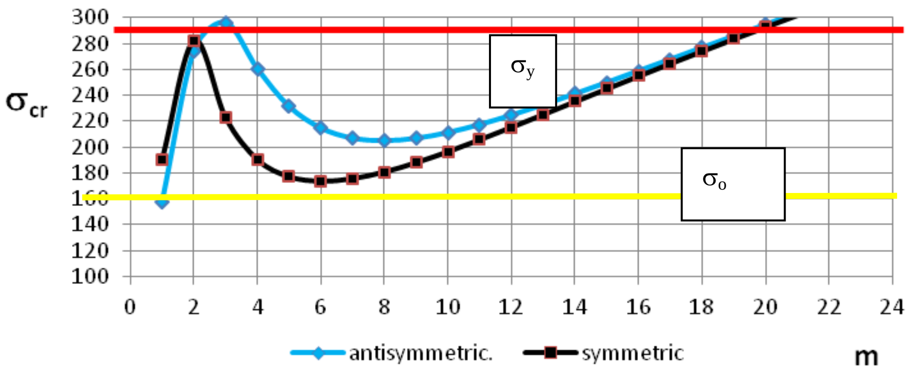

Fig. 2. Buckling stress versus number of half-waves *m* for symmetry and antisymmetry conditions imposed along cross-section symmetry axis (σ_y-aluminum yield limit, σ_o -proportional limit)

In Fig. 2 the calculation results for a column of a channel cross-section are shown. The calculations are based on J_2 deformation theory and Ramberg-Osgood relation.

ACKNOWLEDGMENT

This contribution is a part of the project funded by the National Science Centre Poland, allocated on the basis of the decision No. 2012/07/B/ST8/0409.

REFERENCES

[1] Wittenberg T. C., de Jonge A., Plasticity correction factors for buckling of flat rectangular GLARE plates, DUT, Int. Council of the Aeronautical Sciences, 482, 13, 2002, pp. 1-482.

[2] Kołakowski Z., Kowal-Michalska,K. (eds.), Selected problems of instabilities in composite structures, Technical University of Lodz, A Series of Monographs, Lodz. 1999.

NUMERICAL BUCKLING SOLUTIONS OF CYLINDRICAL SHELLS WITH ONE TRANSVERSAL CUT UNDER DIFFERENT CONDITIONS OF AXIAL COMPRESSION

V.L. KRASOVSKY, O.V. LYKHACHOVA
Department of Structural Mechanics and Strength of Materials
Prydniprovs'ka State Academy of Civil Engineering and Architecture
Chernyshevskogo 24a, 49-600 Dnepropetrovsk, Ukraine

Within a unified finite-element approach, the numerical buckling analysis of axially compressed elastic cylindrical shells with one transversal cut is realized in ANSYS software. The research studies two buckling solutions: 1) geometrically linear buckling solution for the definition of eigenvalues N^{cr}; 2) geometrically nonlinear stress-strain state solution for the evaluation of buckling loads N^{lim}. Simulations have been performed for 5 loading schemes (Fig. 1) which represent the loading nature (force loading - schemes 1, 3, 5 or kinematical loading - schemes 2, 4) and three different conditions of applying an axial compression (with out-of-plane edge rotation - schemes 1, 2; with parallel edge displacement - schemes 3, 4; with out-of-plane edge displacements - scheme 5).

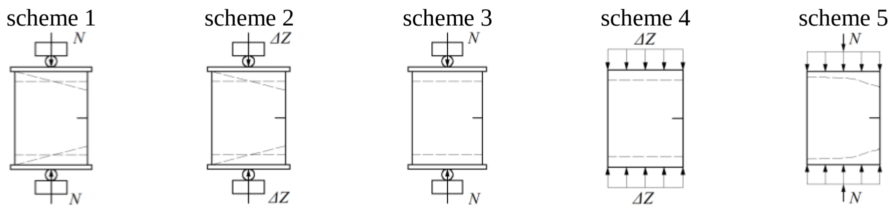

Fig. 1. Loading schemes (in buckling moment)

The numerical investigation has been carried out on 3-D FE models of elastic orthotropic shells of the following mechanical and geometrical characteristics: modulus of elasticity E_x = 6.9 MPa, E_y = 3.45 MPa (x matches with the generatrix, y corresponds to the circumferential direction); shear modulus G = 1.92 MPa; Poisson's ratio ν_x = 0.3, ν_y = 0.15; radius R = 50 mm, length L = 100 mm, thickness h = 0.23 mm (L/R = 2.0, R/h = 217); cut length l = 0, 8, 16, 30, 60, 80 mm (l corresponds to an angle γ = 0, 9°.2, 18°.3, 34°.4, 68°.8, 91°.7); longitudinal size of the cut a = 2 mm. For the loading schemes 1, 2, 3, FE models contain isotropic elastic models of the two rigid cylindrical disks (E= 2×10^{15} Pa, ν = 0.3; R = 50 mm, H = 3 mm). FE meshes of the shells and rigid disks are created by standard elements SHELL181 and SOLID185, respectively. The total number of elements varies between 33500 and 36700, including shell FE between 12800 and 16000 depending on l. Longitudinal displacements of models are fixed in the middle section of the shell height. Radial and tangent displacements are restricted on the external surfaces of rigid disks (schemes 1, 2, 3) and on the edges of the shells (schemes 3, 4, 5). An axial compression is applied as longitudinal concentrated forces (schemes 1, 3) or displacements (scheme 2) to the external surfaces of rigid disks and as uniform longitudinal forces or displacements (schemes 4 and 5, respectively) distributed on the edges.

General features of linear and geometrically nonlinear buckling solutions are presented in Fig. 2 as the dependences "$\overline{N}^{i} - l$" for 5 loading schemes. Here, $\overline{N}^{i} = N^{i} / N^{cl}$; $N^{cl} = 2\pi E h^{2} / \sqrt{3(1-\nu^{2})}$ is the critical axial compressive force found for an isotropic shell with parameters E = 5.175 MPa, ν = 0.225. $\overline{N}^{cr}$ are lower than $\overline{N}^{\lim}$ in all cases, except small cuts (γ>18°). For γ<18° linear solutions are close for the schemes 1-4. When γ =18° $\overline{N}^{cr}$ reaches values of (0.46-0.49) N^{cl} . Then linear solutions diverge, and if γ =91°.7 bifurcation buckling loads are 0.22, 0.35, 0.41, 0.53 N^{cl} respectively for the schemes 1-4. For the scheme 5 the dependence "$\overline{N}^{cr}$ - l" is rather different. It is a smooth descending curve which falls to 0.022 N^{cl} for γ=91°.7. The dependence "$\overline{N}^{\lim}$ - l" for the scheme 5 is similar but for the schemes 1-4 these curves are more complicated. A sharp drop of $\overline{N}^{\lim}$ is replaced by a rather intensive increase with a following smooth decrease of buckling loads. Note that the loading nature has almost no effect on $\overline{N}^{\lim}$. At the same time $\overline{N}^{\lim}$ found for the schemes 3, 4 are much more higher than $\overline{N}^{\lim}$ found for the schemes 1, 2.

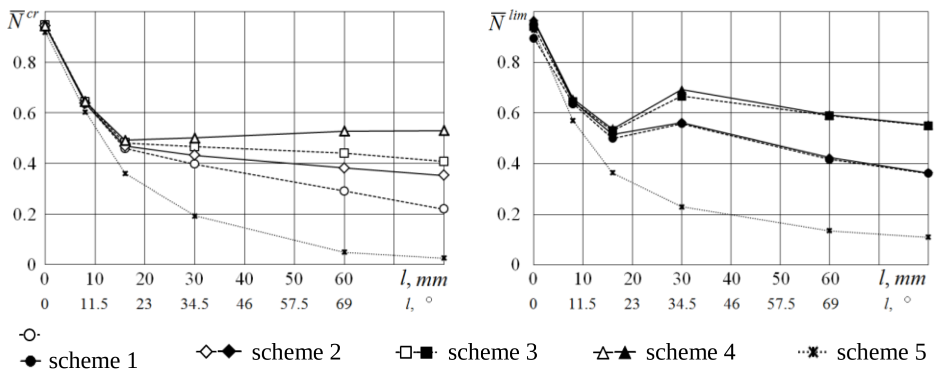

Fig. 2. Dependences "$\overline{N}^{i} - l$" for different loading schemes

This work is supported by Alexander von Humboldt Foundation (Institutional academic cooperation program, grant no. 3.4 - Fokoop - UKR/1070297).

REFERENCES

[1] Krasovsky V.L., Marchenko V.A., Schmidt R., Influence of manner of applying axial compression on the behaviour of a cylindrical shell under local action, Stability of Structures, Lodz, 13, 2012, pp. 389-396.

[2] Лихачёва О., К вопросу определения несущей способности продольно сжатых цилиндрических оболочек с одним поперечным разрезом, Вісник Придніпровської державної академії будівництва та архітектури, Днепропетровск, 7-8, 2012, сс. 87-95.

[3] Lykhachova O.V., Schmidt R., Deforming and buckling of axially compressed elastic cylindrical shells with transversal cut in experiments and numerical simulation, Shell Structures: Theory and Applications, (eds.) W. Pietraszkiewicz, J. Gorski, London, 3, 2013, pp. 219-222.

INFLUENCE OF EDGES REINFORCMENT OF LONGITUDINAL COMPRESSED CYLINDRICAL SHELL ON ITS BEHAVIOUR AT LOCAL CROSS-SECTION IMPACT

V.L. KRASOVSKY, V.A. MARCHENKO
Department of Building Mechanics and Strength of Materials, Prydneprovsk State Academy of Civil Engineering and Architecture
Chernyshevsky 49a, 49000 Dnepropetrovsk, Ukraine

It is known [1, 2], that character and conditions of application of the basic loading (Fig. 1) influence the feature of behavior of longitudinal compressed cylindrical shells at cross-section local impacts (LQI). To the full these features are shown at typical kinematic LQI with bilateral connection of a shell and an impact. At such impacts the basic axial compressing loading (force N_0) in the beginning is set, then - consistently increasing radial moving (W) is set, thus is traced reaction of a shell to cross-section influence (Q).

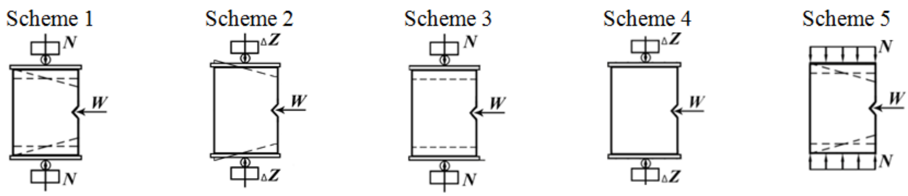

Fig. 1. Loading scheme

The purpose of this research consist in studying of influence on behavior at LQI longitudinal compressed shell of a reinforcement of its edges face rings. The core loading of a shell was carried out under the scheme 5 [1, 2], that corresponds to the appendix on its end faces of in regular intervals distributed longitudinal compressing efforts. Thus radial displacements of edge are limited but the exit of end faces from a plane is possible.

Designations: relative axial force $\overline{N}_0 = N / N^{cl}$; parameter of kinematic influence $\overline{W} = W / h$; parameter of reaction of a shell to influence $\alpha = Q(R/h)^{0.5} / (Eh^2)$; *R*, *h* - radius and thickness of an shell; *E*, μ - Young modulus and Poisson ratio of material; N^{cl} - classical value of critical axial force $N^{cl} = 2\pi Eh^2 / [3(1-\mu^2)]^{0.5}$.

Research was made using program complex ANSYS. Shells were modeled by finite elements SHELL281, frames - BEAM189. Geometry of shells: *2R*=86 mm; *h*=0.271 mm *(R/h*=160*)*; length *L/R*=2.0. Frames of square cross-section incorporated to a shell without eccentricity. The size of section changed from 6 mm up to 12 mm with a step of 2 mm. A material of shells and frames - steel X18H9н (*E*=195 GPa*;* μ =0.3).

Results of numerical research are presented in Fig. 2, *a* by a family of dependences « $\alpha - \overline{W}$ » at $\overline{N}_0 = 0.4 N^{cl}$ which to the full reflect behavior is longitudinal compressed shells at considered LQI. Here, the curve 1 answers the core loading shells under the scheme 1 (power axial compression with free turn of a plane of round end faces [1, 2]), a curve 7 - loading of a shell under the scheme 5. Curves 2, 3, 4, 5, 6 correspond to shells with the party of a frame 12, 10, 8, 7.5, 6 mm, accordingly. Dependences «$\alpha - \overline{W}$» for the shells loaded under the scheme 5 and 1 at various values of N_0, are presented in Fig. 2b,c.

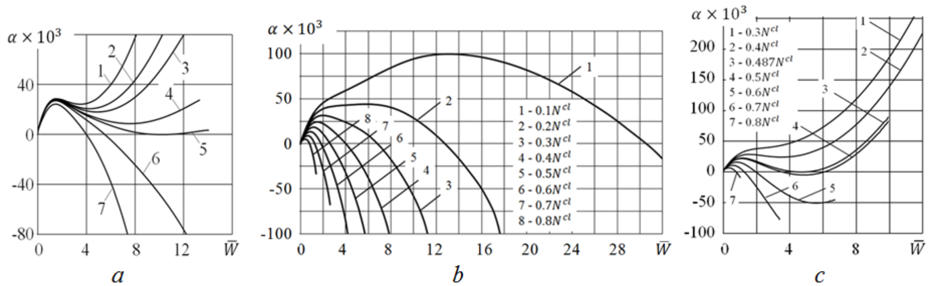

Fig. 2. Dependences «$\alpha - \overline{W}$»

The resulted dependences, first of all, expand representation about influence of conditions of fastening of edges on behavior of longitudinal compressed shells at LQI. In this case the received curves «$\alpha - \overline{W}$» reflect possible in practice transitive situations from initial conditions of fastening of edges of a shell under the scheme 5 to the scheme 1. Besides they expand representation about the mechanism of buckling of real shells. In particular, specify existence for a shell with the supported edges steady supercritical forms with one dent. In this case it means, that for the investigated shells equipped by face frames of square section with the side of 7.5 mm, loaded under the scheme 5, equally effective loadings which makes $\overline{N}_0 = 0.4N^{cl}$ represents the bottom local critical force $\overline{N}_+$ (at which probably existence steady supercritical forms with one local dent). It is necessary to note, that at the core loading researched shells under the scheme 1 size $\overline{N}_+ = 0.487$. The amplitude of subcritical dent thus makes $\overline{W} = 4.47$ (fig.1,*c*). In this case at the bottom local critical force $\overline{N}_+ = 0.4$ amplitude of a local dent makes $\overline{W} \approx 9$. Character of curve 5 shows, that, basically, for a shell with face frames it is possible to receive values $\overline{N}_+$ which less the than received size $\overline{N}_+ = 0.4$, however their realization is possible only at greater amplitudes of movings.

The research was sponsored by the Fund of Humboldt Grant no. 3.4-Fokkop-UKR/1070297.

REFERENCES

[1] Krasovsky V., Marchenko V., Influence of manner of applying axial compression on the behavior of a cylindrical shell under local action, Stability of structures XIII-th - Symposium, Zakopane, 2012, pp. 389-396.

[2] Krasovsky V., Marchenko V., The influence of boundary conditions on the behavior of an axially compressed shell with quasi-static lateral perturbation, Bulletin СевНТУ.- Sevastopol: Publishing house SevNTU, 2013. Issue 137: Mechanics, power, ecology - С.166-172 [in Russian].

CORNER RADIUS EFFECT IN THIN-WALLED SQUARE SECTION COLUMNS ON THE LOCAL BUCKLING OF WALLS UNDER AXIAL COMPRESSION

M. KRÓLAK, R. MANIA, M. KAMOCKA
Department of Strength of Materials, Lodz University of Technology
Stefanowskiego 1/15, 90-924 Łódź, Poland

1. INTRODUCTION

During axial-compression of thin-walled square section steel columns, we can determine the local buckling critical stress from the formula valid for a long uniformly-compressed rectangular plate simply supported at all edges (1) [1]:

$$\sigma_{kr} = 4\frac{\pi^2 D}{b_0^2 t} = \frac{\pi^2 E}{3\left(1-\nu^2\right)}\left(\frac{t}{b_0}\right)^2 \tag{1}$$

where: E is Young modulus of column material, ν Poisson's ratio, b_o - single wall width of square column or rectangular plate, t - wall thickness (or plate thickness). For typical girder design the critical stress values of local buckling are very small in comparison to the structural steel yield point. Then the mechanical strength properties of applied material couldn't be fully used in considered columns [3].

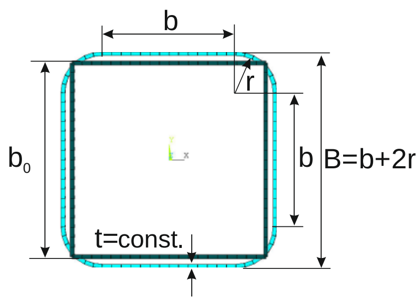

Fig. 1. Square section column cross section with corner radius

2. THE FORMULATION OF PROBLEM

We consider a thin-walled square section columns with corner radius, as it is shown in Fig. 1. The local buckling of thin-walled columns under axial compression with radius corner ($r \neq 0$) and without radius corner ($r = 0$, $b = b_0$) is analysed. The wall thickness and cross-section area of all columns are the same, then the relationship can be established:

$$b = b_0 - \frac{\pi}{2} r \tag{2}$$

For given data: l, b_0, t, E, ν and assumed radius corner r, using the formula (2), one can calculate the width b of a flat part of column wall with assumed radius corner. In the case when b = 0, we obtain a cylindrical shell with a total radius $r_c = 2/\pi \cdot b_0 = 0.63662$.

3. RESULTS of CALCULATIONS

The computations of local buckling critical stresses of considered thin-walled square section column with radius corner, exposed to axial compression, were performed with application of the finite element method software ANSYS. The exemplary, detailed computations were executed for the following data: the wall column width without radius corner $b_0 = 1$ m; column height $l = 3b_0 = 3$ m; the flat wall elements width $b = b(r)$; considered wall width: t = 1, 2, 4 mm; Young modulus for steel columns E =200 GPa; Poisson's ratio ν = 0.3. The results are shown in Fig. 2.

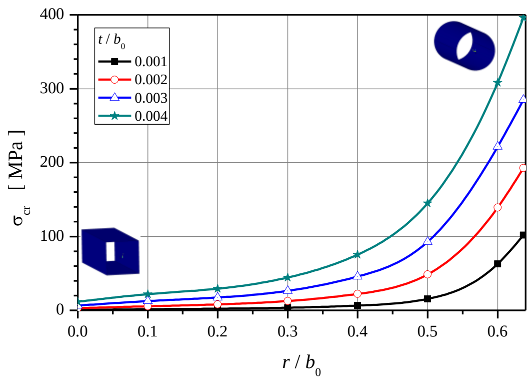

Fig. 2. Corner radius-critical stresses curve

4. COCLUSIONS

From the performed computations and exemplary diagram one can simply conclude that for compressed columns made of the same material with the same boundary conditions, the local buckling stress of walls increases with the increase of radius corner value. It leads also to increase of the ultimate load of considered columns. Introduction of even small radius corner is a design tool to control a local buckling stress value and effective strength utilization of column material.

REFERENCES

[1] Volmir A.S., Ustoiczivost deformirujemych system, Nauka, Moskwa, 1967.

[2] Krolak M. (ed.), Buckling, postbuckling and load carrying capacity of thin-walled orthotropic structures, Monographs, TU of Lodz, 1995 (*in Polish*).

[3] Krolak M., Mania J.R. (eds), Stability of thin-walled plate structures, Vol. 1 of Statics, Dynamics and Stability of Structures, S. of Monographs, TU of Lodz, 2011.

BUCKLING OF STEPPED BEAMS RESTING ON AN ELASTIC FOUNDATION

K. KULIŃSKI, J. PRZYBYLSKI
Faculty of Mechanical Engineering and Computer Science
Częstochowa University of Technology
Armii Krajowej 21, 42-201 Częstochowa, Poland

1. INTRODUCTION

The stability of beams under compressive load with different ends support, stepped cross-section and resting on elastic foundations has been the subject of interest by many researchers. In terms of Winkler foundation, reaction forces are proportional to the deflection of a beam at any point and the foundation characteristics are modeled by using the system of fixed linear springs. The constant of proportionality of these springs is known as the subgrade modulus. For the problem description both classical mathematical methods and finite element analysis have been used.

2. PROBLEM FORMULATION

In this paper the influence of structural parameters of the beam with two ends fixed resting on Winkler foundation on its buckling critical force has been discussed. The change in the beam's cross-section results from two piezoceramic plates perfectly bonded at top and bottom surfaces of the beam, where the adhesive layer connecting mentioned elements is treated as negligible. The influence of piezoelectric stimulation on buckling load has also been discussed.

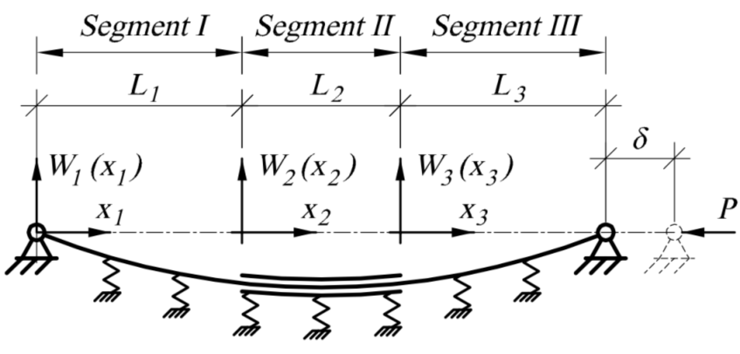

Fig. 1. Scheme of the analyzed beam under prescribed axial end displacement

For the performed analysis there have been adopted five different supports of beam ends which prevent their longitudinal displacements. The considered beams have:

- both ends pinned,
- both ends fixed,

- one end fixed, the other one pinned,
- one end fixed, the second one fixed with ability to slide in direction perpendicular to the longitudinal axis of the beam (guided support),
- one end pinned, the second one fixed with ability to slide in direction perpendicular to the longitudinal axis of the beam (guided support).

For the general mathematical formulation of the problem, the energy method has been applied. When a function, which is the solution of the governing equation, is substituted into boundary conditions one obtains a set of linear homogeneous equations with respect to integration constants. Equating to zero the determinant of matrix consisting unknown integration coefficients, the transcendental equation is obtained. Finally, after numerical solution of this equation, the critical force can be found for any given buckling shape of the beam. A number of calculations with different geometrical parameters of the beam and piezoceramic patches have been performed to show an influence of those parameters on the critical force.

Applying the electric field to piezoceramics, dependently on the electric field vector direction, the longitudinal compressive or stretching force can be induced. The value of this force is determined by the applied voltage, the relationship between piezoceramics length to the beam length as well as the relationship between piezosegment axial stiffness to the beam stiffness. The range of the critical buckling force modifications by the mentioned force has also been studied in this paper.

After analysis of the obtained numerical results one can be stated that both the higher system stiffness and the higher value representing foundation stiffness parameter result in the greater values of the system critical load. Moreover, a significant influence on the buckling force have both the piezosegment localization and the generated piezoelectric force.

Obtained results of the critical bucking forces for different types of beam end supports, different values of Winkler elastic foundation coefficient and piezoceramic plates have been compared with those presented in [1]. Results concerning controllability of the critical buckling load by the residual force have been compared with [2]. In both cases, obtained results show a good agreement.

REFERENCES

[1] Eryilman A., Atay M. T., Coskun S. B., Buckling of Euler Columns with a Continuous Elastic Restraint via Homotopy Analysis Method, Journal of Applied Mathematics, Vol. 2013, Article ID 341063, 8 pages, 2013. doi:10.1155/2013/341063.

[2] Przybylski J., Zagadnienia statyki i dynamiki smukłych układów mechanicznych ze zintegrowanymi elementami piezoceramicznymi, wyd. Politechniki Częstochowskiej, Częstochowa, 2012, pp. 36-74.

LOAD CAPACITY OF COLD-FORMED COLUMN MEMBERS OF LIPPED CHANNEL SECTION WITH PERFORATIONS OF DIFFERENT ARRANGEMENTS SUBJECTED TO COMPRESSION LOADING

M.P. KULATUNGA
School of Engineering & Built Environment, Glasgow Caledonian University
Glasgow, UK

M. MACDONALD
School of Engineering & Built Environment, Glasgow Caledonian University
Glasgow, UK

1. ABSTRACT

This paper describes the results obtained from experimental, numerical, and theoretical investigations into the load capacity of column members of lipped channel cross-section with perforations of different arrangements subjected to compression loading. Most of structural cold-formed steel members are typically manufactured with pre-punched perforations to accommodate, for example, electrical, plumbing and heating services. Due to the position, orientation and the shape of perforations, the elastic stiffness and ultimate strength of a structural member can be vary. The buckling behaviour of cold-formed steel structural members with lipped channel cross-section were used as columns, with perforations of different shapes studied and comparisons of the finite element results and the test results are also made with existing design specifications and conclusions are drawn on the basis of the comparisons.

2. INTRODUCTION

Cold-formed steel sections are widely used in storage racks, building structures, transportation machineries, domestic equipment, and other applications. The uses of cold-formed steel products are many and varied due to various characteristics such as their high strength-to-weight ratio, reliability and accuracy of profile, and ease of manufacture [1]. The behaviour of a structural member with perforations can vary with perforation size, position, shape and number of perforations and can limit the advantages of these structures [2], [3]. Hence, these can make the design and analysis of these members more complex.

3. NUMERICAL AND EXPERIMENTAL INVESTIGATIONS

The numerical results presented have been determined through the non-linear buckling analysis of column members of lipped channel cross-section with perforations using ANSYS finite element modelling software. In this study, a set of specimens of the same cross-section but with different perforation positions was tested as shown in Fig. 1.

Column lengths were kept constant, with perforations located at the mid-height of the column. Five cold-formed steel columns were tested to failure with fixed-fixed end conditions. Tensile tests of the lipped channel column materials were also carried out to determine the material properties.

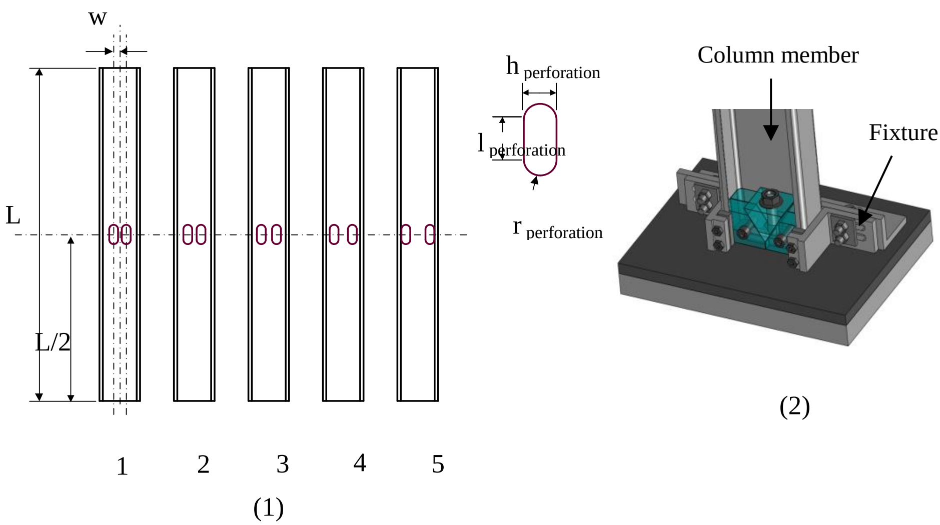

Fig. 1. (1) Perforation shapes and positions & (2) Fixed-end fixture

4. CONCLUSION

The ultimate strength of cold-formed steel lipped channel sections with perforations under pure compressive loading was shown to be accurately predicted by the Finite Element Analysis. As noticed during the experimental investigation, the presence of slotted holes on the web reduced the axial stiffness and also it can be clearly seen that a higher reduction in axial stiffness can be observed when the perforations are located near to the corners. The buckling investigation conducted has proven that the cold worked flat portions of the cross-section have lower yield strength compared to the corners. The FEA model in conjunction with the modifications proposed to the buckling design recommendations studied in this research work, and, based on the parametric study findings, this enables engineering judgements to be made before manufacturing the final product.

REFERENCES

[1] Rhodes, J., Design of Cold-Formed Steel Members: Elsevier Applied Science, England, 1991.

[2] Yu, W.W., Cold-Formed Steel Structures. 3rd ed. Canada: John Wiley & Sons Inc. ISBN 0-471-34809-0, 2000.

[3] ENV 1993-1-3: Eurocode 3, design of steel structures; part 1.3: General rules supplementary rules for cold formed thin gauge members and sheeting, 2009.

BUCKLING AND VIBRATIONS OF SEVEN-LAYER BEAMS WITH CROSSWISE CORRUGATED MAIN CORE

E. MAGNUCKA-BLANDZI, Z. WALCZAK
Institute of Mathematics, Poznan University of Technology
Piotrowo 3A, 60-965 Poznan, Poland

1. INTRODUCTION

Currently, layered structures are very common and used in many industries. Many articles are devoted to them. Theoretical base for thin-walled sandwich beams is presented in [1]. We refer the readers also to [2]. Carrera in the paper [2] formulated the zig-zag hypotheses for multilayered plates. Magnucki et al. [4] presented analytical and numerical (FEM) calculations as well as experimental verification of the obtained results devoted to a sandwich beam with a crosswise or lengthwise corrugated core. The considered beam was made of an aluminum alloy. The plane faces (outer layers) and the corrugated core were glued together. The present work was inspired also by the results obtained in the paper [3].

The subject of the study is one orthotropic thin-walled sandwich beam with trapezoidal core and three-layer facings. The outer layers of facings are flat, but inner layers are trapezoidal corrugated - in perpendicular direction to the corrugation of the main core. The beam is with crosswise corrugated main core and lengthwise corrugated inner layers of facings (Fig. 1). Metal of the flat or corrugated sheets is isotropic.

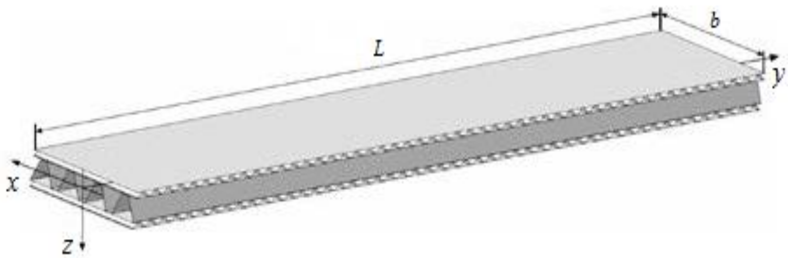

Fig. 1. Scheme of the beam with crosswise corrugated main core

The mathematical and physical model of this beam is formulated, which contains the hypothesis of deformation of the cross section, including the displacement and strain fields, and rigidities of the layers in particular directions.

2. ANALITICAL STUDIES

The analytical study includes formulation of mathematical model, the crucial parts of which are: the hypotheses related to deformation of the cross section of the beam, the description of displacement and stress fields for particular layers, formulation of equations of motion, and their solution.

The field of displacements of the cross section of the beam, strains and stresses are defined as follows:

- the outer sheets

$$v(y,z) = -t_{c1}\left(\zeta \frac{dw}{dy} \pm x_2\phi(y)\right),\ \varepsilon_y = -t_{c1}\left(\zeta \frac{d^2w}{dy^2} \pm x_2 \frac{d\phi}{dy}\right),\ \gamma_{yz} = 0\ ,\ \sigma_y = E\varepsilon_y\ ,$$

- the lengthwise corrugated cores of faces

$$v(y,z) = -t_{c1}\left\{\zeta \frac{dw}{dy} - \left[\zeta \pm \left(\frac{1}{2} + x_1\right)\right]\phi(y)\right\},\ \varepsilon_y = -t_{c1}\left\{\zeta \frac{d^2w}{dy^2} - \left[\zeta \pm \left(\frac{1}{2} + x_1\right)\right]\frac{d\phi}{dy}\right\},$$

$$\gamma_{yz} = \phi(y)\ ,\ \sigma_y = E_y^{(c2)}\varepsilon_y\ ,\ \tau_{yz} = G_{yz}^{(c2)}\phi(y)\ ,$$

- the inner sheets

$$v(y,z) = -t_{c1}\zeta \frac{dw}{dy},\ \varepsilon_y = -t_{c1}\zeta \frac{d^2w}{dy^2}\ ,\ \gamma_{yz} = 0\ ,\ \sigma_y = E\varepsilon_y\ ,$$

- the crosswise corrugated main core

$$v(y,z) = -t_{c1}\zeta \frac{dw}{dy},\ \varepsilon_y = -t_{c1}\zeta \frac{d^2w}{dy^2}\ ,\ \gamma_{yz} = 0\ ,\ \sigma_y = E_y^{(c1)}\varepsilon_y\ ,$$

where $\phi(y) = v_1(y)/t_{c2}$ - dimensionless function, $\zeta = z/t_{c1}$ - dimensionless coordinate, $x_1 = t_s/t_{c1}$, $x_2 = t_{c2}/t_{c1}$ - dimensionless parameters.

Based on Hamilton's principle the equations of motion are derived for the considered beam and their analytical solutions are given. The detailed calculations have been realised for the simply supported beam subjected to axial compression. The critical load is calculated, and the natural frequency of the beam.

ACKNOWLEDGEMENTS

The project was funded by the National Science Centre allocated on the basis of the decision number DEC-2013/09/B/ST8/00170.

REFERENCES

[1] Ventsel E., Krauthammer T., Thin plates and shells. Theory, analysis and applications, New York, Basel: Marcel Dekker, Inc, 2001.

[2] Carrera E., Historical review of Zig-Zag theories for multi-layered plates and shells, Applied Mechanics Reviews 56(3), 2003, pp. 287-308.

[3] Magnucki K., Kuligowski P., Krus M., Magnucka-Blandzi E., Bending and buckling of orthotropic sandwich beams with three-layer faces, Coupled instabilities in metal structures. Proceedings of the 6-th International Conference on Coupled Instabilities in Metal Structures held in Glasgow, Scotland, 2012, pp. 587-594.

[4] Magnucki K., Jasion P., Krus M., Kuligowski P., Wittenbeck L., Strength and buckling of sandwich beams with corrugated core, Journal of Theoretical and Applied Mechanics 51, 2013, pp. 15-24.

POST-BUCKLING ANALYSIS OF CORRUGATED SHELL UNDER EXTERNAL PRESSURE AND CONCENTRATED LOADS

M. MALINOWSKI
Faculty of Mechanical Engineering, University of Zielona Góra, Poland
Szafrana 4, 65-516 Zielona Góra, Poland

1. INTRODUCTION

Shell structures, in particular vessels or retort furnaces are widely used for storing loose materials, liquid or are used for the heat treating process. In these thin-walled structures pre-buckling, buckling state and post-buckling conditions play a major role in design process and should be precisely analyzed. The retort of furnace usually is a circular cylindrical shell with smooth wall and is made of stainless steel. An alternative method of increasing the shell stiffness and general instability resistance of the cylindrical shell is the introduction of corrugations. The buckling and vibration of corrugated composite cylinder is presented by Ross and Little [1, 2]. The elastic buckling of pressure vessels with ellipsoidal heads was analyzed by Magnucki [3].

In this paper an analysis of corrugated shell based on the non-linear procedure is presented. The equilibrium paths for elastic and elastic-plastic mechanical properties were plotted. The results of the analyses were obtained with the use of ANSYS system.

2. BASIC ASSUMPTION

A corrugated shell proposed in the paper consists of an ellipsoidal head and a flange and is simply supported to head wall and the bottom part of the shell. The main dimensions of the shell are presented in Fig. 1. The shell is restrained on the flange and subjected to external pressure p and concentrated loads F_i at temperature $T=350^oC$. Mechanical properties of material: Young's modulus E=191GPa, Poisson's ratio $\nu=0.3$, yield strength $R_{p0,2}$=202MPa. The geometrical parameters: R=0.71m, L=1.8m, b=0.8m, h_c=0.015m, L_c=0.08m, R_c=0.018m, t=3, 4mm, t_h=4, 5mm. Load capacity is ΣF_i=1200kg.

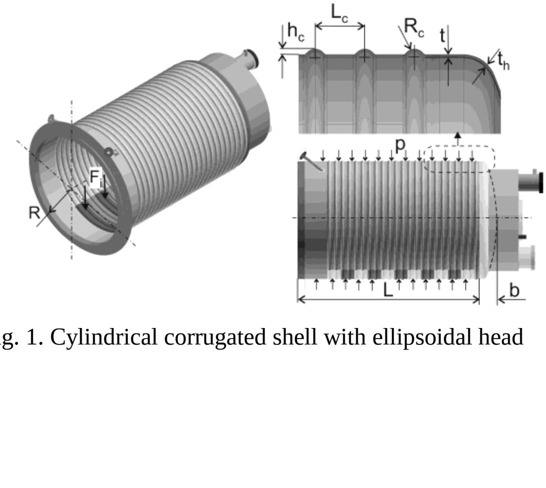

Fig. 1. Cylindrical corrugated shell with ellipsoidal head

3. FEM ANALYSIS AND RESULTS

The FEM mesh of corrugated shell is created by element SHELL181. To start the non-linear procedure based on the arc-length method small initial geometrical imperfections have been introduced into the perfect model. The shape of imperfections had the form of: a) only the first eigenmode; b) the first 10 eigenmodes. The maximum deviation from the perfect structure was equal w_0/t=1, 2. The analysis has been performed to check the influence of elasticity and bilinear characteristic of material on stability. Examples of equilibrium paths are shown in Fig. 2. The equilibrium paths are stable and for two cases a snap-through phenomena is observed.

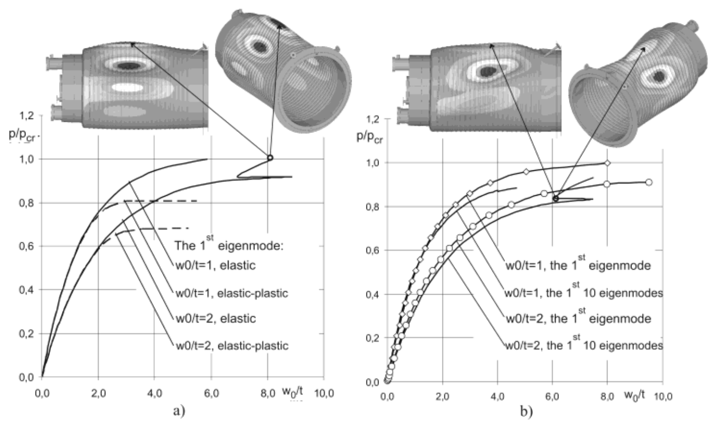

Fig. 2. Equilibrium paths of corrugated shell: elastic and elastic-plastic properties, t=3mm, t_h=4mm (a); elastic properties, t=4mm, t_h=5mm (b)

4. CONCLUSIONS

Load is not axially symmetric and clearly affects the buckling shapes and has the influence on stability in post-critical range. According to the results shown in the paper the dimensionless pressure for non-linear (elastic-perfect plastic) and linear mechanical properties are about 20-25 percent lower. The calculated deformations of the shell and equilibrium paths with or without snap-through indicate a relatively high sensitivity of the shell on the wall thickness, material model, and single or multimode imperfection pattern.

REFERENCES

[1] Ross C., Little S., The buckling of a corrugated carbon fibre cylinder under external hydrostatic pressure, Ocean Engineering, 28, 2001, pp. 1247-1264.

[2] Ross C., Little A., Köster P., Tewkesbury G., Vibration of a thin-walled carbon fibre corrugated circular cylinder under external water pressure, Thin Walled Structures, 44, 2006, pp. 542-553.

[3] Magnucki K., Strength and optimization of thin walled vessels, PWN, 1998, pp. 168 (in Polish).

ON CRITICAL AND SUPERCRITICAL REGIMES OF RESPONSE OF TIMOSHENKO BEAM ON ELASTIC FOUNDATION TO MOVING LOAD

A. I. MANEVICH, A. S. ZEMLICH

Department of Computational Mechanics and Strength of Materials
Dniepropetrovsk National University,
Gagarin av. 72, 49050 Dniepropetrovsk, Ukraine

The stationary response of a Timoshenko beam (TB) on the elastic foundation to a moving load is studied with emphasis on critical velocities and features of supercritical regimes. Investigations of dynamics of the TB on elastic foundation were carried out beginning from 1950's (S. H. Crandall, 1957, J. D. Achenbach and C. T. Sun, 1965, and others) and have been summarized in [1], [2]. There has been shown that the responses for infinite and semi-infinite beams at constant velocity of the load always approach stationary running waves ("steady-state solutions"), and three critical (or characteristic) values of velocity exist in TB (in distinction on a single critical velocity in classical Euler-Bernoulli model), at which amplitudes of waves become unbounded (in case of concentrated load). The first critical velocity corresponds to the minimal phase velocity v_*, two others relate to velocities of shear and longitudinal waves v_s and v_l.

But complete analysis of all types of the beam responses in different ranges of velocity, that depend on parameters of the beam and foundation, becomes rather complicated for the TB, especially in supercritical cases (Fryba L. in [2, part 5, p. 23.2] has distinguished 18 possible cases). In addition, this complex picture has not a transparent physical interpretation.

The aim of this report is to show that the description of various response types in entire range of the load velocity and understanding of the physical essence of the problem are considerably simplified by analyzing dispersion curves (phase velocity - wave number) for free waves and parametrical curves in plane of two parameters of the characteristic biquadrate equation. It is shown that one should discern two types of dispersion curves, depending on a normalized foundation stiffness parameter.

For the first type dispersion curves, relating to weak and moderate foundations, three abovementioned critical velocities exist, and the minimal critical value rises with increasing foundation stiffness. Four general cases of the beam response depending on the load velocity (in intervals $v < v_*$, $v_* < v < v_s$, $v_s < v < v_l$, $v > v_l$) and three special cases ($v = v_*$, $v = v_s$,, $v = v_l$) are possible. Peculiarities of these responses also can be predicted based on the dispersion relations.

In case of the second type dispersion curves (stiff foundation) the first value v_* coincides with v_s, so only two critical velocities remain, and they do not change at further increase of foundation stiffness. Three general cases of response (in intervals $v < v_s$, $v_s < v < v_l$, $v > v_l$) and two special cases ($v = v_s$, $v = v_l$) are possible.

On the whole, solutions for all the cases are defined by a few analytical expressions.

The parametrical curves in plane of two parameters of the characteristic equation give additional possibilities for prediction of the sequence of regime changes with increasing velocity.

The mapping between the characteristic velocities and supercritical regimes, from one side, and shape of the dispersion relations and parametrical curves, from other side, gives a clear understanding of the physical nature of the problem.

REFERENCES

[1] Grigoliuk E. I., Selezov I. T., Nonclassical theories of oscillations of rods, plates and shells. - in: "Itogi nauki i tekhniki", Series: Mekhanika tviordykh deformiruemykh tel, 5, Moscow, VINITI (1973) (in Russian).

[2] Fryba L., Vibration of Solids and Structures under Moving Loads, 1st edition, 1972, Noordhoff; 3rd edition, Thomas Telford Ltd., 1999.

EXPERIMENTAL BUCKLING TESTS OF FML PROFILES

R. J. MANIA
Department of Strength of Materials, Lodz University of Technology
Stefanowskiego 1/15, 90-924 Łódź, Poland

1. INTRODUCTION

For different structural members one can find different theoretical approach which allow for considered structural member the strength, load carrying capacity or failure conditions to determine. Each one of standing for application methods are based on some assumptions and requirements. Therefore their applicability for specific structure element requires some kind of validations. This should be achieved before the real structure creation than in monitoring its behaviour in real loading conditions. For years an effective way of comparison has been experimental testing of scaled or full dimension members [3]. In the case of aircraft thin-walled structures this method is of special meaning especially for loads which can be source of these elements buckling [4].

The subject of this research were thin-walled profiles made of Fiber Metal Laminate material type, with 3-2 stacking sequences where 0.3 mm aluminium was of 2024 T3 lot and composite layers were made of glass fiber reinforced epoxy resin (TVR 380 M12/R). Each one of composite layers was created of two 0.26 mm prepreg plays of specific orientation angle - equal or different, but always giving sequence symmetry with respect to plate mid-plane, to avoid coupling effects. Considered profile shapes and overall dimensions are given in Fig. 1. These dimensions correspond to fuselage stringer size and fulfil thin-walled plate theory limits. Three specimens of each case of stacking were manufactured. All specimens were subjected to axial uniform compression.

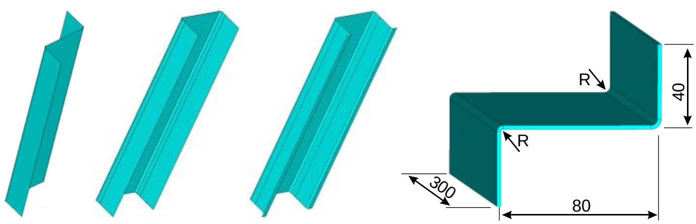

Fig. 1. Cross-section shapes and dimensions of tested profiles

2. FULL SCALE MODEL BUCKLING TEST PROCEDURE

The buckling experiments were carried on in the classical tensile test machine. It was equipped with special supporting rigs with milled flat bottom groves allowing freedom of rotation (Fig. 2), where profile loaded edges were constrained [4]. With two pairs of back-to-back bonded strain gauges - one pair in the geometrical centre of the web and one in the middle of flange edge, compressive and bending strains were measured.

The deflection of these two locations were measured with two laser beam devices. All data was registered for further processing.

a) 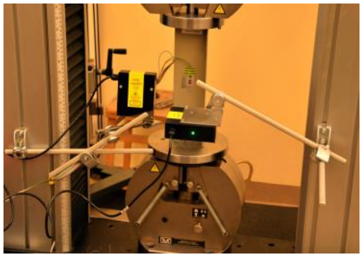

Fig. 2. Experimental test rig with measuring devices

There are many 'widely used' techniques for buckling load determinations based on measured strains and/or deflections [2]. Some of them were applied in this research to buckling load determination [4]. The exemplary results obtained with strain inversion method are presented in Fig. 3 with reference to FEM computation results. The broader comparison of all performed analysis with their mutual comparison, will be given during the Symposium.

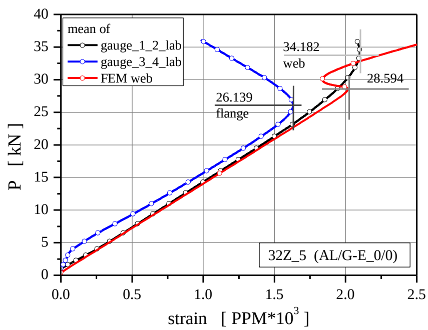

Fig. 3. Buckling load determination with 'strain inverse method'
an example of Z-shape profile investigation

ACKNOWLEDGMENTS: Research carried out within the project UMO-2012/07/B/ST8/04093 funded by the state funds designated by NCN.

REFERENCES

[1] Mania R.J., Buckling and post-buckling of FML compressed open cross section profiles, 3rd Int. Conf. on Buckling and Postbuckling Behaviour of Comp. Lami. Shell Struc., Braunschweig, 2015.

[2] Rhodes J., Zaras J., Determination of critical loads by experimental methods. Kolakowski Z., Kowal-Michalska K. (eds.), Statics, dynamics and stability of structures, Vol. 2, TUL Series of Monographs, 2012, pp. 477-499.

[3] Singer J., Arbocz J., Weller T., Buckling Experiments: Experimental Methods in Buckling of Thin-Walled Structures, Willey, 1998.

[4] Verelom J., The development of a design tool for Fibre Metal Laminates compression panels, PhD, Delft TU, 1995.

MAXIMUM ELASTIC BUCKLING RESISTANCE OF COLUMNS OF CONSTANT VOLUME

J. MARCINOWSKI
Institute of Building Engineering, University of Zielona Góra
Szafrana 1, 65-516 Zielona Góra, Poland

J. L. Lagrange (1770) was probable the first scientist who attempted to determine the optimum shape of a compressed column with respect to the stability criterion. Clausen (1853) confirmed that a "bellied" column is the strongest. A. Volmir mentions in his monograph some works of Soviet scientists from late fifties of XX-th century and presents an interesting solution. Also today many investigators study the mechanical behaviour of columns looking for its optimal shape.

In this paper, the optimal column was defined as the strongest, elastic column of a given length and volume which can carry the highest axial load without buckling. Pin-ended columns loaded by the force applied at the movable end are considered. Shape of the column which is a solid of revolution is defined by the function $r(x)$ defining the current radius of circular cross section. The solid, cylindrical column of the constant radius r_0 and the length L is treated as the starting point of the optimisation procedure leading to the strongest column. It was assumed that the initial volume $V_0 = \pi\, r_0^2\, L$ remains constant, it means that some portion of material can be shifted to the other location in such a way that the column will remain the solid body of revolution.

Due to the symmetry of the problem, it was assumed that all considered functions $r(x)$ are symmetric with respect to the section $x = L/2$ (comp. Fig.1).

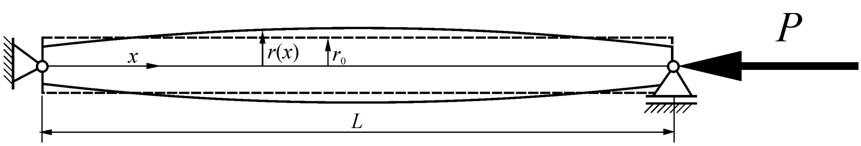

Fig. 1. The compressed column

In the problem defined above, the searched profile curve defining the shape of the column being the solid of revolution depends on two variable parameters C_1 and C_2. One can express this fact writing the profile function in general form like this: $r(x) = r(x;\, C_1,\, C_2)$. The first parameter is determined from the condition that volume remains constant. This condition can be expressed in the following form

$$\int_0^L \left[r(x; C_1, C_2)\right]^2 dx = r_0^2\, L \tag{1}$$

As a result the only one variable parameter remains because from (1) the parameter C_2 can be expressed by C_1. In this stage of the analysis the parameter C_1 is the single, variable parameter of the problem.

To find the parameter C_1 defining the searched optimal column's shape the energetic criterion of the column's stability was exploited. The Rayleigh quotient in the following form was used

$$P(C_1) = E \frac{\int_0^L \left(w_b^I\right)^2 dx}{\frac{4}{\pi}\int_0^L \frac{w_b^2}{\left[r(x;C_1)\right]^4} dx} \quad , \tag{2}$$

in which w_b is the buckling mode function adopted in the form of the single half wave sinus. Solving this equation for the whole possible range of the parameter C_1 one can find the particular value corresponding to the highest value of P. In such a way the profile curve $r^{opt}(x)$ of optimal column was obtained.

The value of P obtained from Eqn. (2) is approximate and its exact value was determined on the basis of two differential equations of stability of pin-ended column. The first one adopts the form

$$E\,\frac{\pi}{4}\left[r^{opt}(x)\right]^4 w^{II}(x) + P\,[w(x) + f(x)] = 0\,, \tag{3}$$

in which E - the Young's modulus, $w(x)$ - the searched buckling function, $f(x)$ - the function defining the initial imperfection, and P - the axial force. The function $f(x)$ was adopted as the single half wave sinus with very small amplitude. This differential equation was solved numerically for different values of P. The searched critical force was obtained as the value of P causing the significant (let us say L/10) deflection $w(x)$.

The other differential equation used to determination of the exact value of P_{kr} was the following

$$E\,\frac{\pi}{4}\left[r^{opt}(x)\right]^4 w^{II}(x) + P\,w(x) + M = 0 \tag{4}$$

in which M - the bending moment applied at both ends of the column treated as a load disturbance. In calculations it was assumed that M is very small. Similarly as above the searched critical force was obtained as the value of P causing the significant deflection $w(x)$. Equations (3) and (4) with proper boundary conditions were solved numerically by means of *Mathematica* system. All other derivations and calculations were performed in this system as well.

Optimum shapes were obtained for four different classes of functions. Final results were confirmed also in numerical analyses performed by means of the commercial system based on the finite element method.

It is interesting that in all analysed cases the resulting maximum elastic buckling resistance was about 30 % greater than its counterpart for the case of the cylindrical column of constant radius and the same volume.

GBT-BASED BUCKLING ANALYSIS OF RACK SYSTEMS IN THE FRAMEWORK OF ECBL APPROACH

S. DE MIRANDA, D. MELCHIONDA
DICAM, University of Bologna
Viale Risorgimento 2, 40136 Bologna, Italy

V. UNGUREANU, D. DUBINA
Politehnica University of Timisoara, Ioan Curea 1, 300224 Timisoara, Romania
Romanian Academy - Timisoara Branch
Mihai Viteazu 24, 300223 Timisoara, Romania

The Erosion of Critical Bifurcation Load (ECBL) is a practical and convenient tool to characterize the instability behaviour of thin-walled cold-formed steel members [1]. It represents a way to adopt the actual European buckling curves for cold-formed sections by calibrating new α imperfection coefficients. This approach avoids the use of curves obtained for hot-rolled ones and allows to design more accurately complex elements like rack systems. In order to apply the ECBL approach, it is necessary to study the critical and post-critical behaviour of the members. In particular, this approach applies in the instability mode interaction with the erosion of the critical bifurcation load referred to a case of interaction of two or more buckling modes associated with the same critical load.

As it is well known, the Generalized Beam Theory (GBT) is a powerful tool to study thin-walled members and GBT finite element analyses can be effectively used to evaluate the effects of mode interaction. The GBT was originally proposed by Schardt in the 60s [2] and is a thin-walled beam theory able of capturing cross-section in-plane and out-of-plane (warping) deformation through the inclusion of additional degrees of freedom, the so-called “cross-section deformation modes”. Later, many authors have contributed to the improvement of the GBT. In particular, most part of the contributions came from Davies and co-workers [3] and from Camotim and co-workers [4].

With this in mind, the systematic use of the GBT to find the mode interaction points is presented in this work. Reference is made to the formulation of the GBT with shear deformation recently presented in [5] that, thanks to new definitions of the kinematic parameters and of the generalized deformations, allows establishing a clear relationship between the GBT results and those of the classical beam theories [6], an important issue to apply the GBT in the current engineering practice.

In the present work, much attention is devoted to analyse how the boundary conditions and the section properties affect the mode interaction points. As an example, Fig. 1(a) shows the results of a parametric analysis of the rack member RSB125 without holes loaded in compression. Several analyses have been performed varying the thickness, the half-wavelengths and considering various boundary conditions, like Simple support-Simple support (SS), Simple support-Clamped (SC), Clamped-Clamped (CC). In particular, in this example the thickness ranges between 0.7 mm and 3.2 mm, the half-wavelengths between 5 mm and 5000 mm so covering the most design-interesting geometrical dimensions. Local-distortional, local-global and distortional-global interaction points are shown in Fig. 1(b). As it can be noted, they tend to create well delimited areas. Also intermediate boundary conditions, with warping restrained, can be taken into account. These numerical results are useful in the ECBL approach in order simplify the design process and also open a way to find simplified functions describing mode interaction behaviour.

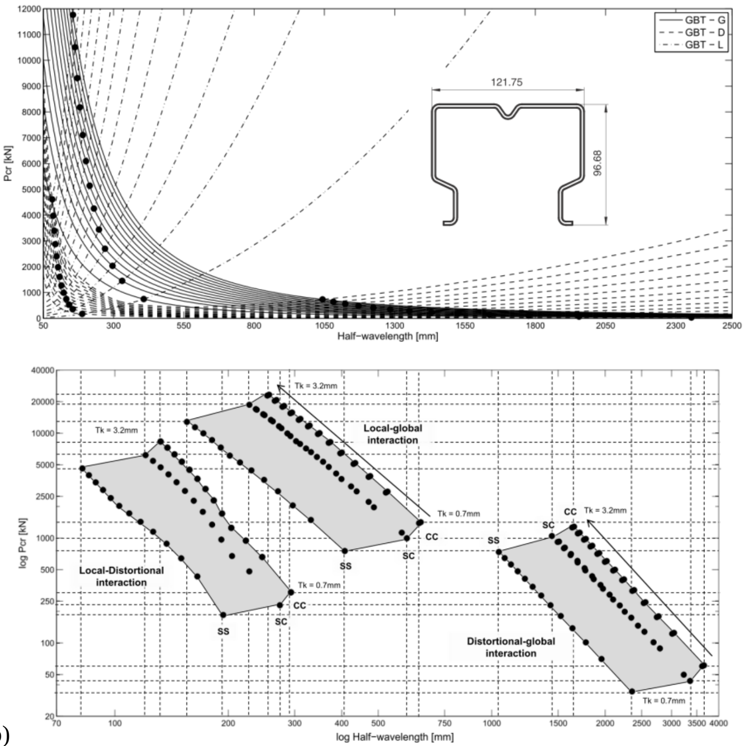

(a)

(b)

Fig. 1. RSB125 mode interaction points

REFERENCES

[1] Dubina D., Ungureanu V., Instability mode interaction: From Van Der Neut model to ECBL approach, Thin-Walled Structures 81, 2014, pp. 39-49.

[2] Schardt, R.P., Verallgemeinerte Technische Biegetheorie, Springer, Berlin, 1989.

[3] Jiang C., Davies J.M., Design of Thin-Walled Purlins for Distortional Buckling, Thin-Walled Structures 29, 1997, pp. 189-202.

[4] Abambres M., Camotim D., Silvestre N., GBT-based elastic–plastic post-buckling analysis of stainless steel thin-walled members, Thin-Walled Structures 83, 2014, pp. 85-102.

[5] de Miranda S., Gutierrez A., Miletta R., Ubertini F., A generalized beam theory with shear deformation, Thin-Walled Structures, 67(2013), pp. 88-100.

[6] de Miranda S., Madeo A., Miletta R., Ubertini F., On the relationship of the shear deformable Generalized Beam Theory with classical and non-classical theories, International Journal of Solids and Structures, 51(2014), pp. 3698–3709.

EXPERIMENTAL AND NUMERICAL ANALYSIS OF FATIGUE DAMAGE OF COMPOSITE PLATES WITH HOLES

A. MUC, M. BARSKI, P. PASTUSZAK
Faculty of Mechanical Engineering, Cracow University of Technology
al. Jana Pawła II 37, 31-864 Kraków, Poland

1. COMPOSITE PLATE

The investigated plates consist of plies, which are made of a glass fabric and epoxy resin. The approximate properties of the single layer are shown in the Table 1. The laminate minimal layer thickness is of t_{LAYER}=0.125[mm]. The dimensions of specimens are as follows: the nominal thickness is equal to t_c=5[mm], the length L_p=250[mm], the width W_p=250[mm] and the radius of the circular hole is equal to R_c=10[mm]. The elliptical shape of the hole is also taken under consideration.

Table 1. Material properties of single layer for glass fibre and epoxy resin

Elastic properties		Strength parameters	
E_{11}	46.00 [GPa]	X_t	245 [MPa]
E_{22}	46.00 [GPa]	Y_t	245 [MPa]
G_{12}	3.600 [GPa]	Z_t	245 [MPa]
ν_{12}	0.130	S_{12}	80 [MPa]

The opposite edges of the analysed plate are clamped. However one edge can move in vertical direction. The considered plate is subjected to uniform compression. In the experiment the load is applied with the aid of the hydraulic device. In the numerical simulations the load is applied by the uniform displacement of one edge (displacement control). The compression cause the stress concentration in the vicinity of the hole. This effect could causes the local failure of the composite material and in consequence global failure of the structure. In the other hand, the investigated structure could also be exposed on a loss of stability in the global sense. This phenomenon should be treated as the form of the global failure of the structure [1]. Therefore the main aim of the presented work is to find out which form of failure will be observed in the case of the investigated plate. Additionally, the character of the local damages of the composite materials are very similar than in the case of the gradually increasing fatigue damages. Thus the currently presented work should be also treated as the introduction to the analysis of the fatigue phenomenon.

The numerical analysis is carried out with the use of commercially available software ANSYS 12.1. The mentioned software is based on the finite element method. Generally, the analysis consists of two stages. At the very beginning, a simple linear buckling analysis is carried out in order to evaluate the value of the critical loading multipliers and the corresponding eigenvectors. These results are very useful, when the influence of the geometric imperfection is taken under consideration. In the second stage, the geometric imperfections are introduced and the displacement in the axial direction is applied. The FEM model of the investigated structure is created with the use of the higher order, multilayered shell elements SHELL281 [2]. The results obtained from the numerical simulations and experiment are very similar. In the Fig 1. the experimental and numerical results are presented.

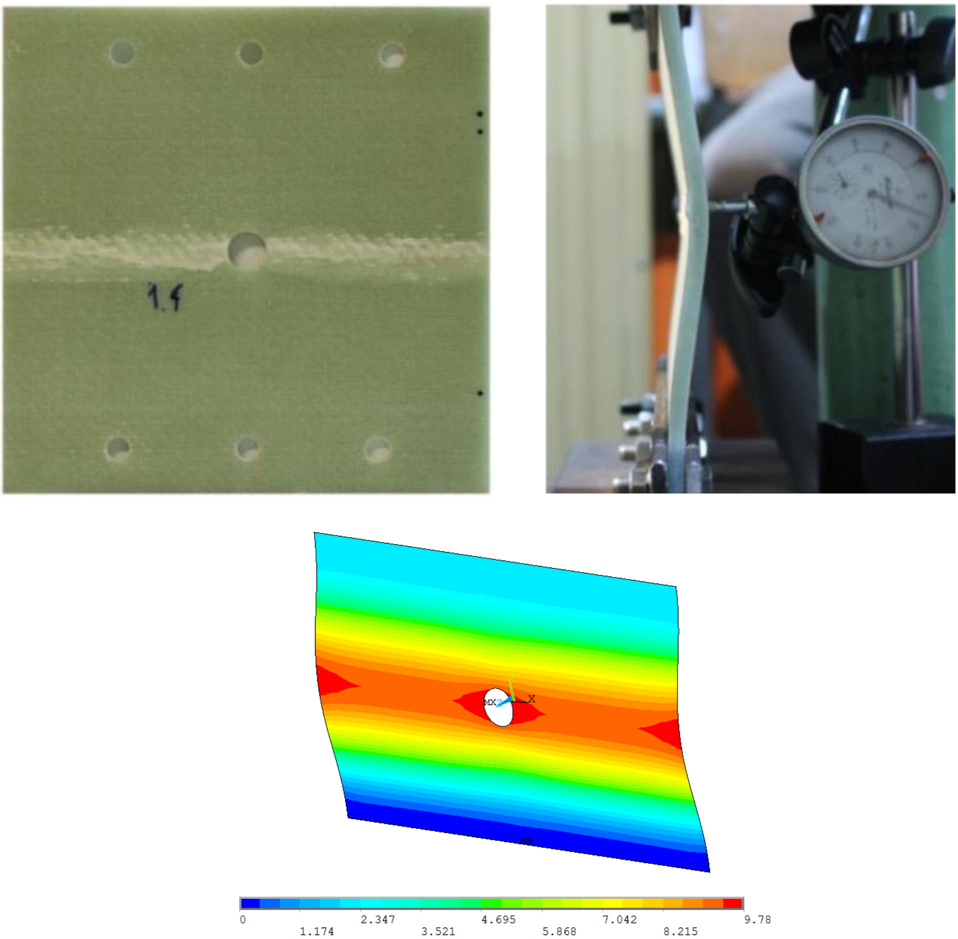

Fig. 1. The obtained results - damaged plate and the form of the loss of stability

REFERENCES

[1] Muc A., Mechanika kompozytów włóknistych, Księgarnia Akademicka, Kraków, 2003.
[2] Barbero E. J., Finite element analysis of composite materials, Taylor & Francis Group, New York, 2008

NUMERICAL ANALYSIS OF DAMAGE IN COMPOSITE CYLINDRICAL PANELS WITH CIRCULAR HOLES

A. MUC, M. BARSKI, A. STAWIARSKI
Faculty of Mechanical Engineering , Cracow University of Technology
al. Jana Pawła II 37, 31-864 Kraków, Poland

1. COMPOSITE CYLINDRICAL PANEL

The investigated composite panel is made of 8 layers with the following stacking sequence: $[0/90/0/90/0]_S$, where "s" denotes a symmetry. The material of each layer is Hexcel TVR 380 M12/R-glass unidirectional prepreg. The properties of the single layer are shown in the Table 1. The dimensions of specimens are as follows: the nominal thickness is equal to t_c=2[mm], the length L_p=300[mm], the width W_p=180[mm], the inner radius R_p=92[mm] and the radius of the circular hole is equal to R_c=10[mm]. The laminate has a nominal fiber volume of v_f=60[%] and a ply thickness t_{LAYER}=0.25[mm].

Table 1. Material properties of single layer for TVR 380 M12/R-glass

Elastic properties		Strength parameters	
E_{11}	46.43 [GPa]	X_t	1534 [MPa]
E_{22}	14.92 [GPa]	Y_t	74.50 [MPa]
G_{12}	5.233 [GPa]	Z_t	74.50 [MPa]
ν_{12}	0.269	S_{12}	57.55 [MPa]

The both ends of the structure are clamped. However one end can move in axial direction. The considered panel is subjected to axial compression and the load is applied by the uniform displacement of the one end (displacement control). The compression cause the stress concentration in the vicinity of the hole. This effect could cause the local failure of the composite material and in consequence global failure of the structure. In the other hand, the investigated structure could also be exposed on a loss of stability. This phenomenon should be treated as the form of the global failure of the structure [1]. Therefore the main aim of the presented work is to find out which form of failure will be observed in the case of the investigated panel.

2. NUMERICAL ANALYSIS

The numerical analysis is carried out with the use of commercially available software ANSYS 12.1. The mentioned software is based on the finite element method. Generally, the analysis consists of two stages. At the very beginning, a simple linear buckling analysis is carried out in order to evaluate the value of the critical loading multipliers and the corresponding eigenvectors. These results are very useful, when the influence of the geometric imperfection is taken under consideration. In the second stage, the geometric imperfections are introduced and the displacement in the axial direction is applied. Due to the expected large magnitude of deformation, the analysis is performed in the geometrically nonlinear range. The nonlinear problem is solved with the aid of the Newton - Raphson algorithm. The FEM model of the investigated structure is created with the use of the higher order, multilayered shell elements SHELL281. These elements are especially dedicated to the analysis of composite structure [2]. They have 6 degrees of freedom in each node, namely 3 translations and 3 rotations. The example of the obtained results are shown in the Fig. 1.

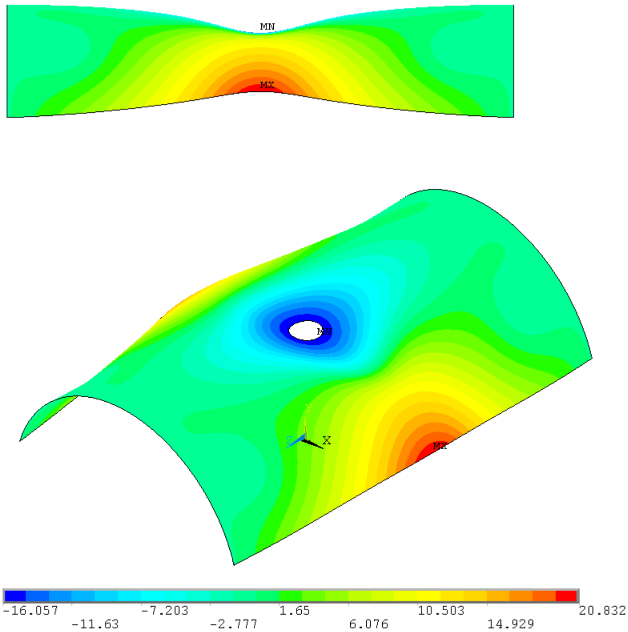

Fig. 1. The radial component of deformation of the composite cylindrical panel with a hole

The presented above shape of deformation is obtained without introducing geometrical imperfection. The final value of the reached axial displacement is equal to UZ=2.5[mm]. The numerical analysis is repeated for the panels with the hole of a different radius. Moreover, in the case of the real shell structure the influence of the imperfection is significant. Thus in the present work the influence of the imperfection is also analysed. Generally, the analysis is limited by the stress concentration localized in the vicinity of the hole, which causes the material damage.

REFERENCES

[1] Muc A., Mechanika kompozytów włóknistych, Księgarnia Akademicka, Kraków, 2003.
[2] Barbero E. J., Finite element analysis of composite materials, Taylor & Francis Group, New York, 2008.

ANALYSIS OF DYNAMIC STABILITY OF ROD STRUCTURES

P. OBARA
Faculty of Civil and Environmental Engineering, Kielce University of Technology
Aleja Tysiąclecia Państwa Polskiego 7, 25-323 Kielce, Poland

1. INTRODUCTION

Analysis of dynamic stability of rod structures was performed in this paper. Two methods: harmonic balance method [1] and small parameter method [2] were used for determination of parametric resonance areas. Both of these methods are based on analysis of the particular solution of the differential equations derived from Floquet's theory. The aim of this work is to present the superiority of small parameter method (SPM) over commonly used harmonic balance method (HBM). Using SPM the simple formula to determine the resonance frequency of the periodic load has been derived. The effects of the shear deformation, rotatory inertia and damping effects on the instability areas of structures are discussed in detail. The analysis uses the finite element method with beam elements without axial deformability. Calculations were performed using the program Mathematica.

2. REGIONS OF DYNAMIC INSTABILITY

The system of equations of motion can be included in the class Mathieu-Hill differential equations with periodic coefficient:

$$\left(\mathbf{M}+\mathbf{M}^{*}\right)\ddot{\mathbf{q}}(t)+\mathbf{C}\dot{\mathbf{q}}(t)+\left(\mathbf{K}-S_o\mathbf{K}_G\right)\mathbf{q}(t)-S_t\cos(\theta t)\mathbf{K}_G\mathbf{q}(t)=\mathbf{0} \tag{1}$$

where:

S_o - static component of periodic force,
S_t - amplitude of periodic force,
θ - frequency of periodic force,
$\mathbf{q}(t)$ - vector of the degrees of freedom,
$\mathbf{M}$ - mass matrix,
$\mathbf{M}^{*}$ - rotatory inertia matrix,
$\mathbf{C}$ - damping matrix,
$\mathbf{K}$ - stiffness matrix,
$\mathbf{K}_G$ - incremental (or geometric) stiffness matrix.

Taking into account the effects of the shear deformation in considering means that above matrices contain correction parameter ζ, which depend on Young's modulus E, Kirchhoff's modulus G, area of cross-section A, moment of inertia I and shear coefficient κ. These matrices were derived by approximation of displacement fields by physical shape functions [3].

Based on (1) the main instability regions on the plane of parameters defining the load (S_0, S_t, θ) and the properties of the structures like the critical force S_e and the free vibration frequency Ω_0, were determined. If we omit damping effects the use of the harmonic balance method requires solving the following equation:

$$\left| \mathbf{K} - \left(S_0 \pm \frac{1}{2} S_t \right) \mathbf{K}_G - \frac{\theta^2}{4} \left(\mathbf{M} + \mathbf{M}^* \right) \right| = 0 \tag{2}$$

whereas in the case of small parameter method (for $S_0 = 0.5 S_e$), for first-order approximation, we obtain the following formula:

$$\theta = 2\Omega_{01} \sqrt{1 \pm \frac{1}{2} S_t K_{G11}^* \frac{1}{\Omega_{01}^2}} \tag{3}$$

where:

Ω_{01} - first free vibration frequency including static component of periodic force,

K_{G11}^* - first element of M-orthonormal geometric stiffness matrix.

The analyses show that both methods give the same results, but compared (2) and (3), it is concluded that the small parameter method is simpler than the harmonic balance method. In the first case it is necessary to use the FEM algorithm and operate on matrices (matrix size depends on the number of degrees of freedom); whereas in the second - it is enough to know the first free vibration frequency and the first element of geometric stiffness matrix.

If we take into account the effects of dissipation forces SPM leads to:

$$\theta = 2\Omega_{01} \sqrt{1 + \frac{1}{2} S_t K_{G11}^* \frac{1}{\Omega_{01}^2} \left(\frac{1}{4} C_{11}^* \pm 1 \right)} \tag{4}$$

where

C_{11}^* - first element of damping matrix.

REFERENCES

[1] Majorana C.E., Dynamic stability of elastic structures: a finite element approach, Computers & Structures 69, 1998, pp. 11-25.
[2] Cunningham W.J., Analiza układów nieliniowych, WNT, Warszawa, 1962.
[3] Gilewski W., Gomuliński A., Physical shape functions: a new concept in finite elements, Finite Elements News 3, 1990, pp. 20-23.

MODIFICATION OF COMPOSITE BEAM CONFIGURATION BY EXPLOSIVELY INDUCED DELAMINATION

M. OSTROWSKI
Invenco R&D company Bernardyńska 21/69 02-904, Warszawa, Poland

1. INTRODUCTION

Passive control of crash or impact event may be based on change of mechanical characteristics due to modification of inner structural connections. The paper covers numerical and experimental analysis of sandwich fabric composite cantilever beam subjected to low velocity impact. A set of metallic electrical conductors was placed between composite layers causing their delamination when subjected to electrical explosion. In result separation of initially connected components in the vicinity of used conductor is obtained leading to change of their mechanical characteristics, allowing for discrete control of global beam behavior.

2. ELECTRICAL BRIDGE WIRE FOR EXPLOSIVE DELAMINATION

Exploding bridge wire (EBW) phenomenon is known from the end of the 18th century [1] and being in use today, mainly for ignition of high explosive materials [2] as well as in physics of high energy [3]. This effect is caused by a rapid heating of a conductor subjected to a pulse of high voltage electric current, what changes its state of matter from solid to vapor, expanding in surrounding continua and forming a strong pressure wave. Afterwards, in result of current discharge through the formed plasma channel, additional heat is applied to the system increasing the effect. Depending of explosion parameters and properties of continua elastic, elasto-plastic or shock waves can be observed. In case of action on the composite, exploding wire embedded between layers acts on adjacent surfaces causing their progressive separation in the vicinity of explosion. Delamination is being extended by the pressure acting in normal direction decoupling adhesive. Figure 1 depicts example delamination process.

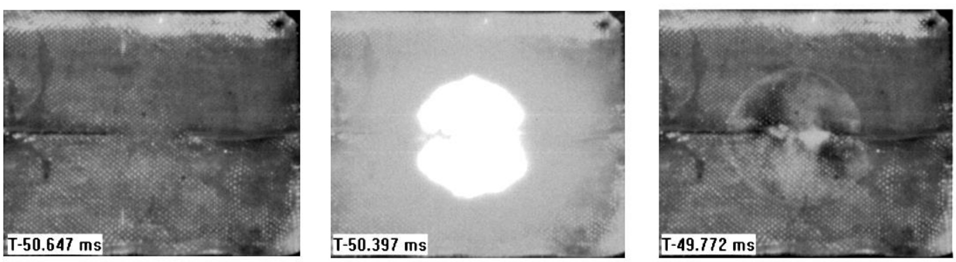

Fig. 1. Sequence of explosive delamination of a composite

3. CANTILEVER BEAM MODIFIED BY INTRODUCED DELAMINATION

A cantilever beam made of layered sandwich composite was modelled with shell finite elements. Problem was solved in a commercial FEM LS-DYNA package using explicit time integration with nonlinear material and geometric formulation. The delamination was simulated by a controlled separation of a connection between layers in the area surrounding the predefined location of the wire. The initiation time of layers' separation was one of controllable parameters allowing for a wide search for solution dependencies. Fig. 2 shows example set of solutions obtained for a beam subjected to an impact at its end for different localization of exploding wire and delamination introduction time set to 52 ms after the beginning of the simulation. Length of the beam was 300 mm, a width 100 mm, thickness between layers midsurfaces 3 mm, delamination area 90 mm × 90 mm.

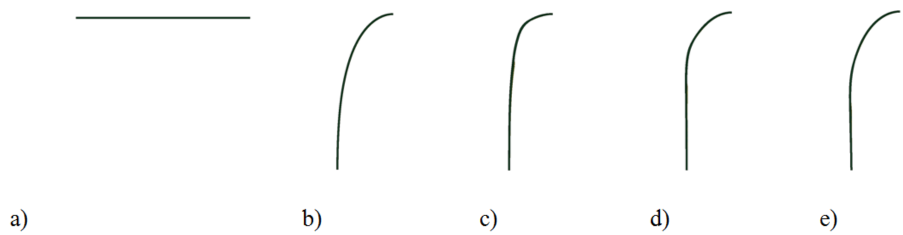

Fig. 2. Results of transverse impact simulation into a sandwich composite beam (side view): a-initial state (0 ms), b - passive state (no delamination, 52 ms), c - delamination centre located 80 mm from the constrained side (52 ms), d - delamination centre located 120 mm from the constrained side (52 ms), e - delamination centre located 160 mm from the constrained side (52 ms)

4. CONCLUSIONS

The embedded electric conductor explosive delamination effect is a high speed phenomenon allowing for control of structural behaviour in impact dynamics events, as well as a robust and controllable laboratory technique for research in field of structural dynamics. The presented results show high influence of the delamination time on beam behaviour when subjected to a transverse impact allowing for the change of localization of its deformation due to the impact. It may be used to preserve the structural integrity as well as, due to the change of the beam's stiffness characteristics, used for mitigation of loads acting on impacting objects.

REFERENCES

[1] Turner B., A study of exploding wires, PhD Thessis , California Institute of Technology, Pasadena, 1960, pp. 1-3.
[2] Hrousis C.A., Christensen J.S., Advances in modeling exploding bridgewire initiation, 14th International Detonation Symposium, Coeur d'Alene, 2010.
[3] Garasi C.J. et al., Multi-dimensional high energy density physics modelling and simulation of wire array Z-pich physics, Physics of Plasma, AIP, Vol. 11/5, 2004.

THREE-LAYERED ANNULAR PLATE WITH ELECTRORHEOLOGICAL CORE

D. PAWLUS
Faculty of Mechanical Engineering and Computer Science, University of Bielsko-Biała
Willowa 2, 43-309 Bielsko-Biała, Poland

1. INTRODUCTION

Approximation of the change of properties from solid body to viscous fluid known as electrorheological effect and called also as the Winslow effect [1] by the Bingham plastic model accepting in description of the core material, enables to conduct new evaluation process of plate dynamic behaviours. The dynamic sensitivity of plate structure to different values of Bingham model parameters and the analysis of critical and supercritical behaviours are examined in this paper. Some investigations of dynamic behaviours of sandwich annular plates with electrorheological fluid core are presented for example in work by Yeh [2].

2. PROBLEM FORMULTION

The three-layered annular plate is the subject of the analysis. The structure of plate is composed of thin, elastic facings and core with electrorheological properties. The plate edges are clamped. Plate is loaded on facings with stress linearly increasing in time.

The influence of electrorheological properties of core material on dynamic behaviour was examined in the range of critical parameters of plate work. At the moment of time of the loss of plate dynamic stability (established according to criterion presented in work [3]) the change of core material behaviour occurs from elastic body to properties of viscous fluid-suspension. The influence of the viscosity constant of rheological form of core material and the values of shear stress in core Bingham model on the final results is subjected to the detailed analysis. The static value of shear stress in the equation of Bingham body (see, Eqn. 1) has been accepted as equal to values of critical radial and circumferential stresses calculated at the moment of the loss of plate dynamic stability.

The classical theory of sandwich plates with the broken line hypothesis has been used. The nonlinear geometric relations expressed by Kármán’s equations describe the deformation of facings. The preliminary deflection and additional deflection increasing in loading time are equal for each plate layer. The solution to the problem of dynamic deflections of three-layered plates with viscoelastic core is presented in work [4] in detail. Shown form of the system of differential equations is here modified by the physical relations of Bingham model core material. These relations are expressed by equations [1]:

$$\tau_{rz_2} = \eta \cdot \dot{\gamma}_{rz_2} + \tau_{r\max} \qquad \tau_{\theta z_2} = \eta \cdot \dot{\gamma}_{\theta z_2} + \tau_{\theta\max} \tag{1}$$

where: η - plastic viscosity constant, $\dot{\gamma}_{rz(\theta z)_2}$ - shear rate in radial and circumferential directions, respectively, $\tau_{r(\theta)\max}$ - static yield stress in radial and circumferential directions, respectively.

3. NUMERICAL EXAMPLE

The observations have been led for plates with facing thickness h' equal to: $h' = 0.001$ m, core thickness equal to $h_2 = 0.002$ m, inner radius $r_i = 0.2$ m, outer radius $r_o = 0.5$ m. Facings are made of steel. The example of plates compressed on outer edge, which buckling is in the form of m = 7 circumferential waves, is shown in Fig.1 for values of core Kirchhoff's modulus equal to: $G_2 = 0.5$ MPa. The supercritical vibrations shown in Fig. 1 are observed for greater than $\eta = 17$ Pas·values of viscosity constant η. For the smaller value of viscosity constant η the run of curves $\zeta_{1max} = f(t^*)$ in supercritical region of plate work is limited.

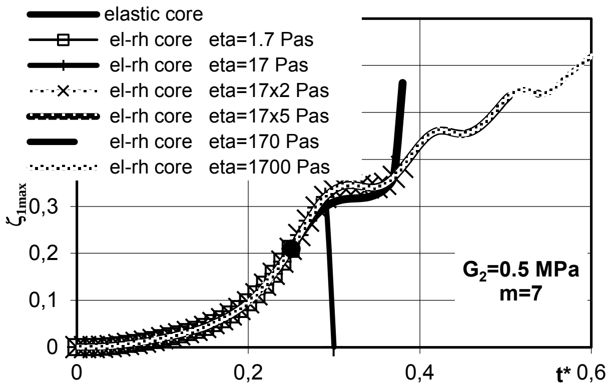

Fig. 1.Time histories of deflections of waved plates $G_2 = 0.5$ MPa, m = 7 compressed on outer edge

4. CONCLUSION

The observations show the strong influence of core material properties on plate dynamic, supercritical behaviour. Results indicate the possibility of controlling of plate work and limitation of the supercritical vibration field. Presented results and observations could be useful in plate structure design for suitable control its dynamic behaviour and work field.

REFERENCES

[1] Jordan T.C., Shaw M.T., Electrorheology, Transactions on Electrical Insulation, Vol. 24, No. 5, 1989, pp. 849-878.
[2] Yeh JY, Vibration control of a sandwich annular plate with an electrorheological fluid core layer, Smart. Mater. Struc., 16, 2007, pp. 837-842.
[3] Volmir, C., Nonlinear dynamic of plates and shells, Moscow, Science, 1972 (in Russian).
[4] Pawlus D., Dynamic stability of three-layered annular plates with viscoelastic core, Scientific Bulletin of the Technical University of Lodz, 1075, Lodz, 2010 (in Polish).

STATECZNOŚĆ DWUKIERUNKOWO POFAŁDOWANYCH ŚRODNIKÓW KSZTAŁTOWNIKÓW ZIMNOGIĘTYCH

W. PERLIŃSKI, B. MICHALAK
Katedra Mechaniki Konstrukcji, Politechnika Łódzka
Al. Politechniki 6, 90-924 Łódź, Polska

1. WPROWADZENIE

Konstrukcje stalowe z jednokierunkowo pofałdowanymi środnikami są wykorzystywane w wielu krajach. Wykorzystanie konstrukcji tego typu dotyczy zarówno konstrukcji mostowych jaki i budownictwa. Analizę stateczności tego typu środników można znaleźć w wielu pozycjach literatury, wymieńmy tu dla przykładu [1, 2]. Wadą tego typu jednokierunkowego pofałdowania jest to, że nie można otrzymać płaskiej linii zagięcia pomiędzy środnikiem i pasami dźwigara, stąd nie można zastosować takiego pofałdowania w kształtownikach giętych na zimno. Natomiast pofałdowanie dwukierunkowe pozwala wykorzystać ten sposób wzmocnienia sztywności środników w kształtownikach giętych na zimno.

Przedmiotem rozważań będą środniki kształtowników giętych na zimno pofałdowane sinusoidalnie w dwóch kierunkach (Rys. 1). Celem rozważań jest analiza stateczności tak pofałdowanych środników. Analizie zostaną poddane: ściskane równomiernie pasmo płytowe, płyta prostokątna ściskana równomiernie w dwóch kierunkach, środnik w postaci płyty prostokątnej obciążonej złożonym stanem naprężeń ściskających, oraz środnik ścinany. Analizę stateczności sprężystej modelu powłokowego pofałdowanego środnika przeprowadzono używając programu ABAQUS.

2. MODEL ELEMENTÓW SKOŃCZONYCH

Wartości sił krytycznych i postacie utraty stateczności określono korzystając z programu ABAQUS. Zastosowano model materiału liniowo sprężystego i czterowęzłowe elementy powłokowe o 5 stopniach swobody w węzłach typu S4R5 (Rys. 1).

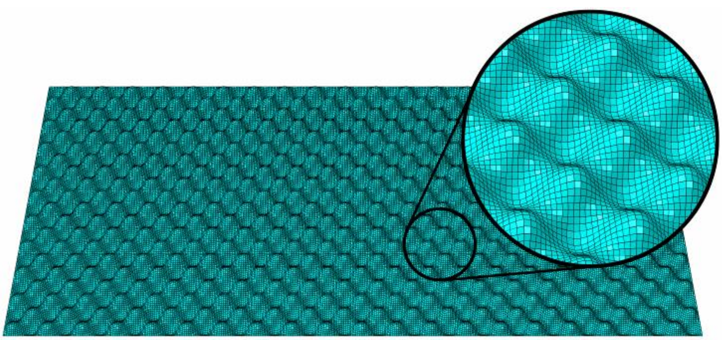

Rys. 1. Model pofałdowanego środnika w metodzie elementów skończonych

Elementy S4R5 o odebranym jednym stopniu swobody w węzłach możemy zastosować w przypadku analizy cienkich płyt o małych odkształceniach. Powierzchnię środkową modelowano analitycznie wprowadzając siatkę punków o gęstości 1×1mm. Powierzchnia ta następnie została posiatkowana na elementy skończone o takich samych wymiarach.

Obliczenia przeprowadzono dla dwóch rodzajów warunków brzegowych: swobodnego podparcia i brzegu zamocowanego.

2. ANALIZA NUMERYCZNA

Celem analizy numerycznej jest ocena wpływu stosunku f/l (f - wyniosłość fałdy sinusoidalnej, l - długość okresu pofałdowania) i stosunku t/l (t - grubość blachy środnika) na wartości sił krytycznych. Na rys.2 przedstawiono przykładowo zależność wartości siły krytycznej dla ściskanego pasma płytowego w zależności od stosunku f/l ,gdzie t/l jest przyjętym parametrem. W trakcie prezentacji zostaną przedstawione wyniki dla środnika ścinanego i poddanego złożonym naprężeniom ściskającym.

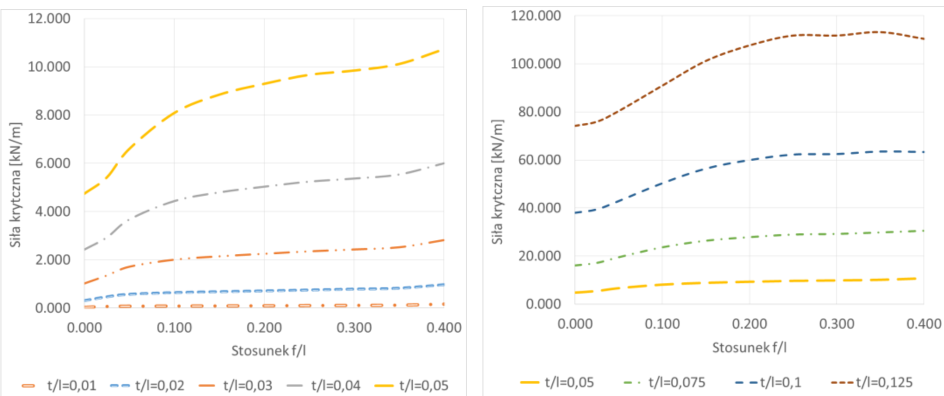

Rys. 2. Wartości sił krytycznych dla ściskanego pasma płytowego

Z wykresów na Rys. 2 można stwierdzić, że większe przyrosty wartości sił krytycznych wraz ze wzrostem f/l występują dla środników o małym stosunku t/l . Natomiast dla środników o dużym stosunku t/l wzrost wartości siły krytycznej wraz ze wzrostem f/l osiąga pewne maksimum. Dla rozpatrywanego przypadku maksimum to występuje przy wartościach $f/l = 0.25 \div 0.35$.

LITERATURA

[1] Eldib M.E.A.-H., Shear buckling strength and design of curved corrugated steel webs for bridges, Jour. Construc. Steel Research, 65, 2009, pp. 2129-2139.

[2] Kuchta K., Design of Corrugated Webs under Patch Load, Journal of Advanced Steel Construction, Vol. 3, No. 4, 2007, pp. 737-751.

POSTBUCKLING OF IMPERFECT PLATE SUBJECTED TO SHEARING LOAD

M. PSOTNÝ
Department of Structural Mechanics, Slovak University of Technology
Radlinského 11, 810 05 Bratislava, Slovakia

1. INTRODUCTION

The stability analysis of thin plate subjected to shear is presented. The non-linear FEM equations are derived from the variational principle of minimum of potential energy. To obtain the non-linear equilibrium paths, the Newton-Raphson iteration algorithm is used. Corresponding levels of the total potential energy are defined. The peculiarities of the effects of the initial imperfections are investigated using user program. Obtained results are compared with those gained using ANSYS system.

2. THEORY

Restricting to the isotropic elastic material and to the constant distribution of the residual stresses over the thickness, the total potential energy can be expressed as:

$$U = \int_A \frac{1}{2}\left(\boldsymbol{\varepsilon}_m - \boldsymbol{\varepsilon}_{0m}\right)^T t\,\mathbf{D}\left(\boldsymbol{\varepsilon}_m - \boldsymbol{\varepsilon}_{0m}\right)dA + \int_A \frac{1}{2}\left(\mathbf{k} - \mathbf{k}_0\right)^T \frac{t^3}{12}\mathbf{D}\left(\mathbf{k} - \mathbf{k}_0\right)dA - \int_A \mathbf{q}^T \mathbf{p}\, dA \qquad (1)$$

The system of conditional equations one can get from the condition of the minimum of the increment of the total potential energy $\delta\, \Delta U = 0$. This system can be written as:

$$\mathbf{K}_{inc}\, \Delta\, \boldsymbol{\alpha} + \mathbf{F}_{\mathrm{int}} - \mathbf{F}_{ext} - \Delta\, \mathbf{F}_{ext} = \mathbf{0} \qquad (2)$$

where $\boldsymbol{K}_{inc}$ - the incremental stiffness matrix of the plate,
$\boldsymbol{F}_{\mathrm{int}}$ - the internal force of the plate,
$\boldsymbol{F}_{ext}$ - the external load of the plate,
$\Delta\boldsymbol{F}_{ext}$ - the increment of the external load of the plate, more details in full text.

3. FEM NONLINEAR ANALYSIS

The FEM computer program using a 48 DOF element has been used for analysis. FEM model consists of 8×8 finite elements. Full Newton-Raphson procedure, in which the stiffness matrix is updated at every equilibrium iteration, has been applied. Interactive change of the pivot member during calculation is necessary for obtaining required number of L-D paths. Obtained results are compared with results of the analysis using ANSYS system, where 32×32 elements model is created. Element type SHELL143 (4 nodes, 6 DOF at each node) is used. The arc-length method was chosen for analysis, the reference arc-length radius is calculated from the load increment. Only fundamental path of nonlinear solution has been presented.

4. EXAMPLE

Illustrative example of steel plate loaded in shear (Fig. 1) is presented as load – displacement paths. The initial displacements are assumed as the out of plane displacements only as a combination of first three buckling modes: $d_0=\alpha_i$*mode i. Parameters α_i are mentioned in this figure.

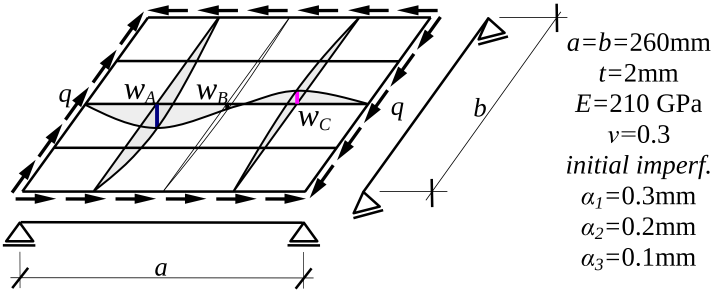

Fig. 1. Notation of the quantities of the plate loaded in shear

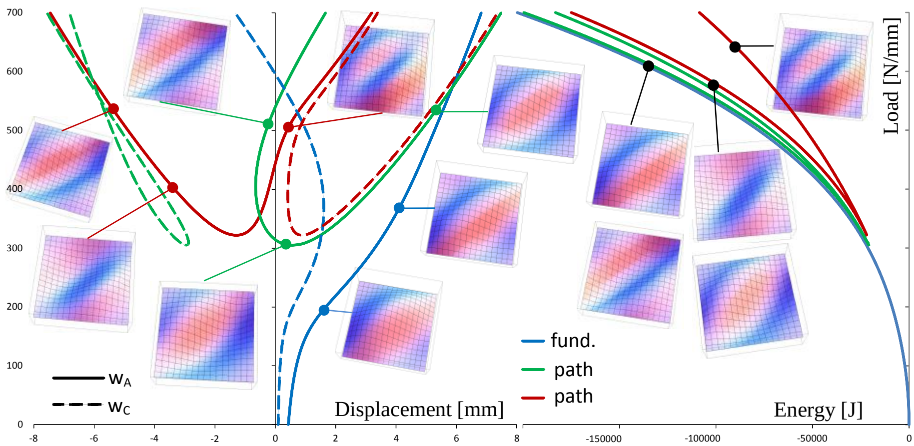

Fig. 2. Buckling and post-buckling of thin plate with the initial displacement

Presented non-linear solution of the post-buckling behaviour of the plate is divided into two parts. On the left side we have load versus nodal displacement parameters relationship, on the right side the relevant level of the total potential energy is drawn. Due to the mode of the initial imperfection the nodal displacements w_A, w_C have been taken as the reference nodes (see Fig. 1). In Fig. 2 there are presented first three loading paths representing various forms of change between buckling shapes. Fundamental path corresponds with the minimum value of total potential energy, thus there is no presumption of a snap-through. However, for some different shapes of initial imperfection, the level of the total potential energy of the fundamental stable path can be higher than the total potential energy of the secondary stable path. This is the assumption for the change in the buckling mode of the slender web.

BUCKLING ANALYSIS OF COLD FORMED SILO COLUMN

K. REJOWSKI, P. IWICKI
Department of Structural Mechanics University of Technology
Narutowicza 11/12, 80-952 Gdańsk, Poland

1. INTRODUCTION, SCOPE OF THE WORK

Silos are built of thin-walled horizontally corrugated curved sheets strengthened by vertical columns [1]. The wall sheets carry circumferential tensile forces caused by horizontal wall pressure of a bulk solid and vertical columns carry vertical compressive forces exerted by wall friction from a bulk solid. Wall sheets may be assumed as elastic foundation of the columns. In the design practice it is necessary to use a simple models instead of analysis of the whole 3D silos [2]. The Eurocode 3 [3] gives a simplified formula to calculate the buckling strength of vertical silo columns resting on elastic lateral foundation.

The aim of the research is to perform a linear buckling analysis (LBA) of a silo column, modelled by shell elements and supported in lateral or torsional direction by an elastic foundation constant along the column length. Influence of the foundation stiffness on the column buckling resistance was investigated. The calculated load factor was compared to the recommendations given by Eurocode 3 and to similar results of the whole silo modelled by shell elements analysed in paper [4].

2. NUMERICAL ANALYSIS OF COLUMN

As the parametric study consider the column supported by lateral (k) and torsional (k_θ) elastic foundation (modelling the silo walls) continuously distributed along the column length (Fig. 1). The column was loaded by vertical continues load imposed by a bulk solid according Eurocode 1 [5]. The analysis was performed program ABQUS [6].

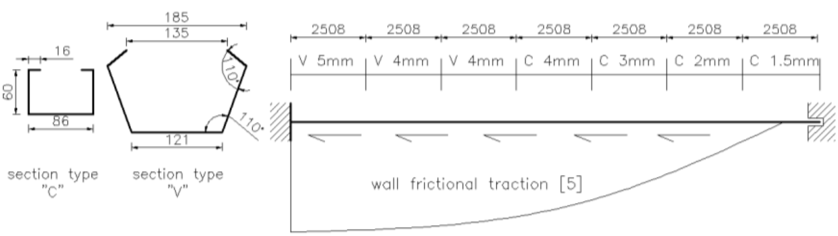

Fig. 1. Analysed silo column

The increase of foundation stiffness caused nonlinear rise of the column buckling load (Fig. 2). For low lateral and torsional foundation stiffness a global buckling of the column occurred, at higher stiffness local, distorsional or torsional buckling took place. According to recommendations given by Eurocode 3 the load factor is low (0.4) and in a real silo 3D FE analysis [4], it was 5.5 for LBA and 3.2 GNA.

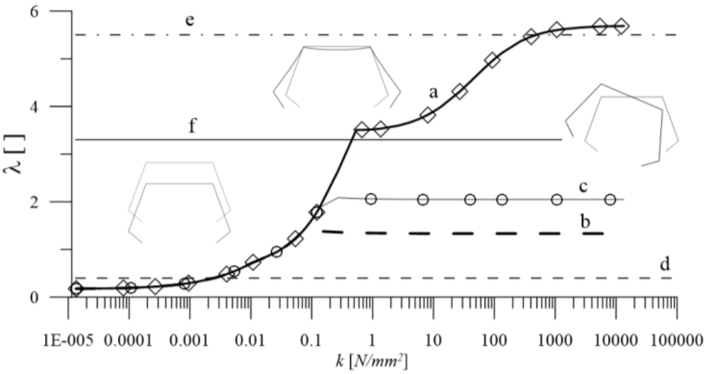

Fig. 2. Evolution of column limit and buckling load factor λ against lateral foundation stiffness for: a) $k_\theta=\infty$, b) $k_\theta=0$, c) $k_\theta=67$ *Nm/rad*, d) according Eurocode 3, e) FE LBA [4] , f) FE GNA [4]

3. CONCLUSIONS

The effect of bracing stiffness on the critical and limit load of the cold-formed column was investigated. Comparing calculated buckling load factor with the results of the 3D silo shell FE analysis one can estimate the column foundation stiffness. The lateral foundation stiffness according Eurocode 3 is much lower than calculated in FE model [4]. Further investigation of the column foundation in both torsional and lateral direction are needed.

The financial support of the Polish National Research Centre NCN in the frame of the Grant No 2011/01/B/ST8/07492 " Safety and optimization of cylindrical metal silos containing bulk solids with respect to global stability " and of the Polish National Centre for Research and Development NCBR in the frame of the Grant POIG.01.03.01-00-099/12 "Innovative method of dimensioning and construction of large industrial silos made from of corrugated sheets" is gratefully acknowledged.

REFERENCES

[1] Wójcik M., Iwicki P., Tejchman J., 3D buckling analysis of a cylindrical metal bin composed of corrugated sheets strengthened by vertical stiffeners, Thin-Walled Structures, 49, 2011, pp. 947-963.

[2] Iwicki P., Sondej M., Buckling analysis of cold formed stell column, Stability of Structures XIII-th Symposium - Zakopane 2012, pp. 283-288.

[3] EN1993-4-1. Eurocode 3: Design of steel structures. Part 4-1: Silos, tanks and pipelines - Silos. Brussels, CEN, 2007.

[4] Iwicki P., Rejowski K., Tejchman J., Wyboczenie cylindrycznego silosu z blachy falistej wzmocnionego słupami w analizach statycznych i dynamicznych, Inżynieria i Budownictwo (in press).

[5] EN1991-1-4. Eurocode 1: Basis of design and action on structures. Part 4: Actions in silos and tanks. Brussels, CEN, 1995.

[6] Abaqus, Theory Manual, Version 6.8, Hibbit, Karlsson & Sorensen Inc, 2008.

DISTORTIONAL INSTABILITY OF AXIALLY LOADED COLD ROLLED SIGMA PROFILES

K. RZESZUT, K. CIESIELCZYK
Institute of Structural Engineering, Poznan University of Technology
Piotrowo 5, 60-965 Poznan, Poland

A. GARSTECKI
Higher Vocational State School in Pila
Podchorazych 10, 64-920 Pila, Poland

1. INTRODUCTION

Application of thin-walled cold formed sections increased the importance of local and distortional instability phenomena which may appeared at a similar or lower load level as global instability. Distortional buckling of compression members is associated with the deformation of the contour in a form of symmetrical or asymmetrical closing or opening of the section and change the angle between adjacent walls. Distortional buckling of compression members has been widely discussed in literature. In [1] Lau and Hancock proposed distortional buckling formulas for columns made of cold-rolled channel cross-sections. The distortional buckling analysis was also carried out by Schafer [3]. The comparative analysis conducted by Szymczak and Werochowski in [4] showed that the critical distortional stresses calculated according to the designing code obtain overestimated values in relation to the formulas proposed by Hancock and Schafer.

In this paper the distortional buckling analysis of cold-rolled sigma profiles was performed. In the first part of the study critical distortional stress was calculated based on Eurocode recommendations and Hancock and Schafer formulas. In the second part, the FEM numerical model was created in order to verify the assumptions introduced in the analytical analysis and to investigate the interactive buckling, which is not taken into account in analytical formulas.

2. PROBLEM FORMULATION

The critical distortional buckling stress for edge or intermediate stiffener according [2] should be obtained from:

$$\sigma_{cr,s} = \frac{2\sqrt{KEI_s}}{A_s} \tag{1}$$

where: K is the spring stiffness per unit length and A_s, I_s are the effective characteristics of the effective cross-sectional area of stiffener. Alternatively, the critical distortional buckling stress can be calculated from the equations formulated by Lau and Hancock:

$$\sigma_{cr} = \frac{E}{2A_f}\left[(\alpha_1+\alpha_2) - \sqrt{(\alpha_1+\alpha_2)^2 - 4\alpha_3}\right] \quad (2)$$

where: A_f is the cross-sectional area of the flange and lip, α_1, α_2, α_3 are coefficients dependent on the geometric characteristics or from formula proposed by Schafer:

$$\sigma_{cr} = \frac{k_{\varphi fe} + k_{\varphi we}}{k_{\varphi fg} + k_{\varphi wg}} \quad (3)$$

where: $k_{\varphi fe}$, $k_{\varphi we}$, $k_{\varphi fg}$, $k_{\varphi wg}$ are elastic and "geometric" rotational spring stiffness from the web and flange.

In the numerical examples the simplified model was used, where the sigma cross-section was replaced by channel cross-section with spring supports as shown in Fig. 1a. The analysis was carried on several cold-formed symmetrical sigma profiles (flange width b = 70 mm, wall thickness t = 1.5 mm and the lip width c = 16 mm). The results of the calculations are presented in the table (Fig. 1b).

a)

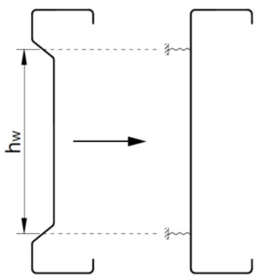

b)

H [mm]	Shafer [MPa]	Lau-Hancock [MPa]	EN 1993-1-3 [MPa]
140	423.01	341.56	323.61
200	266.90	245.75	250.69
230	216.18	211.25	228.85
260	172.60	177.27	211.89
300	124.87	129.06	194.19
350	81.65	102.43	117.28

Fig. 1. Examples a) simplified model, b) critical distortional buckling stress

The next stage of research will cover numerical analysis using the finite element method in order to determine the degree of accuracy of the adopted simplified model and to determine which of the presented analytical methods provides the best results.

REFERENCES

[1] Lau S.C.W., Hancock, G.J., Inelastic buckling of channel columns in the distortional mode. Thin- Walled Structures, 10, 1990, pp. 59-84.

[2] PN-EN 1993-1-3, Eurokod 3. Projektowanie Konstrukcji stalowych. Część 1-3: Reguły ogólne. Reguły uzupełniające dla konstrukcji z kształtowników i blach profilowanych na zimno, Polski Komitet Normalizacyjny, 2006.

[3] Schafer B. W., Distortional buckling of cold-formed steel columns, Final Report of AISI, 2000.

[4] Szymczak C., Werochowski W., Dystorsyjna niestateczność osiowo ściskanych kształtowników giętych z usztywnionymi stopkami, Inżynieria i Budownictwo, 2/2005.

FLANGE VERTICAL BUCKLING OF I-SHAPED STEEL GIRDERS

Shu. SHIMIZU, T. UEDA, Shi. SHIMIZU
Department of Civil Engineering, Shinshu University
Wakasato 4-Chome, 380-8553 Nagano, Japan

G. FUJITA, N.TANAKA
Miyaji Engineering Co. Ltd.
Yawata-Kaigandori 3-Chome, 290-8580 Ichihara, Japan

1. BUCKGROUND AND INTRODUCTION

This paper deals with the flange vertical buckling of an I-shaped "non-hybrid" steel girder having the practical section dimensions. On flange vertical buckling, Basler et al. [1] presented a formula to verify the occurrence of vertical buckling of an I-shaped steel girder by using the width-thickness ratio of the web plate. Two authors of the current paper carried out an experimental test on the hybrid steel girders, and in the test [2], unexpected vertical buckling was observed in a test model.

With above background, the authors conducted the numerical studies [3] on the flange vertical buckling of the I-shaped "hybrid" steel girders having smaller section dimensions than practical based on the experimental model. Through these studies, the authors pointed out that occurrence of vertical buckling is owing to the thickness of flange and web plate and not to the width-thickness ratio. This fact suggests that the new collapse model is required to establish the procedure for verification of vertical buckling.

2. NUMERICAL MODEL AND RESULT

In the current paper, flange vertical buckling behaviour on the "non-hybrid" steel girders, having the shapes and dimensions of practical girders, is studied. The typical numerical model has its depth of 2 500 mm, web thickness of 8.5 mm, flange width and thickness of 600×37 mm, and the span length of 29 800 mm, and the grade SM570 steel with the yield stress of 596 MPa is assumed. Fig. 1 shows the outline of the typical numerical model. In the analysis, 2 point loadings are considered and the left side loading is kept to be larger by 1 % than the right side loading as same to authors' previous studies.

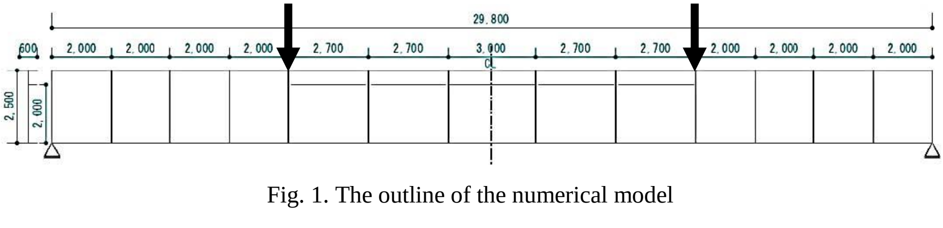

Fig. 1. The outline of the numerical model

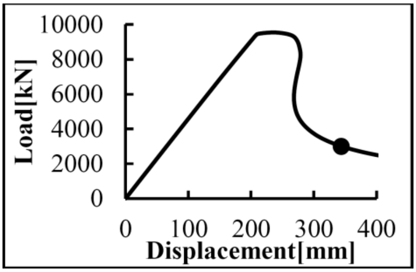

Fig. 2. Load-deflection relation

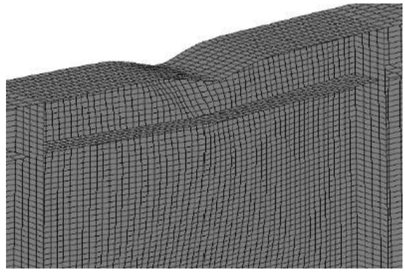

Fig. 3. Deformation pattern

Fig. 2 shows the load-deflection relationship of the numerical model in which vertical buckling occurs. As with the previous studies, after the peak load, the load reduces drastically. Fig. 3 shows the deformation pattern of the numerical model at the stage indicated with the black point (●) in the Fig. 2.

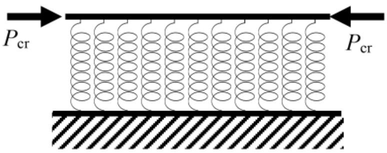

Fig. 4. A Column on the elastic foundation

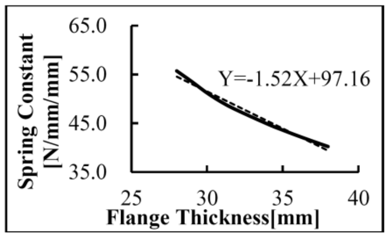

Fig. 5. Spring constant-flange thickness relation

Timoshenko presented a formula to estimate the buckling load P_{cr} of a bar elements supported by many springs (Fig. 4) as $P_{cr} = \sqrt{\alpha EI}$, here the constant α [N/mm/mm] is corresponding with the spring constant per a unit length. The authors consider that this formula is applicable to flange vertical buckling. Fig. 5 shows the spring constant that has been calculated by the Timoshenko's formula and author's numerical results.

3. CONCLUSION

1) Vertical buckling in the numerical model assuming the practical girders occurred.
2) The spring constant could be approximated by a straight line.

REFERENCES

[1] Basler,K & Thürlimann B., Strength of Plate Girders in Bending, *Proc ASCE*, Vol.87, ST6, 1961, pp. 153-181.
[2] Dowling,P.J. (ed)., Constructional Steel Design, An International Guide, Elsevier, 1992.
[3] Shimizu S., Zhang J., Tanaka N., Akehashi K., Nakai H., An Experimental Study on Ultimate Strength Behaviour of Hybrid Steel Plate Girders, Steel Construction Engineering, JSSC (Japanese Soc. of Steel Constr.), 10: 2003, pp. 51-60. (in Japanese).

STABILITY OF A STEEL WELDED GIRDER WITH BENDING AND SHEAR FORCES INCLUDED

R. SYGULSKI
Polytechnic Faculty, The President Stanisław Wojciechowski Higher Vocational State School in Kalisz, Poznańska 201-205, Kalisz, Poland

M. GUMINIAK, Ł. POLUS
Institute of Structural Engineering, Poznan University of Technology
Piotrowo 5, 60-965 Poznan, Poland

1. INTRODUCTION AND PROBLEM FORMULATION

The stability of the elements of a steel welded girder subjected to bending and shear forces is considered (Fig. 1).

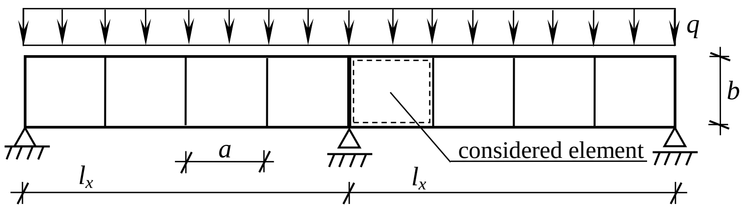

Fig. 1. Steel girder with vertical stiffeners

The correct determination of the critical load is essential in the design process. This issue was investigated and solved in analytical terms by Timoshenko [1]. The Finite Element Method (FEM) is applied to numerical investigation of the stability of the steel welded girder with the bending and the shear forces included. Suitable numerical algorithms of FEM were presented e.g. by Rakowski and Kacprzyk [2]. Others, e.g. Shi [3], Chinnaboon, Chucheepsakul and Katsikadelis [4] have used the Boundary Element Method (BEM) to solve the buckling problem of thin plates of any shape including the plates with holes.

2. NUMERICAL EXAMPLES

The element of the steel welded girder is considered and modelled as the rectangular simply-supported plate of dimensions $a = b = 2.0$ m, subjected to N_x and N_{xy} in-plane forces with linear and constant distributions, respectively (Fig. 2). The material properties are $E = 205$ GPa, $\nu = 0.3$ and the plate thickness is $h = 0.015$ m. The ABAQUS computational program was used in the analysis. The plate domain is divided into 1600 elements of the S4R and the S8R types and the finite element mesh is regular. The critical loading N_{cr} is expressed using the non-dimensional term $\tilde{N}_{cr} = N_{cr} \cdot a \cdot b / D$, where D is the plate stiffness. The results of calculation are presented in Table 1. Additionally, the stability problem of the plate subjected only to N_{xy} in-plane forces was solved as the simple benchmark test (Table 2). The FEM results were compared with the analytical and the BEM solution according to conception presented in [5].

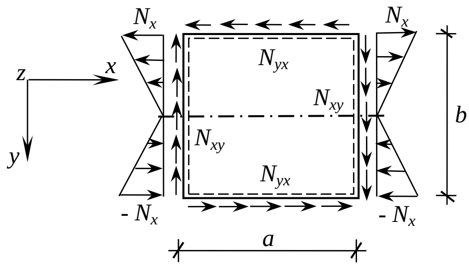

Fig. 2. Considered element of steel welded girder

Table 1. Critical loading value $\tilde{N}_{cr}$. Assumed the comparative compressing loading: $\tilde{N}_x$

$\tilde{N}_{xy}/\tilde{N}_x$	0.0	0.025	0.05	0.1	0.15
FEM (S4R)	251.837	250.498	247.032	236.685	224.229
FEM (S8R)	250.069	248.705	245.227	235.037	222.884

Table 2. Critical loading value $\tilde{N}_{cr}$

Loading: N_{xy}	FEM (S4R)	FEM (S8R)	BEM [6]	Analytical [1]
$\tilde{N}_{xy} = \tilde{N}_{cr}$	92.066	91.454	93.051	92.182

3. SUMMARY

The impact of the tangential in-plane loading cannot be avoided. Detailed analysis of the critical load is important in the case of complex structures, included welded girders with stiffeners or holes. This will allow to estimate the maximum value of external loading q.

REFERENCES

[1] Timoshenko S., Woinowsky-Krieger S., Theory of elastic stability, Warszawa, Arkady, 1962 (in Polish).

[2] Rakowski G., Kacprzyk Z., Metoda elementów skończonych w mechanice konstrukcji, Oficyna Wydawnicza Politechniki Warszawskiej, 2005 (in Polish).

[3] Shi G., Flexural vibration and buckling analysis of orthotropic plates by the Boundary Element Method, Int. J. of Solids and Structures, 12, 26, 1990, pp. 1351-1370.

[4] Chinnaboon B., Chucheepsakul S., Katsikadelis, J.T., A BEM-based meshless method for buckling analysis of elastic plates with various boundary conditions, International Journal of Structural Stability and Dynamics, 7, 1, 2007, pp. 81-89.

[5] Guminiak M., Sygulski R., Stateczność początkowa płyt cienkich w ujęciu metody elementów brzegowych, X Sympozjum Stateczności Konstrukcji, Zakopane, 8-12. września, red.: K. Kowal-Michalska, Z. Kołakowski, 2003, pp. 173-180 (in Polish).

WPŁYW NIESTATECZNOŚCI LOKALNEJ NA SZTYWNOŚĆ W KONSTRUKCJACH BLACHOWNICOWYCH

M. SZUMIGAŁA, K. CIESIELCZYK
Institute of Structural Engineering, Poznan University of Technology
Piotrowo 5, 60-965 Poznań, Poland

1. WSTĘP

Zastosowanie w konstrukcjach inżynierskich spawanych przekrojów blachownicowych pozwala na bardziej optymalne dopasowanie wymiarów przekroju do pola rozkładu sił wewnętrznych niż w przypadku zastosowania przekrojów walcowanych. Z tego względu w wielu sytuacjach projektowanie przekrojów blachownicowych jest rozwiązaniem dalece ekonomiczniejszym. Jednak przyjmowanie optymalnych wymiarów blachownic wiąże się z ryzykiem wystąpienia w przekroju zjawiska utraty stateczności lokalnej jak i ogólnej. Zgodnie z zasadami norm europejskich nośność przekrojów klasy 4 zaleca się wyznaczać według teorii nośności nadkrytycznej [1]. Idea obliczeń w stanie nadkrytycznym polega na zamianie przekroju brutto (rzeczywistego) na przekrój efektywny - współpracujący.

2. PRZEKRÓJ WSPÓŁPRACUJĄCY

W [2] zaproponowano dwa sposoby obliczania przekroju współpracującego. Obie metody opierają się na idei zmniejszenia rzeczywistych wymiarów (pola przekroju) ścianek poprzez przemnożenie szerokości przez współczynnik redukcyjny ρ uwzględniający niestateczność ścianki. Podstawowa metoda opisana w zasadniczej części normy (p. 4.3) opiera się na założeniu, że naprężenia ściskające w przekroju współpracującym równe są granicy plastyczności, natomiast druga, alternatywna metoda (załącznik E) jest procedurą iteracyjną i zakłada możliwość uwzględnienia rzeczywistych wartości naprężeń ściskających.

We wspomnianym załączniku przedstawiona została metoda wyznaczania sztywności przekroju współpracującego w stanie granicznym użytkowności. Zakłada się, że efektywny moment bezwładności określa następująca zależność:

$$I_{eff} = I_{gr} - \frac{\sigma_{gr}}{\sigma_{com.Ed,ser}} \left[I_{gr} - I_{eff} \left(\sigma_{com.Ed,ser} \right) \right] \tag{1}$$

gdzie:

- I_{gr} - moment bezwładności przekroju brutto,
- σ_{gr} - maksymalne naprężenia od zginania w stanie granicznym użytkowalności (na podstawie cech przekroju brutto),
- $\sigma_{com,Ed,ser}$ - maksymalne naprężenie ściskające w rozpatrywanym elemencie w stanie granicznym użytkowalności (na podstawie przekroju współpracującego),
- $I_{eff}(\sigma_{com,Ed,ser})$ - moment bezwładności przekroju współpracującego wyznaczony dla maksymalnych wartości naprężeń $\sigma_{com,Ed,ser}$.

Zgodnie z zaleceniami normy zakłada się, że efektywny moment bezwładności jest zmienny na długości przekroju elementu i wyznacza się go dla wybranych przekrojów charakterystycznych (najbardziej wytężonych). Dopuszcza się również założenie, że przekrój będzie stały na całej rozpiętości i wyznaczony dla największej wartości momentu zginającego.

3. ANALIZA NUMERYCZNA

Autorzy postanowili przeanalizować i porównać omówione zalecenia normowe. Obliczenia przeprowadzono dla jednoprzęsłowej belki statycznie wyznaczalnej oraz dla belki statycznie niewyznaczalnej (dwuprzęsłowej oraz dwuprzęsłowej z częścią wspornikową) o przekroju dwuteowym.

W pierwszym etapie porównano pole przekroju współpracującego obliczonego obiema przedstawionymi w [2] metodami. Następnie wyznaczono wartości ugięć przy założeniu stałego przekroju efektywnego w strefie ściskanej i rozciąganej oraz w sposób dokładniejszy - dzieląc belkę na krótsze odcinki, określając iteracyjnie sztywność dla każdego z nich.

Wszystkie wyniki z obliczeń uzyskanych metodami analitycznymi zostaną porównane z wynikami otrzymanymi z analizy numerycznej przy wykorzystaniu metody elementów skończonych dla modelu 3D.

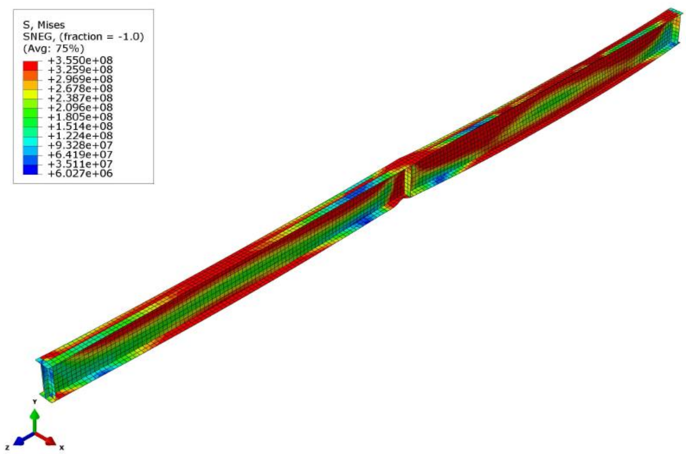

Rys. 1. Mapa naprężeń [Pa] wg hipotezy H-M-H w jednym z analizowanych modeli

BIBLIOGRAFIA

[1] Piekarczyk M., Wykorzystanie nadkrytycznej rezerwy nośności w projektowaniu konstrukcji stalowych, Wydawnictwo Politechniki Krakowskiej, 2002, pp. 11-61.

[2] PN-EN 1993-1-5, Eurokod 3, Projektowanie konstrukcji stalowych, Część 1-5: Blachownice, Polski Komitet Normalizacyjny, 2008.

LOCAL AND DISTORTIONAL BUCKLING IN THIN-WALLED BARS WITH Z-SECTIONS SUBJECTED TO WARPING TORSION

A. SZYCHOWSKI
Department of Structure Mechanics, Metal Structures and Computer Methods
Kielce University of Technology
Al. 1000 - lecia Państwa Polskiego 7, 25 - 323 Kielce, Poland

1. INTRODUCTION

Thin-walled bars with open sections and flat walls are sensitive to different modes of buckling (local, distortional and overall). At the same time, when in torsion, these bars are characterised by low strength and low rigidity. In studies [1, 2], the occurrence of the local buckling phenomenon in thin-walled bars, subjected to warping torsion, when other components of the section load were not present, was analysed theoretically and confirmed experimentally. In study [1], Z-sections, C-sections and I-sections, made from internal walls (I-type plates) and cantilever walls (II-type plates) not containing the stiffening of free edges, were taken into consideration. The local critical bimoment (B_{cr}), which causes the local buckling of the bar walls under the torsional load alone, was defined. It was demonstrated that for sections that are unsymmetrical (relative to the axis), e.g. Z-sections, two local critical bimoments are found, which differ in their absolute values. Those are the “left” ($B_{cr,L}$) and the “right” ($B_{cr,R}$) local critical bimoments, depending on the “sense” of the torsional load.

The present study deals with the stability of thin-walled bars with Z-sections. The latter also contain cantilever walls (plates), where the free edge is stiffened (III-type plates), Fig. 1.

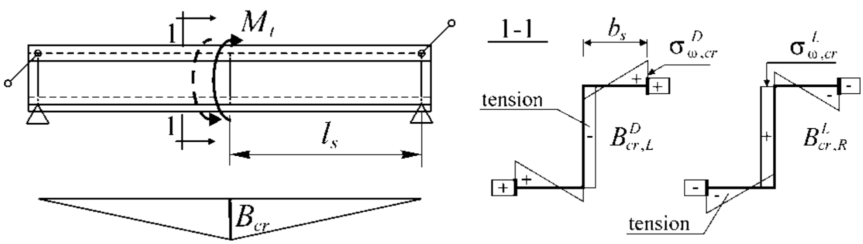

Fig. 1. Thin-walled bar with Z-section made from walls (plates) of I and III type

2. DISTORTIONAL CRITICAL BIMOMENT

In the thin-walled bar with Z-section, subjected to warping torsion (Fig. 1), the phenomenon of distortional buckling can occur [1]. The bimoment which generates this mode of buckling when no other section load components are found was termed “distortional critical bimoment”. It is expressed by the formula (1):

$$B_{cr}^{D} = \frac{\sigma_{\omega,cr}^{D} I_{\omega}}{\omega_{c}} \tag{1}$$

where:

$\sigma_{\omega,cr}^{D}$ - critical warping stress ($\sigma_{\omega,cr}^{D} = k_{\omega}^{D}\sigma_{E,s}$),

k_{ω}^{D} - coefficient of distortional buckling,

$\sigma_{E,s}$ - Euler`s stress for a plate (wall s),

I_{ω} - warping section constant,

ω_{c} - a sectorial coordinate corresponding to critical stress.

The problem of determining coefficients k_{ω}^{D} was solved using the energy method. The cross-section of the thin-walled bar was composed of plates of I and III type. Static and kinematic boundary conditions on the longitudinal edges of the connection were taken into account. Fig. 2 presents the diagrams of coefficients k_{ω}^{D} for the segment of the thin-walled bar with Z-section, when the bimoment distribution is linear.

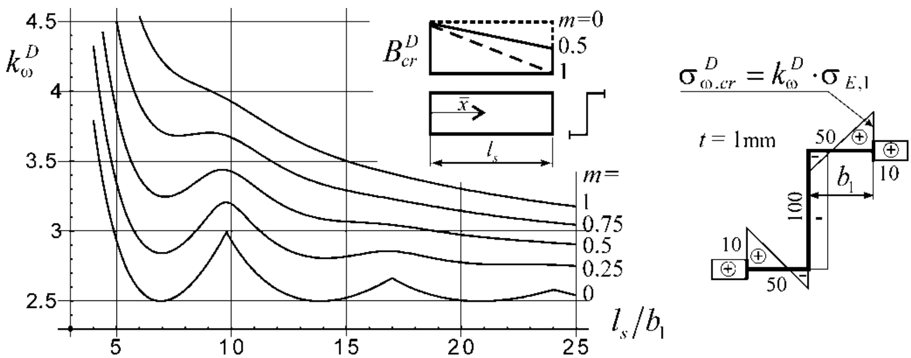

Fig. 2. Diagrams of coefficients k_{ω}^{D}

3. CONCLUSIONS

In the thin-walled Z-section composed of plates of I and III type, local (B_{cr}) and distortional (B_{cr}^{D}) critical bimoments are found, depending on the sense of the torsional load. Those bimoments are associated with different buckling modes (local mode, distortional mode) and have different absolute values.

REFERENCES

[1] Szychowski A., A theoretical analysis of the local buckling in thin-walled bars with open cross-section subjected to warping torsion, Thin-Walled Structures, 76, 2014, pp. 42-55.

[2] Kowal Z., Szychowski A., Experimental determination of critical loads in thin-walled bars with Z-section subjected to warping torsion, Thin-Walled Structures, 75, 2014, pp. 87-102.

WYBOCZENIE PÓŁKI USZTYWNIONEJ KSZTAŁTOWNIKA CIENKOŚCIENNEGO PRZY WZDŁUZNEJ ZMIENNOŚCI NAPRĘŻEŃ

A. SZYCHOWSKI
Department of Structure Mechanics, Metal Structures and Computer Methods
Kielce University of Technology
Al. 1000 - lecia Państwa Polskiego 7, 25 - 323 Kielce, Poland

1. WPROWADZENIE

Współcześnie stosowane kształtowniki cienkościenne o przekroju otwartym charakteryzują się dużymi smukłościami ścianek składowych (półek, środników, itd.). W związku z tym są wrażliwe na zjawiska lokalne związane z utratą stateczności ścianek ściskanych. Z tego punktu widzenia, krawędź swobodną np. półki ściskanej (wspornikowej), wzmacnia się często usztywnieniem krawędziowym, powodując wzrost naprężeń krytycznych wyboczenia [1]. Zmienia się także postać utraty stateczności przekroju z wyboczenia lokalnego na wyboczenie dystorsyjne lub interakcyjną formę obu postaci. W wielu technicznie ważnych przypadkach obciążenia, usztywniona półka kształtownika jest równomiernie ściskana i występuje wzdłużna zmienność naprężeń na długości segmentu pręta. Ściankę taką można w praktyce analizować jako jednostronnie sprężyście zamocowaną „na obrót" płytę wspornikową z podatnym „na ugięcie" usztywnieniem drugiej krawędzi. W pracy [2] przedstawiono wyniki badań stateczności płyt wspornikowych z podłużną krawędzią swobodną przy wzdłużnej zmienności naprężeń i granicznych warunkach podparcia drugiej krawędzi.

W niniejszej pracy zajęto się statecznością sprężyście zamocowanej „na obrót" półki ściskanej (płyty wspornikowej) z podatnym „na ugięcie" usztywnieniem krawędzi, Rys. 1.

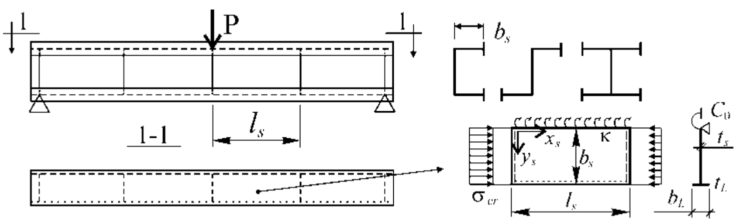

Rys. 1. Wydzielona z segmentu pręta cienkościennego półka ściskana

2. FUNKCJA UGIĘCIA SPRĘŻYŚCIE ZAMOCOWANEJ PŁYTY WSPORNIKOWEJ

Do aproksymacji postaci wyboczenia sprężyście zamocowanej „na obrót" płyty wspornikowej zaproponowano i przetestowano funkcję postaci skończonego szeregu sinusowo - wielomianowego. Dla wskaźnika utwierdzenia krawędzi podłużnej κ (zmieniającego się od 0 (p) do 1 (u)), funkcję ugięcia płyty zapisano w postaci (1):

$$w_s(x_s, y_s) = t_s \sum_{i=1}^{i_o} \left[f_{i2} \cdot \left((1-\kappa)\frac{y_s}{b_s} + \kappa \left(\frac{y_s}{b_s} \right)^2 \right) + \sum_{p=3}^{p_o} f_{ip} \cdot \left(\frac{y_s}{b_s} \right)^p \right] \cdot \sin\left(\frac{i\pi x_s}{l_s} \right) \qquad (1)$$

gdzie:

t_s, b_s, l_s - grubość, szerokość, długość płyty (ścianki *s*),

$\kappa = 1/(1 + 2D_s/b_s C_\theta)$ - wskaźnik utwierdzenia krawędzi podpartej,

C_θ - sztywność obrotowa krawędzi płyty,

D_s - płytowa sztywność zginania,

f_{i2}, f_{ip} - bezwymiarowe, swobodne parametry funkcji ugięcia.

Współczynniki *k* naprężeń krytycznych ($\sigma_{cr}=k\sigma_E$) wyboczenia lokalnego, dystorsyjnego lub interakcyjnego wyznaczono metodą energetyczną. Na Rys. 2 pokazano wykresy współczynników *k* płyty wspornikowej z usztywnieniem krawędzi dla κ=0.5 i różnych wartości parametru (m =1– σ_1/σ_0 , por. Rys. 1) liniowego rozkładu naprężeń.

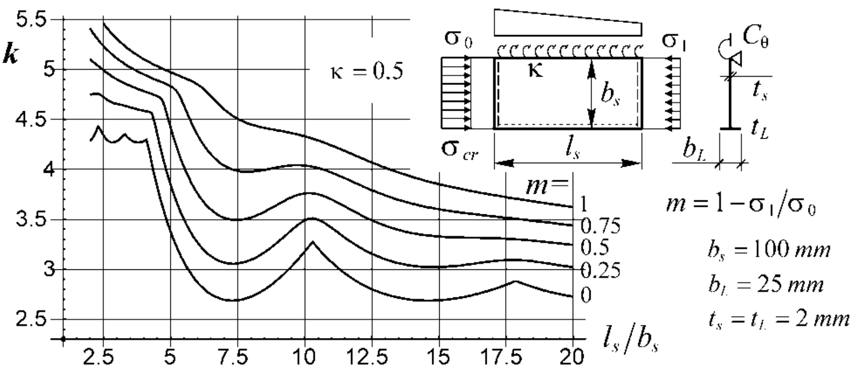

Rys. 2. Wykres współczynników *k* dla κ = 0.5 i m = 0, 0.25, 0.5, 0.75, 1

3. PODSUMOWANIE

Uwzględnienie wzdłużnej zmienności naprężeń i sprężystego zamocowania „na obrót" krawędzi podpartej półki usztywnionej kształtownika cienkościennego pozwala na dokładniejszą ocenę naprężeń krytycznych miarodajnej postaci wyboczenia. Naprężenia te służą do szacowania nośności przekroju np. metodą przekroju efektywnego.

REFERENCES

[1] Bulson P.S., The Stability of Flat Plates. Chatto and Windus. London 1970.

[2] Szychowski A., The stability of eccentrically compressed thin plates with a longitudinal free edge and with stress variation in the longitudinal direction, Thin-Walled Structures, 46, 2008, pp. 494-505.

LOCAL BUCKLING AND INITIAL POST-BUCKLING BEHAVIOUR OF THIN-WALLED CHANNEL BEAMS

C. SZYMCZAK
Department of Theory and Ship Design, Gdańsk University of Technology
Narutowicza 11/12, 80-233 Gdańsk, Poland

M. KUJAWA
Department of Structural Mechanics, Gdańsk University of Technology
Narutowicza 11/12, 80-233 Gdańsk, Poland

1. LOCAL BUCKLING

Thin-walled cold-formed channel beams undergoing pure bending is considered. The flat single and double bends flanges are taken into account (Fig. 1). Local buckling and initial post-buckling behaviour of the compressed flange of the element is investigated. A simple axially compressed column elastically supported along the edge of flange and web connection is taken into consideration as a model of the flange. The total potential energy of the flange is described as a sum of the internal strain energy related to bending and torsion of the flange and the external one dealing with the uniformly distributed elastic springs along the flange edge. Additionally the longitudinal normal stresses σ produce the external potential energy. The governing fourth order differential equation for displacement of the flange centre of gravity v (z) is derived with aid of the total potential energy stationary principle (1)

$$v^{IV} + 2\alpha v'' + \beta^2 v = 0 \tag{1}$$

where: α , β - coefficients expressed by means of the beam geometrical and mechanical parameters and the normal stress σ.

Using the boundary conditions, solution of Eqn. 1 leads to the critical buckling stress σ_{cr} and the buckling mode. Numerical examples dealing the simply supported beams and with the single and double bends flanges are provided. Moreover, the number of half-wave *m* of the buckling mode is determined to obtain the critical stress minimum.

2. INITIAL POST-BUCKLING BEHAVIOUR

In order to examine the initial post-buckling behaviour of the flange the additional nonlinear terms in the strain-displacement relation are taken into description of the total potential energy of the flange. Similarly as above, using the stationary energy principle the governing nonlinear differential equation of forth order for the displacement of the flange centre of gravity v (z) is found. The solution of the nonlinear equation is obtained, by means of the perturbation approach (2), as a series of the linear differential equations.

$$\begin{aligned} v &= \varepsilon v_1 + \varepsilon^2 v_2 + \varepsilon^3 v_3 + \ldots \\ \sigma &= \sigma_{cr} + \varepsilon\sigma^{(1)} + \varepsilon^2\sigma^{(2)} + \ldots \end{aligned} \tag{2}$$

where:

ε - perturbation parameter,

v_1, v_2, v_3 - functions fulfilled boundary conditions,

$\sigma^{(1)}, \sigma^{(2)}$ - derivatives of stress with respect to the perturbation parameter.

The perturbation procedure applied to the simply supported beam leads to $\sigma^{(1)} = 0$, that means the bifurcation point is symmetric and $\sigma^{(2)} > 0$ defined stable points of bifurcation (Fig. 2).

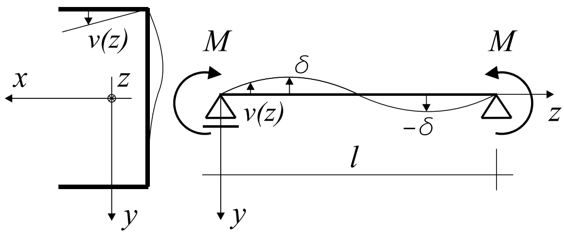

Fig. 1. Thin-walled cold-formed channel beams undergoing pure bending

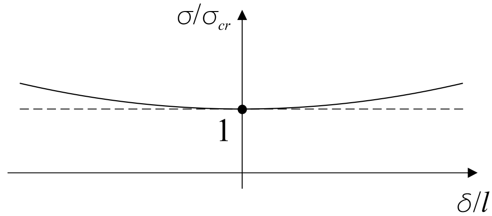

Fig. 2. Bifurcation point and initial post-buckling behaviour

The results obtained show that decreasing of the critical buckling stress upon inevitable geometrical imperfections is not possible. Moreover it is proved that $v_2 = 0$, hence the flange displacement in initial post-buckling state is expressed by the maximum deflection of the flange δ as follows

$$v(z) = \delta\left[\sin\, m\pi z/l - \delta^2 M\, \left(\sin\, m\pi z/l - \sin\, 3m\pi z/l\right)\right] \tag{3}$$

REFERENCES

[1] Paczos P., Stability and limit load of cold-formed thin-walled beams, Poznan University of Technology Press, 2014.

[2] Magnucki K., Paczos P., Kasprzak J., Elastic buckling of cold-formed thin-walled channel beams with drop flanges, Journal of Structural Engineering ASCE, 136 (7), 2010, pp. 886-896.

POSSIBILIY OF USE "3D PRINNTING" IN STATIC AND STABILITY ANALYSES OF THIN-WALLED STRUCTURES

Ł. ŚWIĘCH, M. KALWARA
Department of Aircraft and Aircraft Engines, Rzeszow University of Technology
Powstancow Warszawy 8, 35-021, Rzeszow, Poland

1. INTRODUCTION

Currently, a significant increase in interest of additive manufacturing can be observed. Technology commonly known as 3D printing seems to be good opportunity to manufacture geometrically complicated structures in relatively simple manner. Paper presents overview of experimental investigations carried out to determine the suitability of the technology in the design and testing stage of thin-walled structures.

2. FUSED FILAMENT FABRICATION METHOD

Presented analyses were conducted on thin-walled structures made with use of additive manufacturing method called FFF (Fused Filament Fabrication). Nowadays it is one of the most widespread version of "3D printing" because of relatively low cost of equipment and wide variety of materials from which models can be made. Described method consists in building objects layer upon layer from molten plastic wire, called filament. Geometrical accuracy possible to obtain is about ±0.1 mm.

The scope of available materials starts from standard engineering plastics like ABS, PC, PET, HIPS or Nylon; through biodegradable PLA or rubber-like materials, to composites, e.g. ABS-PC or PLA with carbon fibers.

Mechanical properties of materials listed above allows to build functional mock-ups, prototypes or even short series of complete products.

2. EXPERIMENTAL INVESTIGATIONS

Paper presents result of research program started from testing of mechanical properties carried out on specimens fabricated from different materials. Main parameters of "printing" process and its influence on material's properties were also under consideration.

Next stage of research include manufacturing of structures, geometrical deviations measurements were capture with use of white light scanner. Experimental tests were conducted with use of strength testing machine and deformations were measured by Spatial Digital Image Correlation system (3D DIC).

Range of tested structures covers stiffened plates and panels subjected to shear and compression. Fig. 1 consists example results of postcritical deformation measured for thin-walled cylinder, fabricated from Nylon filament, subjected to compression.

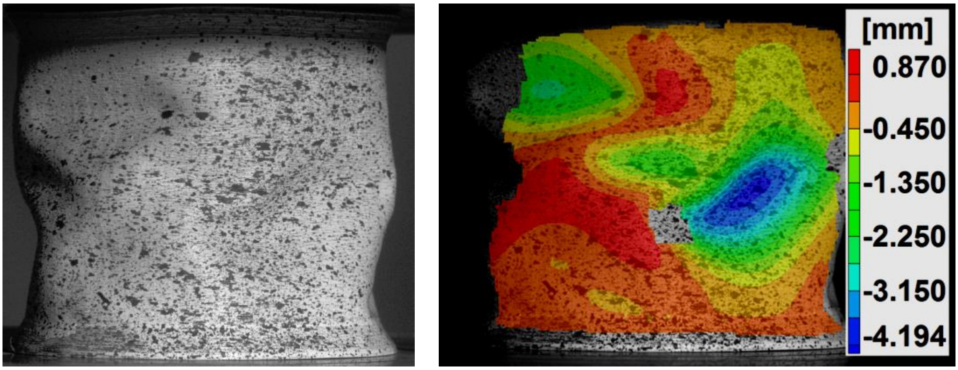

Fig. 1. Example of printed, thin-walled cylinder subjected to compression.
Postcritical deformation (left photo) and
displacement field measured by DIC scanner (right photo)

4. CONCLUTIONS

To sum up, the conducted researche proofs concept of use "3D printing" in experimental investigation of thin-walled structures. Simultaneous use of 3D DIC systems for deformation recording seems to be particularly useful for verification of numerical analyses e.g. by FEM method conducted in geometrically nonlinear stage of deformation.

This publication proposal was made under financial support of The National Centre for Research and Development under grant agreement number LIDER/011/443/L-4/12/NCBR/2013.

REFERENCES

[1] ARAMIS: User manual, GOM mbH, 2010.
[2] ATOS: User manual, GOM GmbH, 2010.
[3] Brzoska Z., Statyka i stateczność konstrukcji prętowych i cienkościennych, PWN, Warszawa, 1965.
[4] Kopecki H., Święch Ł., Zacharzewski J., Comparative analysis of the stress states obtained as a result of numerical calculations and experimental investigations with the 3D digital image correlation method, Statics, Dynamics and Stability of Structural Elements and Systems, Lodz, 2012, pp. 427-446.
[5] Quinn D., Murphy A., Stiffened panel stability behaviour and performance gains with plate prismatic sub-stiffening, Thin-Walled Structures, Elsevier, 2009, pp. 1457-1468.

IMPERFECTION SENSITIVITY ANALYSIS OF COLD-FORMED STEEL MEMBERS

V. UNGUREANU, D. DUBINA
Politehnica University of Timisoara, Timisoara, Romania
Romanian Academy – Timisoara Branch, Timisoara, Romania

A. MADEO, G. ZAGARI, G. ZUCCO, R. ZINNO
MODELING Department, University of Calabria, Cosenza, Italy

The design of cold-formed steel members is generally dominated by interactive buckling. The evaluation of their structural performance requires to account for the presence of local, distortional and global buckling and their interactions [1]. It is well known that experimental limit loads are much lower than predicted by buckling loads, due to the presence of imperfections in real context and interactive buckling that affect the load carry capacity [2÷4]. The presence of imperfections greatly influences the structural behaviour. Therefore it is necessary to evaluate the imperfection sensitivity of these members. Imperfection sensitivity analysis requires the identification of a large number of buckling modes and their interaction. Because of the large number of possible modes and the uncertainly about which ones produce the most dangerous interaction among them, such analysis is prohibitively time consuming.

Path-following analyses based on Riks' method [5] are often used. In spite of the simplicity of its numerical implementation, Riks' method suffers in the case of multiple bifurcations, and moreover the analysis must be fully repeated for each imperfection, making impracticable when combined with Monte Carlo simulation.

The finite element implementation of Koiter asymptotic approach [6] allows to evaluate the pre-critical and initial post-critical behavior of slender elastic structures, also in the presence of strong non-linear pre-critical and in the case of interactive buckling [7, 8]. The method is considered very attractive for its advantages in respect to path-following approach. These consist in an accurate post-buckling analysis and in an efficient imperfection sensitivity analysis with low computational cost. The main difficulties arise in the availability of geometrically coherent structural model and in an accurate evaluation of their high order energy variations. The use of corotational formulation, within a mixed formulation, allows to have a general finite element implementation of Koiter analysis [7].

Therefore, the aim of this work is to apply a robust and efficient methodology [9] to study the imperfection sensitivity of cold-formed steel rack members in compression, with and without perforations [3], as shown in Fig. 1. Using a Monte-Carlo simulation, for a random sequence of imperfections assumed with the shape as linear combination of buckling modes, the equilibrium paths for the imperfect structures are recovered. The load carrying capacity is evaluated statistically. The worst imperfections are detected and the limit load is obtained so allowing the evaluation of erosion of critical bifurcation load [2], as shown in Fig. 2. The maximum erosion detected correspond to the length L=2200 mm. The figure show that brut sections have a higher limit load than net sections, however the slope of sensitivity curves is the same.

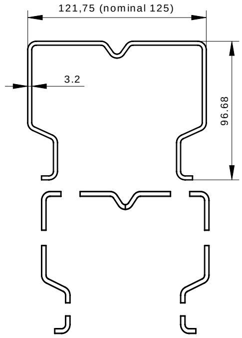

Fig. 1. Geometry of RS125×3.2 rack section in mm (see details in [3])

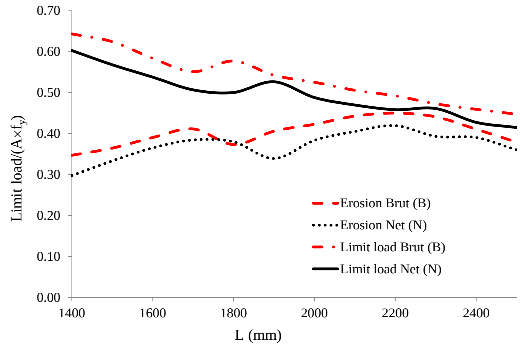

Fig. 2. The minimum limit load normalized to the first buckling load for brut (B) and net (N) section

It can be observed that based on the above parametric study, the obtained erosion are of 0.45 for the brut section (B) and 0.42 for the net section (N), in a good agreement with the ones obtained in [4], i.e. 0.387 for the brut section and 0.395 for the net section.

REFERENCES

[1] Dinis P.B., Camotim D., Cold-formed steel columns undergoing local-distortional coupling: Behaviour and direct strength prediction against interactive failure, Computers & Structures, 147, 2015, pp. 181-208.

[2] Dubina D., Ungureanu V., Instability mode interaction: from Van Der Neut model to ECBL approach, Thin-Walled Structures, 81, 2014, pp. 39-49.

[3] Crisan A., Ungureanu V., Dubina D., Behaviour of cold-formed steel perforated sections in compression: Part 1-Experimental investigations, Thin-Walled Struct., 61, 2012, pp. 86-96.

[4] Crisan A., Ungureanu V., Dubina D., Behaviour of cold-formed steel perforated sections in compression: Part 2-Numerical investigations and design considerations, Thin-Walled Structures, 61, 2012, pp. 97-105.

[5] Riks E., An incremental approach to the solution of snapping and buckling problems, International Journal of Solids and Structures, 15, 7, 1979, pp. 529-551.

[6] Casciaro R., Computational asymptotic post-buckling analysis of slender elastic structures, in: Phenomenological and Mathematical Modelling of Structural Instabilities, M. Pignataro, V. Gioncu (eds.), Vol. 470, CISM - International Centre for Mechanical Sciences, Springer Vienna, 2005, pp. 195-276.

[7] Zagari G., Madeo A., Casciaro R., de Miranda S., Ubertini F., Koiter analysis of folded structures using a corotational approach, International Journal of Solids and Structures, 50, 5, 2013, pp. 755-765.

[8] Barbero E.J., Madeo A., Zagari G., Zinno R., Zucco G., Koiter asymptotic analysis of folded laminated composite plates, Composites Part B: Engineering, 61, 2014, pp. 267-274.

[9] Barbero E.J, Madeo A., Zagari G., Zinno R., Zucco G., Imperfection sensitivity analysis of laminated folded plate, Thin-Walled Structures, 90, 2015, pp. 128-139.

PLASTIC MECHANISMS FOR THIN-WALLED COLD-FORMED STEEL MEMBERS IN ECCENTRIC COMPRESSION

V. UNGUREANU
Politehnica University of Timisoara, Romania
Romanian Academy - Timisoara Branch, Romania

M. KOTEŁKO, J. GRUDZIECKI
Department of Strength of Materials, Lodz University of Technology, Poland

It is very well known that cold-formed steel structures are usually made by thin-walled members of class 4 sections and they are characterised by a reduced post-elastic strength and by a reduced ductility. Since these sections are prematurely prone to local or distortional buckling and they do not have a real post-elastic capacity, the failure at ultimate stage of such members, either in compression or bending, always occurs by forming a local plastic mechanism [1]. This fact suggests the possibility to use the local plastic mechanism to characterise the ultimate strength of such members.

The yield line mechanism analysis has been widely used to study steel members and connections that involve local collapse mechanisms. This method can be used to study post-elastic behaviour, load-carrying capacity, ductility, rotation capacity and energy absorption. A detailed history of yield line mechanism theory has been presented by Zhao [2]. An art review of the application of yield line analysis to cold-formed members has been presented by Hiriyur & Schafer [3] and Ungureanu et al. make an inventory, classify and range geometrical and analytical models for the local-plastic mechanisms aiming to characterize the ultimate capacity of some of the most used cold-formed steel sections in structural applications [4].

Present paper is based on previous studies and on some latest investigations of authors, as well as the literature collected data. It represents an attempt to study the plastic mechanisms for members in eccentric compression.

The approach is a numerical one, in order to identify the plastic mechanisms of members subjected to eccentric compression about minor axis and the evolution of plastic mechanisms, considering several types of lipped channel sections (see Fig. 1).

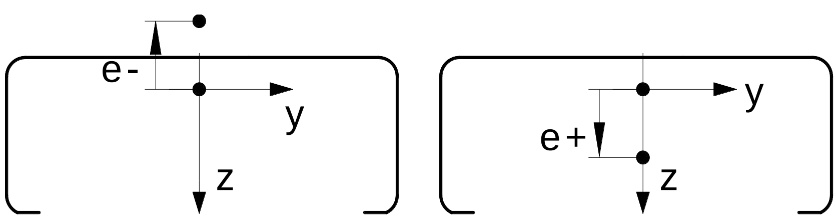

Fig. 1. Example of considered eccentricities

Also, positive and negative eccentricities along the symmetry axis will be investigated, i.e. -10 mm, -5 mm, -2 mm, -1mm, 0 mm, +1 mm, + 2 mm, +5 mm, +10 mm and +20 mm, as shown in Fig. 1.

Fig. 2 presents some plastic mechanisms of thin-walled cold-formed steel members subjected to eccentric compression.

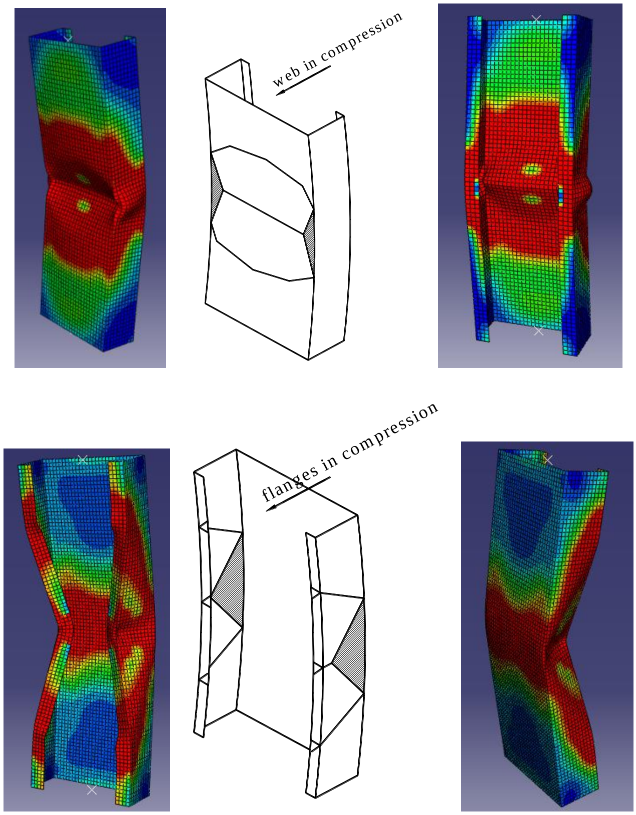

Fig. 2. Plastic mechanisms of members subjected to compression and bending about minor axis

REFERENCES

[1] Dubina D., Ungureanu V., Plastic strength of thin-walled members, Sixteenth Int. Specialty Conference on Cold-Formed Steel Structures, Orlando, Florida, 2002, pp. 324-332.

[2] Zhao X.-L., Yield line mechanism analysis of steel members and connections, Prog. Struct. Engng. Mater., 5, 2003, pp. 252-262.

[3] Hiriyur, B.K.J., Schafer, B.W., Yield-line analysis of cold-formed steel members, International Journal of Steel Structures, 5, 1, 2004, pp. 43-54.

[4] Ungureanu V., Kotelko M., Mania R.J., Dubina D., Plastic mechanisms database for thin-walled cold-formed steel members in compression and bending, Thin-Walled Structures, 48, 10-11, 2010, pp. 818-826.

FINITE ELEMENT MODELLING OF BENDED LAMINATE CHANNEL BEAMS

M. URBANIAK, J. ŚWINIARSKI,
Department of Strength of Materials, Lodz University of Technology,

T NIEZGODZIŃSKI
Department of Dynamics, Lodz University of Technology
Stefanowskiego 1/15, 90-924 Łódź, Poland

1. INTRODUCTION

Engineer running the computing system is focused on the development of computational model, often without being aware of how the software is imperfect in modelling of some phenomena, especially the stability and behaviour of the structure after the stability loss. It is easy to overestimate the considered structure that is built based on a wrong calculation model. Among the engineers carrying out FEM calculations it is well known that the result often depends on the adopted boundary conditions (the way of support and load) and way of solving issues. Analysis of nonlinear stability of thin-walled composite structures (e.g. multilayer laminates) is very important issue. In literature there are still not enough publications on stability and load capacity of thin-walled composite girders loaded with bending moment [1, 2].

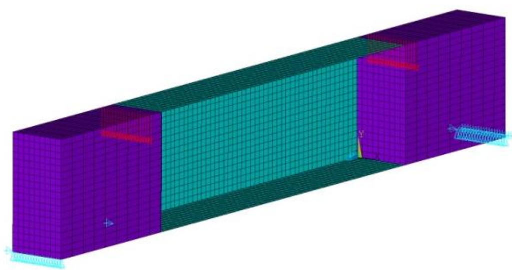

Fig. 1. Model 2 - loading corresponds to four-point bending test

2. NUMERICAL MODELS

For the calculations Ansys v15 finite element method software was used. Two numerical models were prepared. Model 1 includes a fragment of the actual beam located between the handles. The considered part of the channel beams were loaded by stress distribution corresponding to pure bending. Model 2 (Fig. 1) includes the beam with the handles, and the load is the same as at the test stand (four-point bending). For discretization of the composite beam in both cases the multi-layer shell element, defined by eight nodes with six degrees of freedom at each node was applied. In Model 2 to model both handles the cuboid solid element was used, defined by twenty nodes with three degrees of freedom at each node.

3. RESULTS

On the basis of numerical calculations critical moment (M_{cr}) for local buckling was defined which for Model 1 is equal to M_{cr} = 229 Nm, while for Model 2 M_{cr} = 282 Nm. The difference of about 20% is due to obtained different mode of deformation. In the case of the Model 1 on compressed flange two sine half-waves appear and for Model 2 these are three sine half-waves.

The difference between the models in the critical load is due to difference of applying of the load and how the supports are modelled. Similar differences were observed in the results of nonlinear stability compared between the models and the experiment. For the case of a failure mode received from both numerical models and experimental result they are the same (Fig. 2).

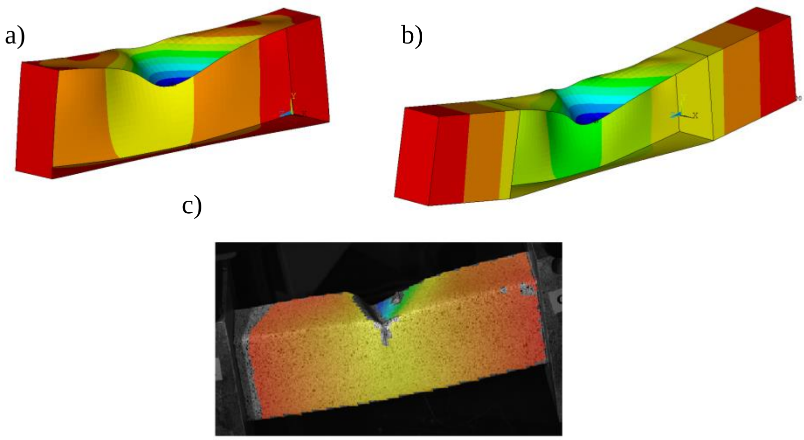

Fig. 2. Failure modes: a) Model 1; b) Model 2; c) Test

The paper has been written under the research project financed by the National Centre for Science - decision number DEC-2011/03/B/ST8/06447

REFERENCES

[1] Bambach M.R., Photogrammetry measurements of buckling modes and interactions in channels with edge-stiffened flanges, Thin-Walled Structures, 47, 2009, pp. 485-504.

[2] Kubiak T., Kaczmarek Ł., Estimation of load-carrying capacity for thin-walled composite beams, Composite Structures, 119, 2015, pp. 749-756.

BUCKLING AND VIBRATIONS OF SEVEN-LAYER BEAM WITH CROSSWISE CORRUGATED MAIN CORE - NUMERICAL STUDY

L. WITTENBECK
Institute of Mathematics, Poznan University of Technology
Piotrowo 3A, 60-965 Poznan, Poland

P. JASION
Institute of Applied Mechanics, Poznan University of Technology
ul. Jana Pawła II 24, 60-965 Poznan, Poland

1. INTRODUCTION

Many applications require the high stiffness and low weight which can be achievable with the use of sandwich structures. Therefore sandwich structures with a various shape of a core are commonly used in many engineering fields. The theory of the sandwich structures are presented in many monographs, for example: Allen [1], Plantema [2], Ventsel and Krauthammer [3]. This theory and its applications is still intensively developed in many contemporary studies. Magnucka-Blandzi and Magnucki [4] discussed strength and stability problems of sandwich beams and its effective design. Magnucki et al [5] and [6] investigated bending and buckling problems of orthotropic sandwich beams with three-layer faces. The present work was inspired also by the results obtained in the paper [5].

The subject of the study is an orthotropic thin-walled sandwich beam with trapezoidal core and three-layer facings. The outer layers of facings are flat, but inner layers are trapezoidal corrugated - in perpendicular direction to the corrugation of the main core. The beam is with crosswise corrugated main core and lengthwise corrugated inner layers of facings. Metal of the flat or corrugated sheets is isotropic. The finite element model is presented in Fig. 1.

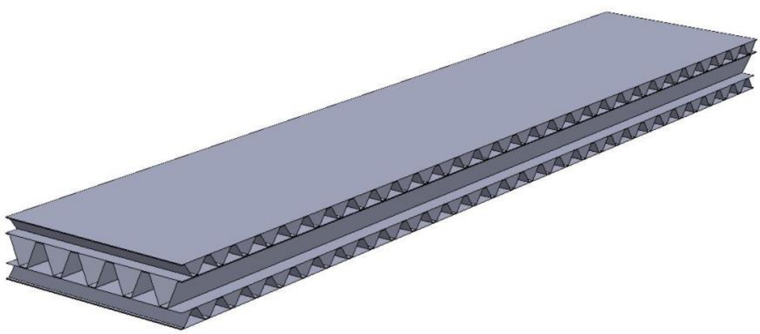

Fig. 1. Numerical model of the beam with crosswise corrugated main core

2. NUMERICAL STUDIES

The geometrically and physically linear analysis were carried out by means of ABAQUS and ANSYS systems. The shell elements were used in three dimensional finite element model. The simply supported sandwich beam with the length L carries a compressive axial force F. The connection between layers of the beam was modelled by means of tie constraints. The load and boundary conditions were applied with using coupling constraints. The arrangement of the load and the supports is illustrated in Fig. 2.

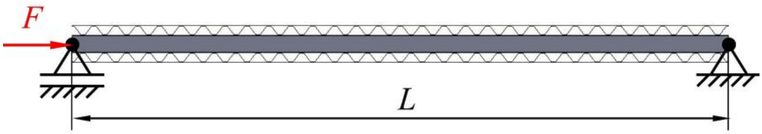

Fig. 2. The scheme of the loaded beam

The critical load and the natural frequencies for the beam with the crosswise corrugated core are determined. The obtained in the numerical (FEM) analyses results will be shown in figures during the Symposium.

ACKNOWLEDGEMENTS

This work was financially supported by the project funded by the National Science Centre (Poland) allocated on the basis of the decision number DEC-2013/09/B/ST8/00170.

REFERENCES

[1] Allen H, Analysis and design of structural sandwich panels, Oxford, London, Edinburgh, New York, Sydney, Paris, Braunschweig: Pergamon Press, 1969.
[2] Plantema F., Sandwich construction: the bending and buckling of sandwich beams, plates and shells, Wiley & Sons, New York, London, Sydney, 1996.
[3] Ventsel E., Krauthammer T., Thin plates and shells, Theory, analysis and applications, New York, Basel: Marcel Dekker, Inc, 2001.
[4] Magnucka-Blandzi E., Magnucki K., Effective design of a sandwich beam with a metal foam core, Thin-Walled Structures 45, 2007, pp. 432–438.
[5] Magnucki K., Kuligowski P., Krus M., Magnucka-Blandzi E., Bending and buckling of orthotropic sandwich beams with three-layer faces, In Proceedings of The 6-th Intl Conference on Coupled Instabilities in Metal Structures, CIMS, J. Loughlan, D.H. Nash and J. Rhodes (Eds.), 3-5 December, Glasgow, UK, 2012, pp. 587-594.
[6] Magnucki K., Jasion P., Krus M., Kuligowski P., Wittenbeck L., Strength and buckling of sandwich beams with corrugated core, Journal of Theoretical and Applied Mechanics, 51, 2013, pp. 15-24.

BUCKLING AND VIBRATIONS OF SANDWICH BEAM WITH VARIABLE MECHANICAL PROPERTIES OF THE CORE

L. WITTENBECK, E. MAGNUCKA-BLANDZI
Institute of Mathematics, Poznan University of Technology
Piotrowo 3A, 60-965 Poznan, Poland

1. INTRODUCTION

The high stiffness and low weight often required in many engineering applications is achievable with the use of sandwich structures. The theory of these structures is the subject of many contemporary studies. There are many monographs devoted to this topic, for example: Plantema [1], Ventsel and Krauthammer [2]. Analytical studies and nonlinear hypotheses of deformation of the field of displacement of were carried out by many investigators. Non-linear zig-zag hypothesis for multilayered plates were presented by Carrera et al. [3]. Magnucka-Blandzi and Magnucki [4] and Magnucki and Magnucka-Blandzi [5] described the strength and stability problems of a sandwich beam with a porous-cellular core and its effective design. Magnucka-Blandzi and Wittenbeck [6] studied compression of simply supported sandwich circular plate consisting of two facings and a core with variable mechanical properties.

The paper is devoted to a sandwich beam consisting of two facings and a core with variable mechanical properties (Fig. 1). The detailed investigation have been realised for the simply supported beam subjected to axial compression. The critical load and the natural frequency of the beam are determined.

2. ANALYTICAL STUDIES

The analytical study includes formulation of mathematical model, the crucial parts of which are: the hypotheses related to deformation of the cross section of the beam (Fig. 1), the description of displacement and stress fields for particular layers, formulation of equations of motion, and their solution.

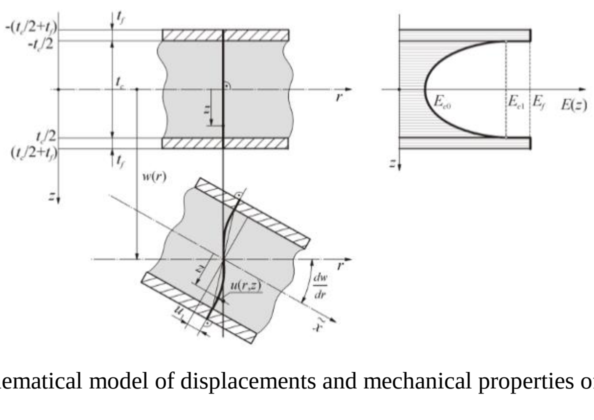

Fig. 1. The mathematical model of displacements and mechanical properties of the beam

Based on Hamilton's principle the equations of motion are derived for the considered beam and analytically solved.

3. NUMERICAL STUDIES

The geometrically and physically linear analysis were carried out by means of ABAQUS system. The shell and solid elements were used in three dimensional finite element model. The connection between layers of the beam was modelled by means of tie constraints. The load and boundary conditions were applied with using coupling constraints. The arrangement of the load and the supports is illustrated in Fig. 2.

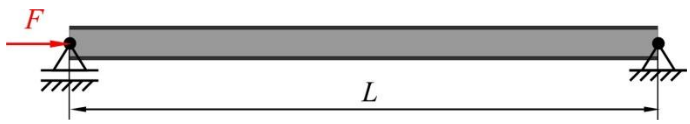

Fig. 2. The scheme of the loaded beam

The critical load and the natural frequencies for the beam with the foam core are determined. The results obtained in the analytical and the numerical (FEM) analyses will be shown during the Symposium presentation.

ACKNOWLEDGEMENTS

The presented research results executed under the subject of No. 04/43/DSPB/0082, were funded with grants for education allocated by the Ministry of Science and Higher Education

REFERENCES

[1] Plantema F., Sandwich construction: the bending and buckling of sandwich beams, plates and shells, Wiley & Sons, New York, London, Sydney 1996.
[2] Ventsel E., Krauthammer T., Thin plates and shells, Theory, analysis and applications, New York, Basel: Marcel Dekker, Inc, 2001.
[3] Carrera E., Brischetto S., A survey with numerical assessment of classical and refined theories for the analysis of sandwich plates, Applied Mechanics Reviews 62, 2009, pp. 1-17.
[4] Magnucka-Blandzi E., Magnucki K., Effective design of a sandwich beam with a metal foam core, Thin-Walled Structures 45, 2007, pp. 432-438.
[5] Magnucki K., Magnucka-Blandzi E., Strength and stability of a sandwich beam with a porous-cellular core, 11-th Symposium Stability of Structures, K. Kowal-Michalska, R.J. Mania (Edit.), Zakopane, Chair of Strength of Materials and Structures, Lodz University of Technology, 2006, pp. 259-266.
[6] Magnucka-Blandzi E., Wittenbeck L., Approximate Solutions of Equilibrium Equations of Sandwich Circular Plate", 11th International Conference of Numerical Analysis and Applied Mathematics 2013, AIP Conference Proceedings 1558, (Eds: T.E. Simos, G. Psihoyios, Ch. Tsitouras), pp. 2352-2355.

BEHAVIOUR OF CONCRETE FILLED STEEL BOX COLUMN WITH CONSIDERING DETACHMENT UNDER 3-D SEISMIC LOAD

S. ZENZAI, S. SHIMIZU
Department of Civil Engineering, Shinshu University
Wakasato 4-Chome, Nagano, 380-8533 Japan

1. INTRODUCTION

Steel box columns used as piers of the motorway viaduct are often filled with the concrete to improve the strength against earthquake.

One of the authors presented two papers on behaviour of partially concrete-filled steel column in the Symposia on Stability of Structures in 2003 and 2009 held in Zakopane [1, 2]. In the 2003 Symposium, detachment of the steel-concrete interface is considered, and in the 2009, influence of the 3-D seismic load is presented. However, the former study dealt with only the static loading, and the latter study was not considering detachment.

Therefore, in the current study, a dynamic analysis is made on a steel box column with considering detachment of the steel plate and the filled-in concrete under the 3-D seismic load by Finite Element Method using MARC 2005r2. The purpose of this study is to disclose influence of detachment of the steel-concrete interface of a concrete-filled steel box column.

2. NUMERICAL MODEL AND THEORY

A typical numerical model is showed in Fig. 1. The column is fixed in all directions at its bottom. At the top of the column, a mass of 900 tons of the superstructure is considered and 3-dimension seismic load is applied.

In the analysis, detachment is realised by the theory of the direct constraints in Marc 2005r2 [3] (Fig. 2). The detachment analysis often requires the special contact and gap elements. However, with the direct constraints are not required special elements.

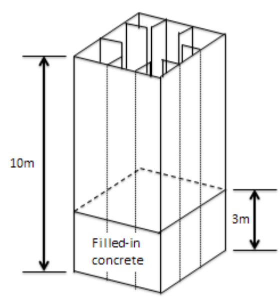

Fig. 1 Numerical model

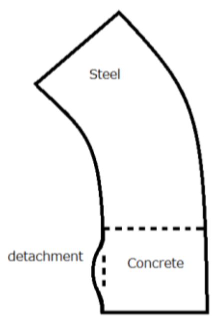

Fig. 2 Detachment of steel and concrete

3. NUMERICAL RESULTS

In Fig. 3, the horizontal displacements at the top of the columns according to time are plotted. In the EW direction, the horizontal displacements of model with detachment is larger than model with no detachment, furthermore, residual displacements is increased.

Fig. 4 shows out-of-plane deformation in steel plate. (Positive value: deformation for the outside of column, Negative value: deformation for the inside of column). The out-of-plane deformation in the steel plate of the model with detachment is transformed in the direction away from the filled in concrete. It is shown that the out-of-plane deformation behaviour of the model with detachment clearly differs from one of the model with no detachment.

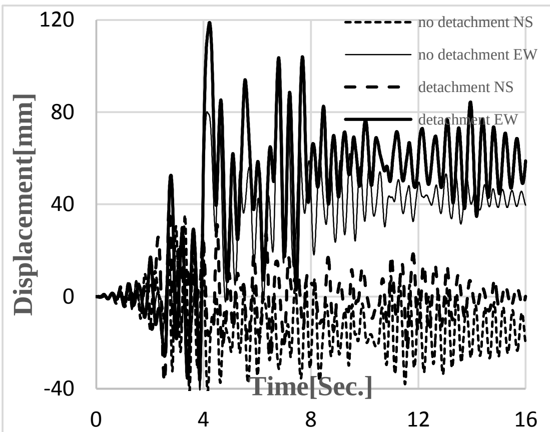

Fig. 3 Horizontal displacements at the top

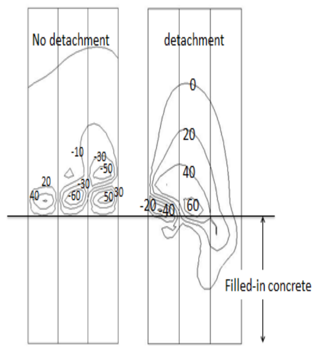

Fig. 4 Out-of-plate deformation

4. REMARKS AND CONCLUSIONS

Horizontal displacements at the top of the columns with considering detachment increase.

The out-of-plane deformation behaviour of the model with detachment clearly differs from one of the model with no detachment.

REFERENCES

[1] Shimizu S., Iwamoto N., Behaviour of a concrete filled steel box column with considering delamination of steel-concrete interface, Proc. of Stability of Structures X, Zakopane, Poland, pp. 379-384.

[2] Shimizu S., Behaviour of steel columns under 3-D seismic load, Proc. of Stability of Structures XII, Zakopane, Poland, pp. 3a-10a.

[3] MSC SOFTWARE, Theory and User Information Version, MSC SOFTWARE, 2005, pp. 508-576.